

POLITECNICO DI TORINO

Master of Science in Mechanical Engineering

Master Thesis

Eco-Driving Optimization of Different Powertrain Architectures Based on Dynamic Programming



Supervisors:

Prof. Federico MILLO

Prof. Luciano ROLANDO

Eng. Luca PULVIRENTI

Candidate:

Marco SCALA

July 2021

Life can only be understood backwards; but it must be lived forwards.

S. Kierkegaard

To my family

Sommario

Al giorno d'oggi i veicoli elettrici ibridi stanno ricevendo molto interesse grazie alle loro potenzialità in termini di riduzione del consumo di combustibile all'interno di limiti realistici di natura economica, infrastrutturale e accettazione da parte del cliente. Comunque, una propulsione ibrida necessita di una strategia di controllo ad hoc: un controllore di alto livello, ovvero il sistema di gestione dell'energia, il quale ottimizzi il flusso di energia all'interno del veicolo.

Utilizzando le tecniche di ottimizzazione globale, come ad esempio la Dynamic Programming (DP), una minimizzazione del consumo di combustibile è possibile attraverso la decisione del migliore profilo di velocità da seguire rispettando tutti i vincoli del problema, e quindi non solo della gestione dell'energia ottimale. In aggiunta, la crescente crescita della connettività dei veicoli di ultima generazione, sta portando ad avere nuovi e migliori sfruttamenti delle tecniche di ottimizzazione globale.

In questo contesto, questo lavoro di tesi è focalizzato sulla ottimizzazione del profilo di velocità di un veicolo in un ambiente interconnesso. Il problema di controllo associato è formulato e risolto attraverso la DP. L'attività di ricerca proposta mira a valutare, tramite simulazione numerica, il potenziale in termini di riduzione del consumo di energia di un uso sinergico tra le tecniche di ottimizzazione globale e la comunicazione del veicolo con l'ambiente circostante. L'approccio proposto è stato testato su un veicolo diesel plug-in ibrido di ultima generazione, già disponibile sul mercato.

Abstract

Nowadays, Hybrid Electric Vehicles (HEVs) are receiving lots of attention thanks to their potentialities in term of fuel consumption reduction within realistic economical, infrastructural and customer acceptance constraints. However, a hybrid powertrain needs an ad hoc powertrain control strategy: a high-level controller, namely the Energy Management System (EMS), that optimizes the energy flow on the vehicle.

Using the global optimization techniques, e.g. Dynamic Programming (DP), a fuel consumption minimization is possible by deciding not only the optimal energy management, but rather the optimal driving schedule. Moreover, the increased connectivity level of last-generation vehicles is paving the way to new and best exploitations of global optimization techniques.

In this framework, this thesis work is focused on the eco-driving optimization of a vehicle in a connected environment. The associated control problem is formulated and solved by means of DP. The proposed research activity aims to assess, through numerical simulation, the potential in terms of energy consumption reduction of a synergic use of global optimization techniques and Vehicle-to-Everything (V2X) information. The proposed approach was tested on a state-of-the-art diesel Plug-in HEV (PHEV) already available on the market.

Acknowledgement

Alla fine di questa tanto entusiasmante quanto impegnativa esperienza universitaria mi sento in dovere di ringraziare tutte quelle persone che mi sono state vicine e mi hanno supportato (e sopportato) durante questi anni importanti della mia vita.

In primis, i miei ringraziamenti vanno alla mia famiglia, il cui ruolo è stato cruciale; grazie per il vostro continuo supporto e incondizionato affetto. Un particolare ringraziamento va a Marco che è stato e sarà sempre un esempio per me.

Vorrei ringraziare particolarmente il Prof. Federico Millo che, grazie alla sua passione, dedizione e straordinaria conoscenza è stato capace di trasmettermi l'amore per la sua materia e mi ha dato l'opportunità di svolgere questo lavoro di tesi, un lavoro ambizioso, stimolante e avvincente in un contesto esterno sicuramente psicologicamente stressante e difficoltoso.

Un ringraziamento particolare al Prof. Luciano Rolando che grazie alla sua invidiabile esperienza e ai suoi preziosissimi consigli è riuscito ad aiutarmi a risolvere le diverse difficoltà incontrare durante questo lavoro di tesi. Vorrei ringraziare di cuore anche il dottorando Luca Pulvirenti per il tempo che mi ha dedicato, il costante confronto durante tutto il percorso mi è stato indispensabile, Luca grazie anche per avermi tenuto sempre alto il morale e spronato a dare il massimo.

Un grazie speciale va anche a tutti i miei amici, una seconda famiglia che mi è stata vicino durante questi anni: le risate, le mille vicende e avventure, le passioni comuni e lo staccare dalla quotidianità sono ricordi indelebili e sono stati di fondamentale importanza per me.

Infine un ringraziamento va anche alla mia costanza, dedizione e meticolosità negli obiettivi che mi pongo, senza i quali non sarei mai stato in grado di raggiungere questo straordinario traguardo.

Index

- Sommario..... VII
- Abstract..... IX
- Acknowledgement XI
- Index..... XIII
- Symbols..... XVII
- List of Tables XXIII
- List of Figures.....XXVII
- 1. Introduction..... 1
- 2. Hybrid Electric Vehicles 5
 - 2.1 Regulation Framework..... 5
 - 2.2 Driving Cycles 9
 - 2.2.1 Type Approval Procedure..... 9
 - 2.2.2 Real Driving Emissions..... 10
 - 2.3 xHEVs Classifications..... 12
 - 2.3.1 Hybridization Level 14
 - 2.3.2 Powertrain Architecture 15
 - 2.3.3 Hybrid Emissions Legislation..... 17
 - 2.4 Energy Management Strategies 19
 - 2.4.1 Introduction..... 19
 - 2.4.2 Dynamic Programming 20

2.5	V2X communication	23
3.	Case Studies.....	25
3.1	Powertrain Specification	25
3.1.1	Experimental Investigation.....	27
3.1.2	Driving Cycles.....	28
3.2	Vehicle Modelling	31
3.2.1	Backward Kinematic Analysis.....	32
3.2.2	Modelling Tools.....	36
3.3	Distance-based Model	40
3.3.1	PHEV Final Drive Energy Minimization	42
3.3.2	CV Fuel Minimization	44
3.3.3	BEV Δ SoC Minimization	45
4.	Results	49
4.1	Speed optimization for PHEV Final Drive Energy Minimization	49
4.1.1	NEDC	49
4.1.2	RDE.....	62
4.2	Speed Optimization for CV Fuel Consumption Minimization	76
4.2.1	NEDC	76
4.2.2	RDE.....	85
4.3	Speed Optimization for BEV Δ SoC Minimization	96
4.3.1	NEDC	96
4.3.2	RDE.....	99
	Conclusions	105

Bibliography..... 107

Symbols

Abbreviations

<i>AC:</i>	Alternative Current
<i>AT:</i>	Automatic Transmission
<i>AWD:</i>	All-Wheel Drive
<i>BMEP:</i>	Brake Mean Effective Pressure
<i>CAV:</i>	Connected and Automated Vehicle
<i>CD:</i>	Charge-Depleting
<i>CF:</i>	Conformity Factor
<i>CS:</i>	Charge-Sustaining
<i>CV:</i>	Conventional Vehicle
<i>DACS:</i>	Direct Air Capture and Storage
<i>DC:</i>	Direct Current
<i>DP:</i>	Dynamic Programming
<i>DPM:</i>	Dynamic Programming Model
<i>DSF:</i>	Dynamic Skip Fire
<i>EM:</i>	Electric Machine
<i>EMS:</i>	Energy Management System
<i>EU:</i>	European Union
<i>EUDC:</i>	Extra Urban Driving Cycle
<i>GHG:</i>	Greenhouse Gas
<i>GLOSA:</i>	Green Light Optimized Speed Advisory
<i>HV:</i>	High Voltage
<i>HPCU:</i>	Hybrid Power Control Unit
<i>ICE:</i>	Internal Combustion Engine

<i>LCA:</i>	Life Cycle Assessment
<i>LD:</i>	Light Duty
<i>Li-NMC:</i>	Lithium Nickel Manganese Cobalt oxide
<i>NEDC:</i>	New European Driving Cycle
<i>PEMS:</i>	Portable Emissions Monitoring System
<i>PM:</i>	Permanent Magnet
<i>PMP:</i>	Pontryagin's Minimum Principle
<i>PMR:</i>	Power-to-Mass Ratio
<i>PHEV:</i>	Plug-in Hybrid Electric Vehicle
<i>PPM:</i>	Parts Per Million
<i>RB:</i>	Rule Based
<i>RDE:</i>	Real Driving Emissions
<i>RT:</i>	Road Transport
<i>RPM:</i>	Revolution Per Minute
<i>RWD:</i>	Rear-Wheel Drive
<i>SA:</i>	Simulated Annealing
<i>SDP:</i>	Stochastic Dynamic Programming
<i>SAS:</i>	Speed Advisory System
<i>SoC:</i>	State of Charge
<i>TTR:</i>	Through-The-Road
<i>UDC:</i>	Urban Driving Cycle
<i>UNFCCC:</i>	United Nations Framework Convention on Climate Change
<i>V2D:</i>	Vehicle-to-Device
<i>V2G:</i>	Vehicle-to-Grid
<i>V2I:</i>	Vehicle-to-Infrastructure
<i>V2N:</i>	Vehicle-to-Network
<i>V2V:</i>	Vehicle-to-Vehicle
<i>V2X:</i>	Vehicle-to-Everything
<i>WLTC:</i>	Worldwide Harmonized Light Vehicles Test Cycle
<i>WLTP:</i>	Worldwide Harmonized Light Vehicles Test Procedure

x_{HEV} : PHEV and/or HEV

Definitions

a : Acceleration
 a_{max} : Upper acceleration limit
 a_{min} : Lower acceleration limit
 C : Cost function
 cap : Battery capacity
 CH_4 : Methane
 CO_2 : Carbon dioxide
 E_{batt} : Total storable energy in the battery
 E_{fd} : Total final drive positive energy
 f_0, f_1, f_2 : Coast down coefficients
 F_{acc} : Acceleration force
 F_{res} : Resistance force
 F_{tot} : Total tractive force at the wheel
 g : Gravitational acceleration
 H_2O : Water (vapor)
 i : Electric battery current
 i_{fd} : Final drive ratio
 i_{gb} : Gearbox ratio
 I_{ICE} : Internal combustion engine inertia
 I_{EM} : Electric motor inertia
 $I_{wh,f}$: Front wheel inertia
 $I_{wh,r}$: Rear wheel inertia
 M_{eq} : Equivalent vehicle mass
 M_{veh} : Vehicle mass

m_f :	Total fuel consumption
N_2O :	Nitrous oxide
O_3 :	Ozone
P_{batt} :	Total battery power request
P_{dmd} :	Total power demand
$P_{el,acc}$:	Electrical accessories power request
P_{gb} :	Inlet gearbox power
P_{gen} :	Mechanical power requested by motor generator
$P_{EM,e}$:	Electrical power requested by motor generator
P_{ICE} :	Mechanical power requested by internal combustion engine
$P_{lim,ICE,min}$:	Internal combustion engine minimum power (function of rpm)
$P_{lim,ICE,max}$:	Internal combustion engine maximum power (function of rpm)
$P_{lim,EM,min}$:	Electric motor minimum power (function of rpm)
$P_{lim,EM,max}$:	Electric motor maximum power (function of rpm)
Q_{lhv} :	Fuel lower heating value
$Q(t)$:	Instantaneous battery charge
Q_{max} :	Maximum battery charge
r_{wh} :	Wheel radius
SoC_0 :	Initial state of charge
SoC_f :	Final state of charge
SoC_{max} :	Upper state of charge limit
SoC_{min} :	Lower state of charge limit
ΔSoC :	State of charge total variation
t :	Time
T :	Total travel time
u :	Power split
v :	Longitudinal vehicle speed
v_{max} :	Upper speed limit
v_{min} :	Lower speed limit
$v_{veh,max}$:	Maximum longitudinal vehicle speed

x :	Total distance travelled by the vehicle
α :	Cost function parameter
δ :	Road grade
η_{gb} :	Total gearbox efficiency
η_{gen} :	Total motor generator efficiency
$\omega_{EM,max}$:	Maximum electric motor rotational speed
ω_{gb} :	Gearbox rotational speed
ω_{wh} :	Wheel rotational speed
$\omega_{wh,max}$:	Maximum wheel rotational speed

List of Tables

Table 1.1: World energy-related CO₂ emissions by sector..... 3

Table 2.1: Characteristic values of Class 3 WLTC [18] 10

Table 2.2: Parameter for RDE compliance divided in zones 12

Table 2.3: Simplified example 1 states and optimal costs-to-go 22

Table 3.1: Vehicle specifications 26

Table 3.2: Main characteristics of the NEDC cycle 29

Table 3.3: Main characteristics of the RDE cycle..... 30

Table 3.4: Computational time comparison between fixed grid and variable grid in PHEV final drive energy minimization model 43

Table 3.5: Computational time comparison between fixed grid and variable grid in CV fuel minimization model..... 45

Table 3.6: BEV battery specifications 46

Table 4.1: Cost function parameter for the sensitivity analysis 50

Table 4.2: Total travel time, final drive positive energy request and final drive positive energy request per kilometre with different values of cost function parameter, for the NEDC performed with a PHEV 53

Table 4.3: Total travel time, final drive positive energy request and final drive positive energy request per kilometre with different values of cost function parameter, for the UDC with V2X communication performed with a PHEV..... 57

Table 4.4: Total travel time, final drive positive energy request and final drive positive energy request per kilometre, comparison among the UDC with and without V2X communication with a fixed value of cost function parameter, performed with a PHEV 61

Table 4.5: Total travel time, final drive positive energy request and final drive positive energy request per kilometre with different values of cost function parameter, for the RDE cycle performed with a PHEV	67
Table 4.6: Total travel time, final drive positive energy request and final drive positive energy request per kilometre with different values of cost function parameter, for the urban RDE cycle with V2X communication performed with a PHEV	71
Table 4.7: Total travel time, final drive positive energy request and final drive positive energy request per kilometre, comparison among the urban RDE cycle with and without V2X communication with a fixed value of cost function parameter, performed with a PHEV	75
Table 4.8: Final travel time, fuel consumption and average fuel consumption with different values of cost function parameter, for the NEDC performed with a conventional vehicle	78
Table 4.9: Final travel time, fuel consumption and average fuel consumption with different values of cost function parameter, for the UDC with V2X communication performed with a conventional vehicle	81
Table 4.10: Final travel time, fuel consumption and average fuel consumption, comparison among the UDC with and without V2X communication with a fixed value of cost function parameter, performed with a conventional vehicle	84
Table 4.11: Final travel time, fuel consumption and average fuel consumption with different values of cost function parameter, for the RDE cycle performed with a conventional vehicle	88
Table 4.12: Final travel time, fuel consumption and average fuel consumption with different values of cost function parameter, for the urban RDE cycle with V2X communication performed with a conventional vehicle.....	91
Table 4.13: Final travel time, fuel consumption and average fuel consumption, comparison among the urban RDE cycle with and without V2X communication with a fixed value of cost function parameter, performed with a conventional vehicle.....	95
Table 4.14: Final travel time, SoC variation and battery energy request per kilometre with different values of cost function parameter, for the NEDC performed with a battery electric vehicle	99

Table 4.15: Final travel time, SoC variation and battery energy request per kilometre with different values of cost function parameter, for the RDE cycle performed with a battery electric vehicle..... 102

List of Figures

Figure 1.1: Global temperature rise between 1970-2020 relative to 1880-1920 mean 2

Figure 1.2: Average concentration of CO₂ in the atmosphere in ppm..... 2

Figure 2.1: Global passenger cars CO₂ emissions and fuel consumption, normalized to the NEDC 7

Figure 2.2: Vehicle speed pattern in the Class 3 WLTC [17] 10

Figure 2.3: Spectrum of vehicle hybridization level [22] 14

Figure 2.4: Scheme of a series hybrid architecture [24]..... 15

Figure 2.5: Scheme of a parallel hybrid architecture [24] 16

Figure 2.6: Hybrid system architectures classified by motor position [25]..... 17

Figure 2.7: Simplified example 1 states and costs [30] 21

Figure 3.1: Powertrain layout of PHEV under investigation [34]..... 28

Figure 3.2: Vehicle speed and gear patterns in the NEDC [16]..... 29

Figure 3.3: RDE speed and altitude profile in function of the distance..... 31

Figure 3.4: Information flow in a backward kinematic analysis [29]..... 32

Figure 3.5: Fuel consumption evaluation in a backward kinematic model [24] 33

Figure 4.1: Speed limits for the first ECE-15..... 50

Figure 4.2: Vehicle speed profile with different values of cost function parameter, for the NEDC performed with a PHEV 51

Figure 4.3: Vehicle speed profile with different values of cost function parameter, for the first ECE-15 performed with a PHEV 52

Figure 4.4: Travel time with different values of cost function parameter, for the NEDC performed with a PHEV	52
Figure 4.5: Final drive positive energy request with different values of cost function parameter, for the NEDC performed with a PHEV	53
Figure 4.6: Trade-off between positive energy request at final level and travel time with different values of cost function parameter, for the NEDC performed with a PHEV	54
Figure 4.7: Speed limits with red or green signal for the first ECE-15.....	55
Figure 4.8: Vehicle speed profile with different values of cost function parameter, for the UDC with V2X communication performed with a PHEV.....	56
Figure 4.9: Travel time with different values of cost function parameter, for the UDC with V2X communication performed with a PHEV.....	56
Figure 4.10: Final drive positive energy request with different values of cost function parameter, for the UDC with V2X communication performed with a PHEV.....	57
Figure 4.11: Vehicle speed profile comparison among different optimizations with a fixed value of cost function parameter, for the UDC performed with a PHEV	58
Figure 4.12: Travel time comparison among different optimizations with a fixed value of cost function parameter, for the UDC performed with a PHEV	58
Figure 4.13: Final drive positive energy request comparison among different optimizations with a fixed value of cost function parameter, for the UDC performed with a PHEV	59
Figure 4.14: Vehicle speed profile comparison among the UDC with and without V2X communication and traffic light signal with a fixed value of cost function parameter, performed with a PHEV.....	60
Figure 4.15: Vehicle speed profile and traffic light signal with a fixed value of cost function parameter, for UDC with V2X communication performed with a PHEV	60
Figure 4.16: Traffic light signals and travel time in a time-distance graph with a fixed value of cost function parameter, for the UDC with V2X communication performed with a PHEV	61
Figure 4.17: Trade-off between positive energy request at final level and travel time for the UDC with and without V2X communication with different values of cost function parameter, performed with a PHEV.....	62

Figure 4.18: Speed limits for the initial part of the RDE cycle	63
Figure 4.19: Vehicle speed profile with different values of cost function parameter, for the RDE cycle performed with a PHEV	64
Figure 4.20: Vehicle speed profile with different values of cost function parameter, for the initial part of urban RDE cycle performed with a PHEV	64
Figure 4.21: Vehicle speed profile with different values of cost function parameter, for the initial part of rural RDE cycle performed with a PHEV	65
Figure 4.22: Travel time with different values of cost function parameter, for the RDE cycle performed with a PHEV	66
Figure 4.23: Final drive positive energy request with different values of cost function parameter, for the RDE cycle performed with a PHEV	66
Figure 4.24: Trade-off between positive energy request at final level and travel time with different values of cost function parameter, for the RDE cycle performed with a PHEV	67
Figure 4.25: Speed limits with red or green signal for the initial part of the RDE cycle ...	69
Figure 4.26: Vehicle speed profile with different values of cost function parameter, for the urban RDE cycle with V2X communication performed with a PHEV	70
Figure 4.27: Travel time with different values of cost function parameter, for the urban RDE cycle with V2X communication performed with a PHEV	70
Figure 4.28: Final drive positive energy request with different values of cost function parameter, for the urban RDE cycle with V2X communication performed with a PHEV	71
Figure 4.29: Vehicle speed profile comparison among different optimizations with a fixed value of cost function parameter, for the urban RDE cycle performed with a PHEV	72
Figure 4.30: Travel time comparison among different optimizations with a fixed value of cost function parameter, for the urban RDE cycle performed with a PHEV	72
Figure 4.31: Final drive positive energy request comparison among different optimizations with a fixed value of cost function parameter, for the urban RDE cycle performed with a PHEV	73

Figure 4.32: Vehicle speed profile comparison among the urban RDE cycle with and without V2X communication and traffic light signal with a fixed value of cost function parameter, performed with a PHEV	74
Figure 4.33: Vehicle speed profile and traffic light signal with a fixed value of cost function parameter, for the urban RDE cycle with V2X communication performed with a PHEV	74
Figure 4.34: Traffic light signals and travel time in a time-distance graph with a fixed value of cost function parameter, for the urban RDE cycle with V2X communication performed with a PHEV	75
Figure 4.35: Trade-off between positive energy request at final level and travel time for the urban RDE cycle with and without V2X communication with different values of cost function parameter, performed with a PHEV	76
Figure 4.36: Vehicle speed profile with different values of cost function parameter, for the NEDC performed with a conventional vehicle	77
Figure 4.37: Vehicle speed profile Travel time with different values of cost function parameter, for the first ECE-15 performed with a conventional vehicle.....	77
Figure 4.38: Travel time with different values of cost function parameter, for the NEDC performed with a conventional vehicle.....	78
Figure 4.39: Fuel consumption with different values of cost function parameter, for the NEDC performed with a conventional vehicle	78
Figure 4.40: Trade-off between fuel consumption and travel time with different values of cost function parameter, for NEDC performed with a conventional vehicle.....	79
Figure 4.41: Vehicle speed profile with different values of cost function parameter, for the UDC with V2X communication performed with a conventional vehicle	80
Figure 4.42: Travel time with different values of cost function parameter, for the UDC with V2X communication performed with a conventional vehicle	80
Figure 4.43: Fuel consumption with different values of cost function parameter, for the UDC with V2X communication performed with a conventional vehicle	81
Figure 4.44: Vehicle speed profile comparison among different optimizations with a fixed value of cost function parameter, for the UDC performed with a conventional vehicle..	82

Figure 4.45: Travel time comparison among different optimizations with a fixed value of cost function parameter, for the UDC performed with a conventional vehicle	82
Figure 4.46: Fuel consumption comparison among different optimizations with a fixed value of cost function parameter, for the UDC performed with a conventional vehicle..	83
Figure 4.47: Vehicle speed profile comparison among the UDC with and without V2X communication and traffic light signal with a fixed value of cost function parameter, performed with a conventional vehicle.....	83
Figure 4.48: Vehicle speed profile and traffic light signal with a fixed value of cost function parameter, for UDC with V2X communication performed with a conventional vehicle.	84
Figure 4.49: Traffic light signals and travel time in a time-distance graph with a fixed value of cost function parameter, for the UDC with V2X communication performed with a conventional vehicle	84
Figure 4.50: Trade-off between fuel consumption and travel time for the UDC with and without V2X communication with different values of cost function parameter, performed with a conventional vehicle	85
Figure 4.51: Vehicle speed profile Vehicle speed profile with different values of cost function parameter, for the RDE cycle performed with a conventional vehicle	86
Figure 4.52: Vehicle speed profile with different values of cost function parameter, for the initial part of urban RDE cycle performed with a conventional vehicle	86
Figure 4.53: Vehicle speed profile with different values of cost function parameter, for the initial part of rural RDE cycle performed with a conventional vehicle.....	87
Figure 4.54: Travel time with different values of cost function parameter, for the RDE cycle with a conventional vehicle	87
Figure 4.55: Fuel consumption with different values of cost function parameter, for the RDE cycle performed with a conventional vehicle	88
Figure 4.56: Trade-off between fuel consumption and travel time with different values of cost function parameter, for the NEDC performed with a conventional vehicle	89
Figure 4.57: Vehicle speed profile with different values of cost function parameter, for the urban RDE cycle with V2X communication performed with a conventional vehicle.....	90

Figure 4.58: Travel time with different values of cost function parameter, for the urban RDE cycle with V2X communication performed with a conventional vehicle	90
Figure 4.59: Fuel consumption with different values of cost function parameter, for the urban RDE cycle with V2X communication performed with a conventional vehicle.....	91
Figure 4.60: Vehicle speed profile comparison among different optimizations with a fixed value of cost function parameter, for the urban RDE cycle performed with a conventional vehicle	92
Figure 4.61: Travel time comparison among different optimizations with a fixed value of cost function parameter, for the urban RDE cycle performed with a conventional vehicle	92
Figure 4.62: Fuel consumption comparison among different optimizations with a fixed value of cost function parameter, for the urban RDE cycle performed with a conventional vehicle	93
Figure 4.63: Vehicle speed profile comparison among the urban RDE cycle with and without V2X communication and traffic light signal with a fixed value of cost function parameter, performed with a conventional vehicle	94
Figure 4.64: Vehicle speed profile and traffic light signal with a fixed value of cost function parameter, for the urban RDE cycle with V2X communication performed with a conventional vehicle	94
Figure 4.65: Traffic light signals and travel time in a time-distance graph with a fixed value of cost function parameter, for the urban RDE cycle with V2X communication performed with a PHEV.....	95
Figure 4.66: Trade-off between fuel consumption and travel time for the urban RDE cycle with and without V2X communication with different values of cost function parameter, performed with a conventional vehicle.....	96
Figure 4.67: Vehicle speed profile with different values of cost function parameter, for the NEDC performed with a battery electric vehicle.....	97
Figure 4.68: Vehicle speed profile with different values of cost function parameter, for the first ECE-15 performed with a battery electric vehicle	97
Figure 4.69: Travel time with different values of cost function parameter, for the NEDC performed with a battery electric vehicle	98

Figure 4.70: SoC profile with different values of cost function parameter, for the NEDC performed with a battery electric vehicle	98
Figure 4.71: Trade-off between SoC variation and travel time with different values of cost function parameter, for the NEDC performed with a battery electric vehicle	99
Figure 4.72: Vehicle speed profile with different values of cost function parameter, for the RDE cycle performed with a battery electric vehicle	100
Figure 4.73: Vehicle speed profile with different values of cost function parameter, for the initial part of urban RDE cycle performed with a battery electric vehicle.....	100
Figure 4.74: Vehicle speed profile with different values of cost function parameter, for the initial part of rural RDE cycle performed with a battery electric vehicle.....	101
Figure 4.75: Travel time with different values of cost function parameter, for the RDE cycle performed with a battery electric vehicle	101
Figure 4.76: SoC profile with different values of cost function parameter, for the RDE cycle performed with a battery electric vehicle	102
Figure 4.77: Trade-off between SoC variation and travel time with different values of cost function parameter, for RDE cycle performed with a battery electric vehicle	103

1. Introduction

After the industrial revolution, which took place between the end of the 18th century and the middle of the 19th one, the agrarian and rural society changed into an innovative and industrialized one. Since this period human activity has become more and more impacting to the environment, due in particular due to the use of fossil fuels i.e. coal, gas and oil; by burning them the carbon dioxide (CO₂) stored in the underground fields is released in the atmosphere. The principal Greenhouse Gas (GHG) are CO₂, water vapor (H₂O), ozone (O₃), methane (CH₄) and nitrous oxide (N₂O), their concentration causing the greenhouse effects. This natural effect is necessary for all ecosystems, in fact without it the average temperature on Earth's surface would be 33°C lower than present (-18°C vs +15°C) [1]. Although greenhouse effect is fundamental, an energy imbalance due to a "radiative forcing" causes a further rise in surface temperature, which is detrimental for the delicate ecosystem balance and causes climate changes that will be more and more evident the higher temperature rise will be. In 2020 the level of mean warming worldwide reached +1.2°C [2] and a further increment risks to overtake the critical thresholds, bringing to large irreversible changes, like the collapse of ecosystems [3][4].

Global warming accelerated from 2014 onward (see Figure 1.1), in fact the deviation of the 60-month running mean from the 1970-2015 linear trend is clear [5]; this phenomenon implies an increase in the Earth's energy imbalance and so a more severe global warming.

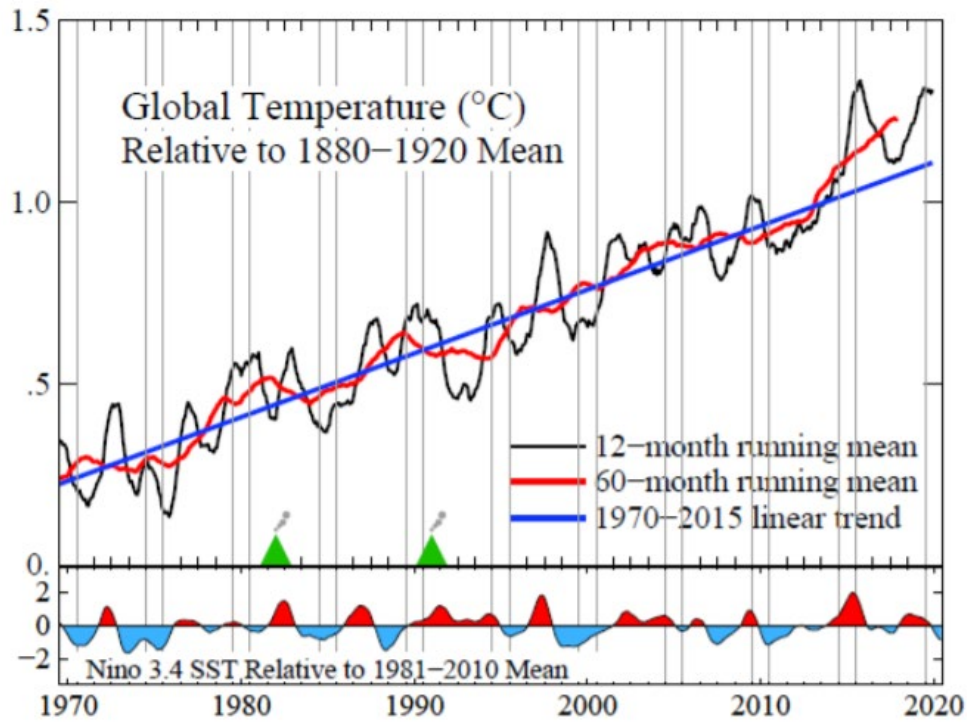


Figure 1.1: Global temperature rise between 1970-2020 relative to 1880-1920 mean

The atmospheric CO₂ concentration over the past 2000 years was rather stable at 270-285 parts per million (ppm) until industrial revolution. Since this period, global CO₂ concentrations have been increasing rapidly: in 2018 concentrations reached 408 ppm (Figure 1.2), in May 2021 grew to 419.1 ppm [6].



Figure 1.2: Average concentration of CO₂ in the atmosphere in ppm

In the last decades global warming has become one of the most important and discussed scientific issues; its effects risk to damage irremediably the environment and the Earth’s fauna and flora. In this framework, in order to minimize these detrimental effects caused by the human activity, policymakers are introducing policies aimed at reducing the CO₂ emissions coming from all the sectors, as an example in 2017 the emissions express in Giga ton of CO₂ by sector are reported in Table 1.1 [7].

Table 1.1: World energy-related CO₂ emissions by sector

Source	Emission [Gt CO ₂]	Emission [%]
Power generator and heat	13588	41.7
Industry	6154	18.9
Road transport	5937	18.2
Buildings	2997	9.2
Aviation and shipping	2049	6.3
Others	1856	5.7
Total	32581	100.0

Focusing the attention on the Road Transport (RT), the CO₂ emissions attributable to the RT was 5937 Gt: 18.2% of total amount of CO₂ emissions due to human activity. It is worth mentioning that in 2015, 51% of global oil demand was due to transport (land transport, aviation and shipping) [8]. Therefore, a transport decarbonization is strictly necessary in the future in order to avoid the dependence on fossil fuels which are non-renewable resources.

2. Hybrid Electric Vehicles

2.1 Regulation Framework

At the 2015 United Nations Framework Convention on Climate Change (UNFCCC), held in Paris, the countries adopted the first-ever global climate deal, aimed at “limiting global warming to well below 2°C” compared to pre-industrial levels and to make an effort to limit the global warming to 1.5°C [9]. The first target means that a net-zero CO₂ emissions must be reached by 2070 to 2085; the second means that the CO₂ emissions must be halved by 2030 and that a net-zero CO₂ emissions must be reached from 2050 onwards [4]. Net-zero emission is possible if the carbon due to human activities equals the carbon captured in the atmosphere through restoring forest or Direct Air Capture and Storage technology (DACs).

Nowadays the transport sector is one of the main sources of GHGs emissions: about 1.35 billion cars are driven worldwide, and this number is destined to grow to 1.8 billion in 2035 [10]. Currently most of them utilize hydrocarbons as a source of energy and it is expected that in 2035/2040 more than 80% of vehicle sales worldwide will still have an Internal Combustion Engine (ICE) [7]. In 2017 the RT accounted for 41.2 million of barrels per day (mb/d), about 40% of world oil demand and this demand is expected, considering the new policies scenario, to increase slightly: 44.9 mb/d in 2040 (that will account for 39% of world oil demand) [7]. In term of CO₂ emission, the RT was due in 2017 of about the 18% of total CO₂ emission linked to anthropogenic causes (19% in 2040) [7]. These small increases in hydrocarbons demand compared to the increase in the number of vehicles will be possible thanks to the new restrictive policies. Globally, in the next 5 years, newly registered vehicle must reduce their fuel consumption up to 30% and more stricter policies

are forecasted in the next future. More in detail regulators are concerned about: improving local air quality, lowering GHG emissions, lowering dependence on imported oil and switching from oil to a more sustainable fuel. Regarding GHG emissions, the regulation for passenger cars in European Union (EU) have been/will be:

- In 1998/1999 through a voluntary agreement, the fleet average emissions target was set to 140 g CO₂/km by 2008/2009. However, despite the initial CO₂ emission reduction (from about 180/200 g CO₂/km in 1998 to about 160/170 g CO₂/km in 2004) it was evident that the target could not be reached without mandatory CO₂ limits.
- In 2009 regulators established that all carmakers had to achieve a fleet average target of 130g CO₂/km from 2015.
- In 2013 the limit was set to 95 g CO₂/km by 2020.
- Lastly in 2017 the limit was set to -15% by 2025 and -37.5% by 2030, both with respect to 2021 average levels.

Moreover, exists an automakers' road map to Battery Electric Vehicles (BEVs) and Plug-in Hybrid Electric Vehicles (PHEVs), for more information see [11]. The EU requires a minimum percentage of sold PHEVs (less than 50 g CO₂/km) or BEVs with the purpose to support a gradual transition to electro-mobility: 15% by 2025 and 30% by 2030 [7]. Similar regulation exists for Light Duty (LD) commercial vehicles, heavy duty vehicles and buses and non-road engines.

The global passenger cars CO₂ emissions and fuel consumption along with the targets are shown in Figure 2.1 [12].

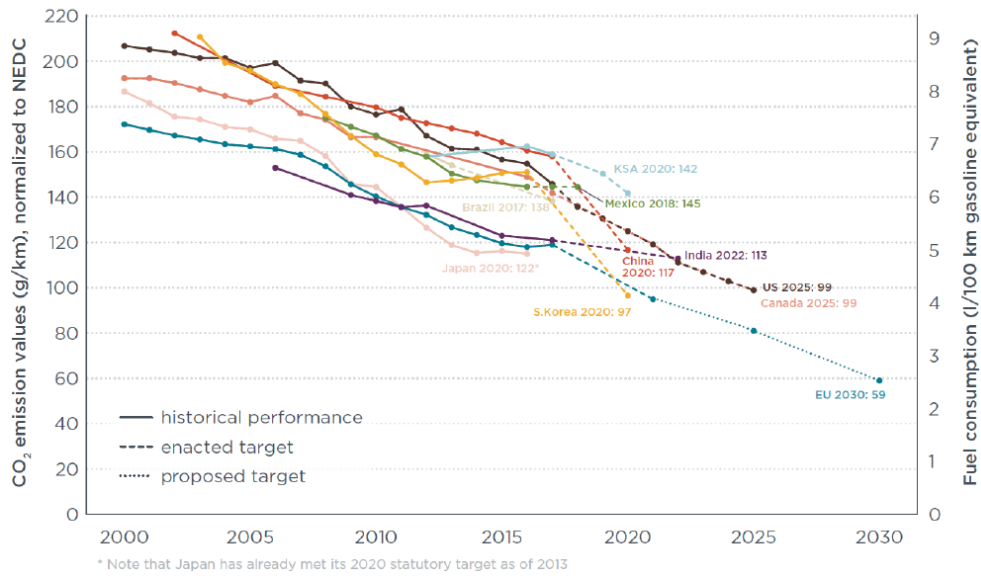


Figure 2.1: Global passenger cars CO₂ emissions and fuel consumption, normalized to the NEDC

There is a similar trend for all principal markets, therefore a great technological effort is necessary to improve fuel economy (3-6% annually on average): in road transport the search for new technologies and fuels is driven by regulators.

However, in the EU the GHG emissions generated by the transport sector have steadily increased between 1990 and 2018 (due to an increasing number of cars driven), despite the trend of other sectors [13].

The CO₂ emission target for passenger cars seems very hard to be reached without a breakthrough in the existing technologies. In order to attempt this challenging target carmakers has to utilize a mix of solution i.e. improve the global ICE efficiency and fuel quality, powertrain electrification, switch to bio fuels or to alternative fuels like natural gas (CH₄). From this portfolio of technologies, powertrain electrification could play a key role, without negatively affecting the vehicle performance; this technology consists in a full or partial powertrain decarbonization: Hybrid Electric Vehicles (HEVs), PHEVs and BEVs represent respectively a medium and a long-term solution. It is predicted that by 2025, 40% of the global LD vehicles will be electrified [14]. In order to have a long-term solution it also assumes primary importance a decarbonization in the energy production.

By considering the CO₂ emitted by a BEV charged using the average EU-27 mix, during its entire life, i.e. the Life Cycle Assessment (LCA), the CO₂ emissions generated by a BEV can be between 17-21% and 26-30% lower if compared to a diesel and a petrol vehicle respectively; it is worth mentioning that in case of 100% coal electricity life cycle GHGs emissions from BEVs are much higher than conventional vehicles [15].

PHEVs and HEVs (xHEVs) combine one or more electric propulsion with a conventional ICE, this can lead to a promising fuel consumption reduction. However, electrification introduces complexity and degrees of freedom due to the cooperation of more power actuators to the vehicle system; in order to manage this complexity, an Energy Management System (EMS) must be developed. Computer-aided software tools are really useful to the research and development of EMS: simulate and predict the fuel consumption benefits will be feasible and economically sustainable. Utilize the future trip information could play a key role to fully exploit all the potentialities of xHEVs, there are two kinds of methods:

- Building predictive models and making assumptions about the future trip.
- Vehicle connectivity using the information from advanced transportation infrastructures like Vehicle-to-Grid (V2G) and Vehicle-to-Vehicle (V2V) communication, collectively referred to as Vehicle-to-Everything (V2X).

Therefore, nowadays the potential of EMS is expanding thanks to the introduction of latest technologies. A key role assumes the exponential growth of computational capabilities, necessary to manage the greater complexity of EMS.

2.2 Driving Cycles

2.2.1 Type Approval Procedure

Legislative driving cycles employed in type-approval tests are used to assess the performance of a category of vehicles (i.e. pollutant emissions, fuel consumption) and the speed profile/length should represent a simplified mean real drive, therefore mean traffic, stop and travel time are taken into account. Type approval procedure is necessary in order to have a standardization. So, the evaluation of fuel consumption of new vehicles is based on regulatory driving cycles, performed in an emissions laboratory. The regulations created around these standardized cycles have contributed to improved fuel economy. The test procedure, driving cycles and regulations differ for different countries and vehicles categories; in this analysis the attention will be focused on the EU regulation for passenger cars.

The New European Driving Cycle (NEDC) chassis dynamometer procedure was the standard in EU until August 2017, consists of several steady-steady test modes: it is really simple to drive and thus results repeatability is ensured [16]. In September 2017 Worldwide Harmonized Light Vehicles Test Cycle (WLTC) has been introduced in EU because of the noteworthy discrepancy between NEDC and the real-world driving conditions: a relevant dynamicity was introduced so the operating points are shifted towards higher loads. The WLTP aims to standardize type approval procedure worldwide and accurately reproduce the mean real-world driving condition, therefore should substitute all other type-approval driving cycle like FTP-75 in the United States or JC08 in Japan. The WLTC impacts on a more fuel consumption and pollutant emissions with respect to other less dynamic cycles e.g. NEDC.

The WLTP varies depending on the vehicle Power-to-Mass Ratio (PMR): three classes are introduced, i.e. Class 1, Class 2 and Class 3 [18]; the last one covers the largest share of

passenger cars in EU. The vehicle speed for Class 3, depending on time is reported in Figure 2.2.

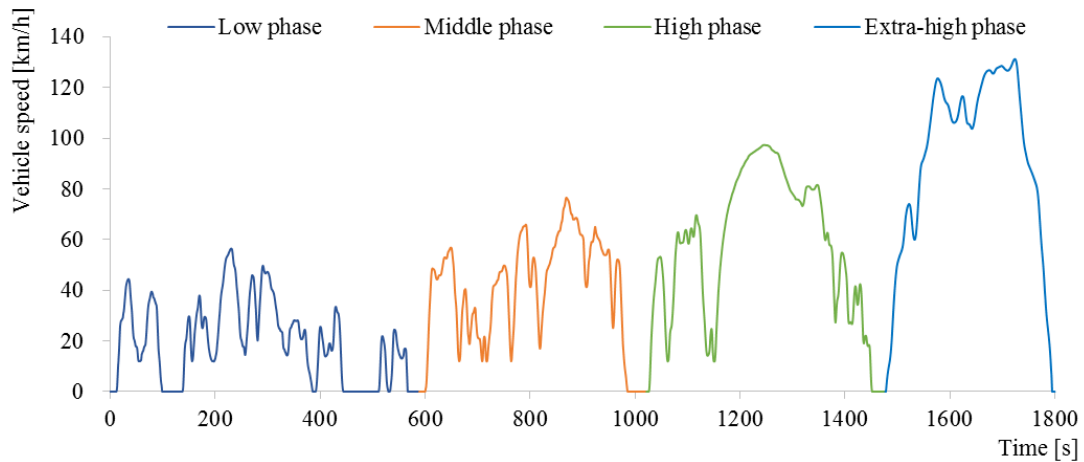


Figure 2.2: Vehicle speed pattern in the Class 3 WLTC [17]

The main characteristic values of WLTC for a Class 3 vehicle are reported in Table 2.1.

Table 2.1: Characteristic values of Class 3 WLTC [18]

Characteristics	Unit	Low	Middle	High	Extra-high	Total
Total distance	m	3095	4756	7158	8254	23262
Total time	s	589	433	455	323	1800
Idle (standing) time	s	156	48	31	7	242
Average speed (incl. stops)	km/h	18.9	39.5	56.6	92.0	46.5
Average speed (excl. stops)	km/h	25.7	44.5	60.8	94.0	53.8
Maximum speed	km/h	56.5	76.6	97.4	131.3	131.3
Maximum acceleration	m/s ²	1.5	1.6	1.6	1.0	1.6

2.2.2 Real Driving Emissions

The standardized driving cycle that are performed in an emission lab are unable to cover the entire envelope of operating points and environmental conditions that the vehicle will be subjected to when driving in the real world. The Real Driving Emissions (RDE) test control vehicle emissions in real world operations, outside the laboratory emission test

where all the conditions are controlled. RDE test is necessary to have a better control of vehicles pollutants emissions, in fact in these test, performed on the road, all the factors present in real life are considered (i.e. road slope, air conditioning, real speed profile, vehicle weight, temperature, etc.) which could lead to different pollutants emissions. Therefore, on the one hand laboratory emission tests are necessary in order to have a standardized emission test procedure where repeatability and comparability between different vehicles are ensured, and on the other hand RDE tests are necessary to assess the real-life vehicle emissions.

RDE testing requirements have been introduced in phases in EU for LD commercial vehicles and passenger cars [19]:

- **RDE monitoring phase** for new type approvals (Euro 6d-temp) from April 2016.
- **RDE type approval testing** from September 2017 where a phase-in Conformity Factor (CF) was introduced.
- **RDE In-Service Conformity requirements** from January 2019 for new car models and from September 2019 for all vehicles.

For emission measurements, Portable Emissions Monitoring System (PEMS) are employed and a CF was introduced in order to correct uncertainty and error of PEMS instruments to be reduced if PEMS technology is enhanced: therefore, the numerical value of the RDE limit is higher than the NEDC limit.

The RDE test must last from 90 to 120 minutes. The route must include three segments: Urban, Rural and Motorway in that order, of at least 16 km each one; the stop period has to be 6-30% of the time duration of the urban segment and each stop no longer than 300 seconds. The main characteristics, divided in zones, are reported in Table 2.2.

Table 2.2: Parameter for RDE compliance divided in zones

Parameter	Urban	Rural	Motorway
Instantaneous speed	$v \leq 60\text{km/h}$	$60\text{km/h} < v \leq 90\text{km/h}$	$v > 90\text{km/h}$
Average speed	$15\text{km/h} \leq \bar{v} \leq 40\text{km/h}$	$60\text{km/h} \leq \bar{v} \leq 90\text{km/h}$	$\bar{v} > 90\text{km/h}$
Trip composition	29-44% of the total trip distance	23-43% of the total trip distance	23-43% of the total trip distance
Distance	$x > 16\text{km}$	$x > 16\text{km}$	$x > 16\text{km}$

Restrictions on other quantities (e.g. payload, ambient temperature, altitude, vehicle conditioning) are imposed, for more information see [20].

2.3 xHEVs Classifications

The HEVs are vehicles where the primary source of energy is the chemical energy stored in the fuel and the secondary source is electricity stored in the battery. On the other hand, the PHEVs can use the electricity as primary source of energy and can be recharged from the electric grid. During the last decades the xHEVs “*have received lots of attention thanks to their potentialities to reduce fuel consumption within realistic infrastructural, economical and customer acceptance constraints*”[21].

Depending on the hybridization degree of the vehicles (reported in the next section) HEVs can reach these energy optimization purposes:

- **Regenerative braking:** kinetic energy can be recovered by an EM and stored into the battery, without waste that energy in heat: it is really important in urban area.
- **Idling reduction:** the ICE can be turned off during stops and low speed.

- **Reduce the clutching losses:** possible if it turns on the ICE when the inlet and outlet gearbox speed are matched and do not require any slip.
- **ICE efficiency enhancement:** the EM assists the ICE in order to operate it near its best efficiency area avoiding the inefficient ones, in fact in conventional vehicles the ICE size is determined by maximum requirements (i.e. top speed, maximum acceleration, etc.) therefore ICE usually works at low efficiencies (in the lower left quadrant of the ICE operating map). Therefore, an ICE downsizing and down speeding will be feasible: a smaller ICE which run at lower rpm is possible thanks to the EM, without compromising performance.
- **Potentially infinite gear ratio:** if the epicyclic train replace the conventional gearbox, it can lead to a fuel consumption reduction thanks to the higher number of ICE operating points that meet the wheel power demand, so a best high efficiency point management.
- **Electrical accessories:** can reduce auxiliary energy request.

Thanks to the additional degree of freedom provided by the EM, the ICE can be better controlled in a hybrid vehicle, improving its emissions at steady-state and during transients, while not sacrificing drivability.

Regarding PHEVs, they can typically operate in two different modes:

- **Charge Depleting (CD):** the vehicle is mainly powered by the EM, therefore the battery must be fully or partially charged initially. This driving mode is usually not suitable for HEVs but only for PHEVs.
- **Charge Sustaining (CS):** the ICE and the EM are used together for propulsion and the State of Charge (SoC) is maintained about constant during the route. Usually a PHEV switches from CD to CS mode when the SoC reaches a specific minimum threshold.

2.3.1 Hybridization Level

The HEVs hybridization level assumes considerable importance to understand the potential and the main features of the HEVs. A classification of today's HEVs based on hybridization level is shown in Figure 2.3: increasing hybridization level leads to a bigger EM and battery size and a smaller ICE.

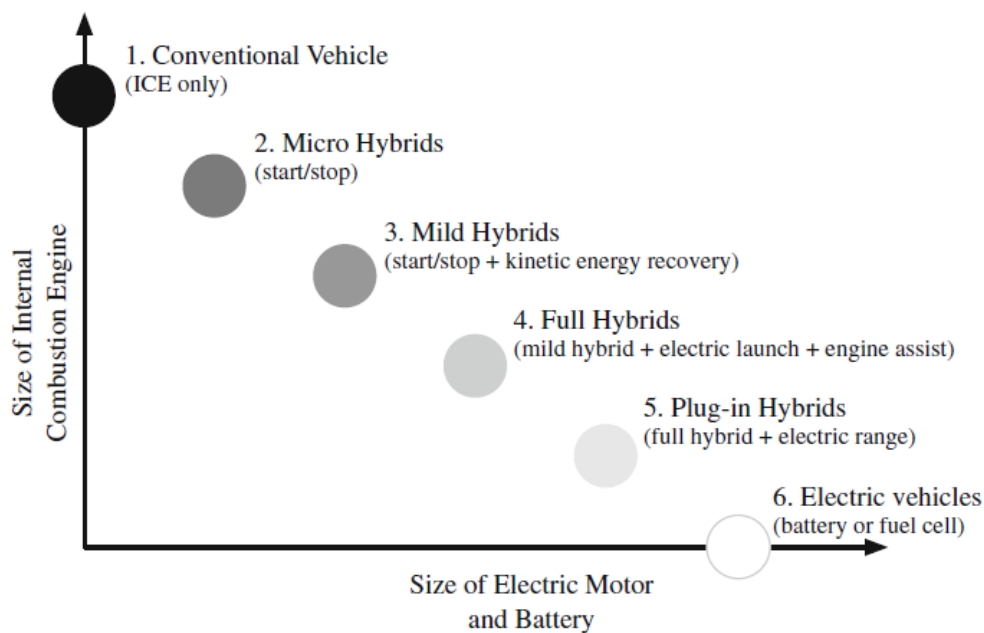


Figure 2.3: Spectrum of vehicle hybridization level [22]

As you can see using the hybridization level the vehicles are classified in:

- **Conventional Vehicle (CV)** where the only source of power is the ICE, therefore there are not degree of freedom for the power: all the power requested at the wheels is provided to the ICE.
- **Micro Hybrid** where it is present a little EM in order to shut down and restart the ICE during the stop; it is useful for vehicle which spent a lot of time at idling in order to reduce fuel consumption.
- **Mild Hybrid** where the ICE is coupled with an EM which can lead also to an e-motor assist and regenerative braking. The electric drive is possible only during coasting and braking phases.

- **Full Hybrid** where EM and battery size guarantee also the electric drive. From this hybridization level the Energy Management System assumes a key role.
- **Plug-in Hybrid** where the battery can be recharged from the electrical grid and so both the CD mode and CS mode are possible.
- **Electric vehicles** where the only source of power is the electric one.

2.3.2 Powertrain Architecture

Another classification of xHEVs can be done considering the powertrain architecture: Series Hybrid, Parallel Hybrid and Complex Hybrid [23].

- **Series Hybrid** where the ICE is only mechanically connected to a generator which is electrically connected to the battery and to the EM. Usually the EM drives the wheels through a fixed gear ratio. The EM is powered by the ICE/generator unit and/or by the battery. If power demand exceeds the output generator power, the battery provides the remaining part otherwise the battery is charged. A simplified scheme of a series architecture is shown in Figure 2.4.

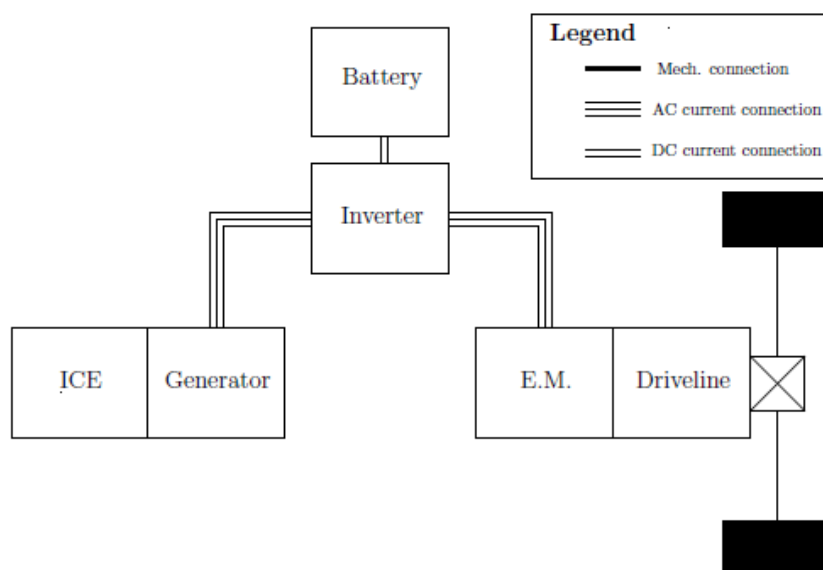


Figure 2.4: Scheme of a series hybrid architecture [24]

- **Parallel Hybrid** where the ICE is mechanically connected to one or more EM. The EM is connected to the wheels by means of a transmission and final drive and to the battery pack through an inverter (Figure 2.5). The overall efficiency can be higher with respect to series architecture because there is less energy conversion.

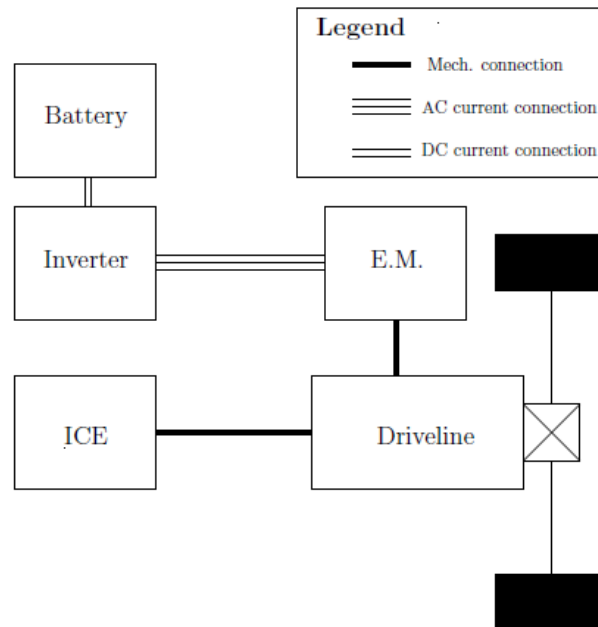


Figure 2.5: Scheme of a parallel hybrid architecture [24]

Once again parallel Hybrid can be classified based on EM position with respect to ICE (Figure 2.6):

- **P0 (P1f)**: the EM is directly connected to the ICE on its front side, considering a longitudinal engine layout. In P0 configuration the regenerative braking and the overall efficiency are limited due to ICE drag and belt losses. Furthermore, the vehicle pure electric mode is not feasible but it is cheap.
- **P1 (P1r)**: the EM is mounted on a crankshaft, directly connected to the ICE on its rear side where is situated the gearbox, so EM cannot be decoupled from ICE (drag losses in regenerative braking).
- **P2**: analogously to P1 configuration, the EM is located upward gearbox, but downstream the clutch, therefore ICE and EM can be disconnected, so avoid

drag losses and coasting operation without engine is possible. The ICE and the EM have a fixed gear ratio, usually equal to 1.

- **P3:** the EM is located between the gearbox and the final drive (differential unit), so its speed is a multiple of wheel speed. P3 configuration enhance P2 capabilities, there are not gearbox losses for EM and there is a variable gear ratio among ICE and EM.
- **P4:** the EM is located on the secondary axle, typically the rear one. Usually it is located upstream the final drive. In this case, the connection to the ICE is Through-The-Road (TTR). P4 configuration have the highest potential for recuperation among parallel configuration and a high market value because permit to have All-Wheel-Drive (AWD).

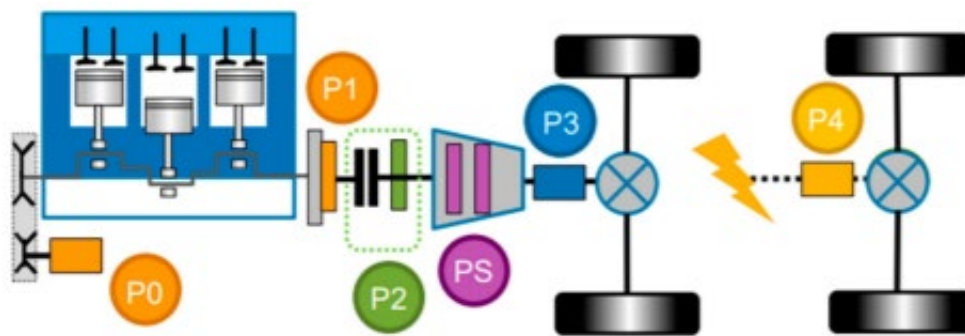


Figure 2.6: Hybrid system architectures classified by motor position [25]

- **Complex Hybrid** this class includes the architecture with a more than one traction motor/ICE, energy and power sources and the series + parallel architecture. These architectures have the highest potential and the highest overall efficiency.

2.3.3 Hybrid Emissions Legislation

The type approval procedure for measuring emissions of xHEVs are different from CVs. It is due to the presence of the battery pack: If a HEV is tested and the final amount of energy stored into the battery is different if compared to the initial one, the fuel

consumption (the only primary source of energy of HEV) will be unfair. Therefore, for HEVs a neutral energy balance must be ensured: SoC variation during the driving cycle must not exceed the 1% of the total chemical energy consumed (Eq. 2.1); if this condition is not guaranteed, a penalty factor is applied to the CO₂ emissions.

$$\Delta SoC < 0.01 \frac{Q_{lhw} \cdot m_f}{E_{batt}} \quad \text{Eq. 2.1}$$

Where:

- Q_{lhw} is the fuel lower heating value.
- m_f is the mass of fuel consumed over the driving cycle.
- E_{batt} is the maximum storable energy in the battery.

For PHEVs (where the primary sources of energy are the electricity and the fuel) the standard procedure is particular unsuitable for two main reasons: PHEVs can operate in CD mode, so for a certain mileage CO₂ emissions are usually neglectable, and test PHEVs only in CS mode is not the correct way because the real advantages of PHEVs are not exploited; in fact the correct way of use is to entirely exploit CD mode, and rely on the ICE only when it is strictly necessary (i.e. when the battery is almost depleted): the charge-sustainability condition is not crucial as for HEVs. Therefore, policy makers have introduced an ad hoc procedure better reflecting their real driving conditions:

- Until August 2017 (measurement performed on the NEDC) there were two tests with some phases with imposed SoC levels, the CO₂ emission was the weighted average of the two tests. For more information, please see the Regulation N°101 Addendum 100.
- Since September 2017 (measurement performed on the WLTC) there are two tests. The first is the Charge Depleting mode where initially the battery is completely charged and the PHEV performs the WLTC cycle until the battery is almost empty [26][27], the ICE can operate to assist the EM and the CO₂ emissions are measured. The second is the Charge Sustaining mode where the battery is at the same level of

the final CD and the energy originates only from ICE and regenerative braking; SoC variation are admitted during the test but the differences between initial and final SoC must be negligible. The emission is a weighted average of the two tests. More details about test procedure can be found in [27].

2.4 Energy Management Strategies

2.4.1 Introduction

In order to exploit all the advantages deriving from a certain degree of hybridization of the powertrain, an EMS must be developed. The EMS optimizes the energy flow on the vehicle thanks to an ad hoc powertrain control strategy, therefore this high-level controller is able to optimize the fuel consumption or other quantity of interest i.e. pollutant emissions, performance, etc.

In literature different categories of controls have been proposed, a primary macro classification consists in model-based and rule-based optimization methods [28].

Model-based methods

The model-based methods can be divided into:

- **Global optimization methods:** e.g. Dynamic Programming (DP), Stochastic Dynamic Programming (SDP), Simulated Annealing (SA) and the genetic algorithms in which a global optimal solution is numerically found [29]. In order to find the global optimal solution a high computational time and a priori information about all the boundary conditions of the problem are required; this leads to an impossibility to implement these strategies on-board. The usefulness of global optimization strategies lies in the fact that it can be used as a benchmark

solution to compare the performance of sub-optimal control strategies like instantaneous and rule-based optimization and it can be used to design rules for rule-based methods [29]. These numerical approaches are based on the minimization of a cost function and a noncausal solution is found since future driving condition is needed.

- **Instantaneous optimization methods:** e.g. Equivalent Consumption Minimization Strategy (ECMS), Pontryagin's Minimum Principle (PMP) where it is implemented instant-wise control decisions therefore only the local optimal solution is found, necessarily sub-optimal; in this case it is an analytical problem formulation which permits to find the solution faster than numerical problem.

Rule-based methods

Most of energy management strategies rely on heuristic control techniques: they can be easily implemented in a powertrain control unit but achieve performance quite far from the optimality. Therefore, the rule-based methods are the most common HEVs supervisory controls thanks to their simplicity and limited computational effort that leads to a feasible real time implementation. They are based on a set of rules that manage the power split between ICE and EM. The rules derive from some significant observed variables like SoC level and power demand. They come from heuristics based on experience or model-based approach [29].

2.4.2 Dynamic Programming

In this dissertation the Dynamic Programming (DP) is used to find the optimal control strategy. The DP was introduced by Richard Bellman in 1957 and it is based on the Bellman's principle of optimality, which states that from any point on an optimal policy, the remaining policy is optimal for the problem with initial conditions that point [29].

DP has been used in many applications among which in the identification of the optimal control strategy in xHEVs. As mentioned above the DP is a numerical model-based method which leads to find the global optimal solution of discretized problems backward in time. Likewise, other model-based methods, the DP must know the cycle a priori and being a numerical problem, a high computational effort is required, therefore is only applicable in simulation environment.

In order to understand how DP works, a simplified example is reported in Figure 2.7.

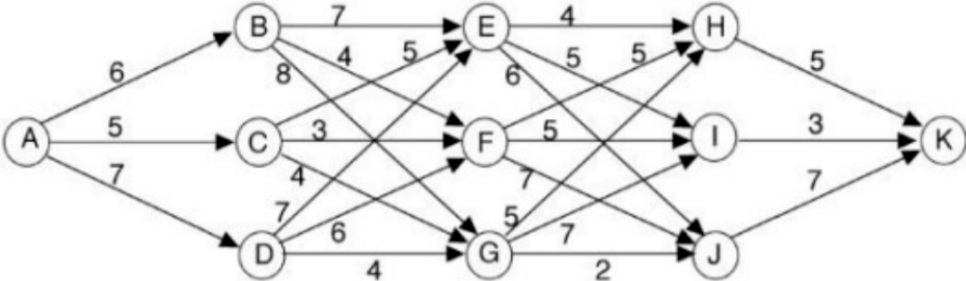


Figure 2.7: Simplified example 1 states and costs [30]

The circled numbers are the states, the arrows represent the potential transition from the previous to the following state and the number associated to the arrows is the cost function (arc cost) numerical value. The state A is the initial state which must be unique, B, C and D represent the feasible discretized states at the time step 1, E, F and G are the states at the following time step, lastly K is the final state (usually can be more than one); therefore the state grid has 3 elements. To find the minimum value of the cost function to go from A to K, should proceed backwards from K to A firstly; it is essential to store the optimal cost-to-go path and so the sum of the arc cost, called cost-to-go function at each state of the grid (Table 2.3). After the backwards run, the DP proceed forwards from A to K along the optimal path.

Table 2.3: Simplified example 1 states and optimal costs-to-go

State	Optimal cost-to-go path	Optimal cost-to-go function
H	H-K	5
I	I-K	3
J	J-K	7
E	E-I-K	8
F	F-I-K	8
G	G-J-K	9
B	B-F-I-K	12
C	C-F-I-K	11
D	D-G-J-K	13
A	A-C-F-I-K	16

The DP involves:

- A dynamic system: described by model equation.
- A cost function: usually to be minimized.
- One or more control signal variable (input) grids: the action made by the system at each time step (e.g. gear, xHEVs operating mode, acceleration). The correspondence between control signal variable and state change is univocal: control variables guide state variable.
- One or more state variable grids: they define where the system is, therefore can mark the evolution of the system (e.g. speed, SoC, ICE state).

In this thesis Dynamic Programming Model (DPM) function is used to find optimal control strategy on a PHEV, BEV and CV [31]. The PHEV work goal is to find the optimal speed profile under imposed maximum and minimum speed limits and optimal power split among EM and ICE that assure to reach the minimum fuel consumption whit a certain total travel time. In the CV and BEV model the goal is to find only the optimal speed profile (whit maximum and minimum constrains) to minimize fuel consumption or SoC variation respectively.

2.5 V2X communication

During the last years V2X communication has been one of the most studied themes in automotive sector thanks to its intrinsic potentialities [32][33][34][35][36][37][38][39][40]. As mentioned above, V2X communication is a vehicular communication system to everything around it; it includes more circumscribe types of communication, e.g. V2G, V2V, Vehicle-to-Infrastructure (V2I), Vehicle-to-Device (V2D) and Vehicle-to-Network (V2N). V2X can influence positively fuel/energy saving, traffic and road safety [34]; this dissertation is focused on the first actual advantage. The V2X communication can lead to eco-driving: it is a really promising technology to reduce fuel consumption significantly, moreover it is relatively simple and low-cost [32]. The V2X offers the opportunity of improving the standard EMS exploitation of xHEVs thanks to predictive information about the imminent route [33].

In the last decade, several studies have demonstrated the possibility to enhance the fuel economy of current vehicles thanks to V2X communication. The optimal vehicle speed and power split can be determined along a given route leading to minor fuel consumption without sacrificing travel time. Look-ahead route information over urban and mixed route scenarios can potentially reduce fuel consumption by 10+% [34]. A study focused on Green Light Optimized Speed Advisory (GLOSA) systems aims at showing the target speed to the driver when approaching a traffic light in order to reduce the number of unnecessary stops (and so lead to lower CO₂ emissions) [35]. Another study of a vehicle equipped with Dynamic Skip Fire (DSF) and integrated in a fleet of Connected and Automated Vehicles (CAVs) thanks to control technologies using vehicle connectivity and automation demonstrated that the energy consumption of future vehicles can be reduced up to 12% [36]. A study on a PHEV architecture using a two-stage DP algorithm has shown a promising fuel economy savings and thanks to DP problem formulation can reduce the computational load [37]. A limited percentage of vehicles with a Speed Advisory System (SAS) have a positive influence on the entire arterial traffic: a SAS-equipped vehicle not

only reduce his own fuel consumption, but also enhance other vehicles fuel economy, more decreases with more SAS-equipped vehicles [38]. For other interesting studies on V2X communication of xHEVs see [33] and [39].

3. Case Studies

3.1 Powertrain Specification

The experimental campaign was performed on a state-of-the-art P2 PHEV schematized in Figure 3.1.

The ICE is a 1950 cc diesel engine, conformed to Euro 6d-temp certification and the EM is a Permanent Magnet (PM) synchronous motor. The motion power is delivered to the rear wheels by means of a torque converter followed by a 9-speed Automatic Transmission (AT) and a final drive. The Li-Ion Nickel-Manganese-Cobalt-oxide (Li-NMC) High Voltage (HV) battery powers the EM through a DC/AC converter (the HV inverter) while a DC/DC converter is necessary for the 12V battery and low voltage electrical loads. The noteworthy vehicle characteristics are summarized in Table 3.1.

Table 3.1: Vehicle specifications

Vehicle			
Cycle	NEDC		WLTC
Test Mass	2040 kg		2162 kg
F0	152.9 N		171.5 N
F1	0.809 N/km/h		0.833 N/km/h
F2	0.0272 N/(km/h) ²		0.0280 N/(km/h) ²
Configuration	Rear Wheel Drive (RWD)		
Transmission			
Type	9-AT w/ Torque Converter		
Speed Ratios	I 5.36	IV 1.64	VII 0.87
	II 3.25	V 1.22	VIII 0.72
	III 2.26	VI 1.00	IX 0.61
Reverse	-4.93	Final Drive	2.65
ICE			
Engine Type	In-line 4 Cylinders Turbo Diesel		
Displacement	1950 cm ³		
Max Power/Max Torque	143 kW @ 3800 rpm / 400 Nm @ 1600-2800 rpm		
Compression Ratio	15.5:1		
EM			
Type	PM Synchronous Motor		
Max Power/ Max Torque	90 kW @ 2000 rpm / 440 Nm @ 0-1750 rpm		
Max Speed	5000 rpm		
HV battery			
Type	Li-NMC		
Rated Voltage	365 V		
Capacity	13.5 kWh / 37 Ah		
Number of Cell in Parallel	1		
Number of String	63		
Cooling System	Water Cooled		

3.1.1 Experimental Investigation

The study relied on a huge amount of experimental data. It is used an AWD chassis dynamometer and RDE scenarios equipping the vehicle with PEMS [41].

The Hybrid Power Control Unit (HPCU), connected to the HV inverter, allows the driver to select between four driving modes [41]:

- **Hybrid Drive:** the EMS autonomously decides the operating mode depending on the route profile and the driving situation. Usually the ICE propels the vehicle in combination with the EM. It is the default mode.
- **Electric Drive:** the vehicle is propelled only by the EM; therefore, it operates in CD mode. No fuel is needed, guaranteeing zero tail pipe emissions, but it is requested a certain minimum SoC.
- **E-Save Drive:** the vehicle operates only in CS mode so both the ICE and the EM are used for propulsion. This mode allows the Electric Drive at a later stage.
- **Charge Drive:** the vehicle is propelled only by the ICE and a power surplus constantly charging the battery. Usually this mode is not convenient due to efficiencies issues; in fact, power losses should be taken into account in case of recharging from ICE which are avoided when the battery is recharged directly from the grid.

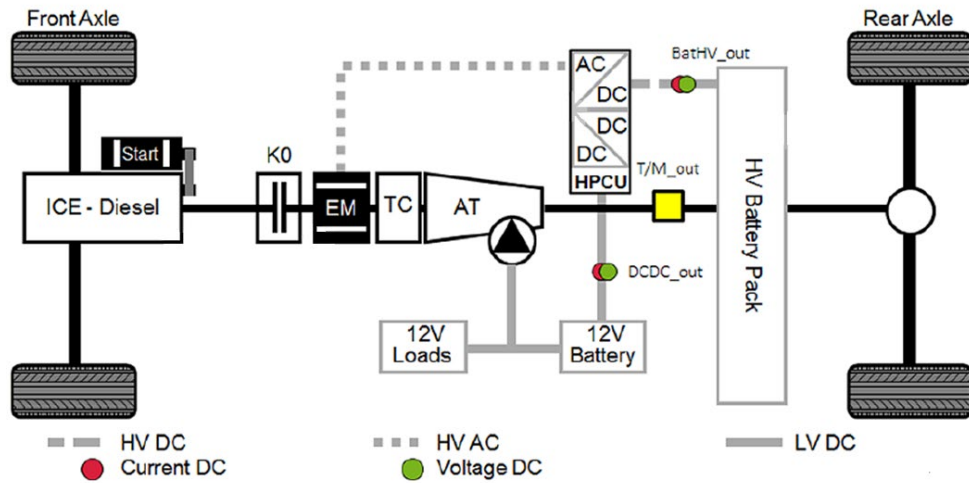


Figure 3.1: Powertrain layout of PHEV under investigation [34]

3.1.2 Driving Cycles

3.1.2.1 NEDC

As mentioned above, the NEDC consists of several steady-steady test modes; it was mainly used for the vehicle model debugging thanks to its simplicity. The NEDC is composed in the first part by four Urban Driving Cycle (UDC) segments, the ECE-15, while in the second part one Extra Urban Driving Cycle (EUDC). The vehicle speed profile and gear-imposed scheme can be seen in Figure 3.2 and the cycle main characteristic values are reported in Table 3.2.

Table 3.2: Main characteristics of the NEDC cycle

Characteristics	Unit	ECE-15	EUDC	NEDC
Distance	m	1013	6955	11007
Total time	s	195	400	1180
Idle (standing) time	s	57	39	267
Average speed (incl. stops)	km/h	18.4	62.6	33.6
Average speed (excl. stops)	km/h	23.87	68.6	42.24
Maximum speed	km/h	50	120	120
Average acceleration	m/s ²	0.599	0.354	0.506
Maximum acceleration	m/s ²	1.042	0.833	1.042
Total positive difference in altitude	m	0	0	0
Total negative difference in altitude	m	0	0	0

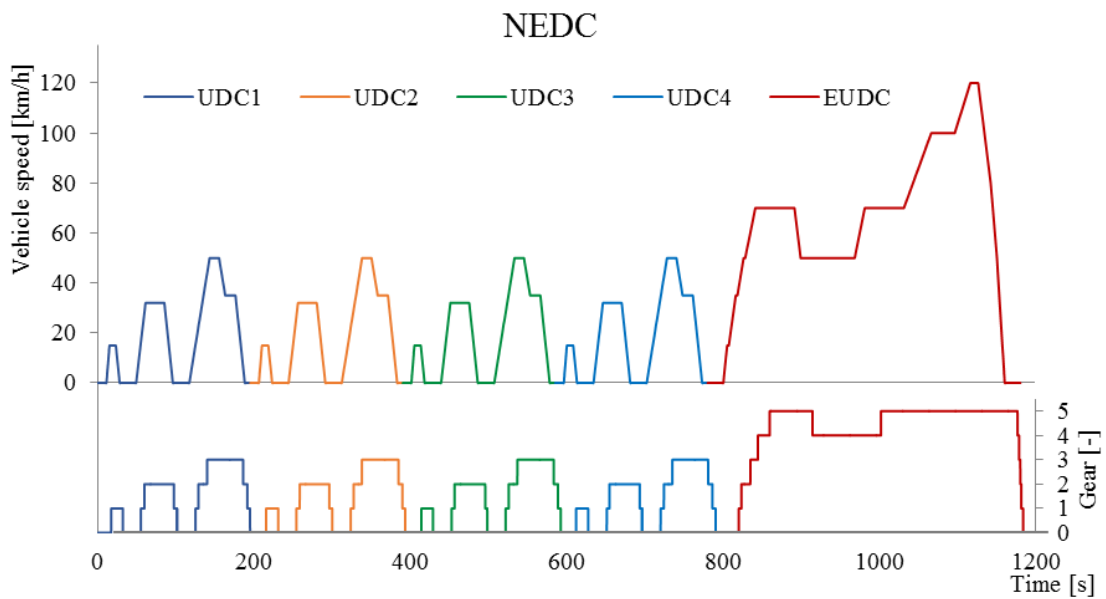


Figure 3.2: Vehicle speed and gear patterns in the NEDC [16]

3.1.2.2 RDE

The RDE cycle taken into account in this analysis was conducted on the roads in the surroundings of Turin under a pre-defined RDE compliant route [20] to completely characterize the powertrain control logic. The mean features are listed in Table 3.3.

Table 3.3: Main characteristics of the RDE cycle

Characteristics	Unit	Urban	Rural	Motorway	RDE
Distance	m	24665	30945	40875	96485
Total time	s	2577	1591	1364	5532
Idle (standing) time	s	389	14	6	409
Average speed (incl. stops)	km/h	34.5	70.0	107.9	62.8
Average speed (excl. stops)	km/h	40.6	70.6	108.4	67.8
Maximum speed	km/h	63.0	90.1	138.1	138.1
Average absolute acceleration	m/s ²	0.381	0.350	0.260	0.343
Maximum absolute acceleration	m/s ²	3.94	4.22	2.92	4.22
Total positive difference in altitude	m	230	241	268	739
Total negative difference in altitude	m	243	133	395	771
Maximum altitude	m	277	359	352	359
Minimum altitude	m	241	243	225	225

The RDE cycle is composed by 3 phases: Urban, Rural and Motorway travelled in that order. The vehicle speed profile and the altitude with respect to the distance is reported in Figure 3.3.

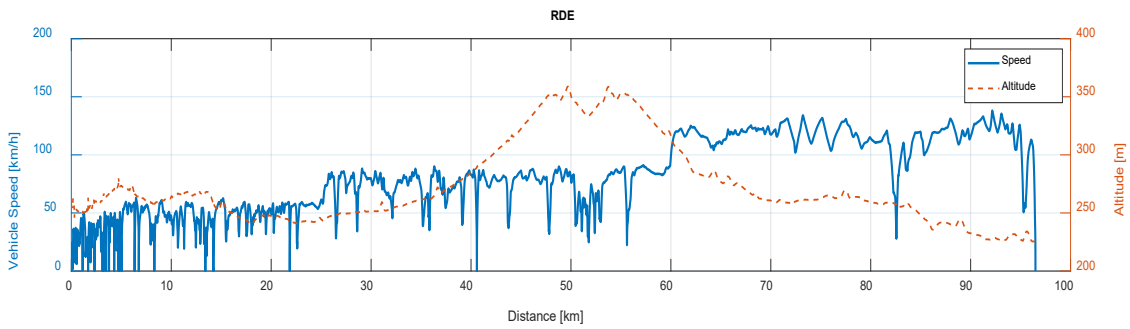


Figure 3.3: RDE speed and altitude profile in function of the distance

3.2 Vehicle Modelling

The development and optimization of an EMS suitable for xHEVs in order to simulate fuel consumption and/or pollutant emissions requires a reliable simulation tool. The development of the energy management strategy of a xHEV is not economically sustainable if performed only experimentally. In fact, a huge number of experimental data is needed for a correct impact evaluation of different energy management strategies for different mission profile. The complexity of xHEVs and the necessity to simulate long driving cycles do not permit the use of detailed models for EMS: look-up tables approaches are usually preferred [42]. However, these approaches with modern powertrain are inadequate: xHEVs with downsized turbocharged engine tested on dynamic cycle and start & stop strategies lead to high dynamic behaviour which cannot be taken into account only with the use of look-up tables approaches [24].

The three most common modelling approaches suitable for EMS development are:

- Backward kinematic approach.
- Quasi static approach.
- Dynamic approach.

In the next section the backward kinematic approach is analysed because is the used in this work, for more info about quasi static and dynamic approaches see [43] or [24].

3.2.1 Backward Kinematic Analysis

The backward kinematic analysis starts from the main vehicle characteristics, the speed of the vehicle and the road grade and go back in a backward kinematic process to the engine speed and to the engine torque through wheel rotation speed and the total transmission ratio (Figure 3.4).

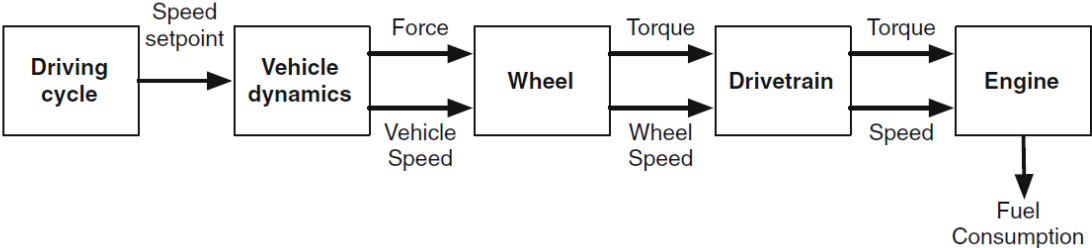


Figure 3.4: Information flow in a backward kinematic analysis [29]

The driving cycle is divided into small steps where all the variables are assumed constant. Instantaneous fuel consumption and emission rate can be found through interpolation of look-up table where they are expressed in function of engine speed and engine torque (or similar quantity like Brake Mean Effective Pressure (BMEP)). All the dynamics are neglected using this approach; in fact, all the input and calculated quantities are considered a sequence of stationary states, so simulation results can differ from the experimental data. Finally, cumulative data are obtained thanks integration over the entire driving cycle (Figure 3.5). To assess only the fuel consumption, the backward kinematic analysis returns acceptable results.

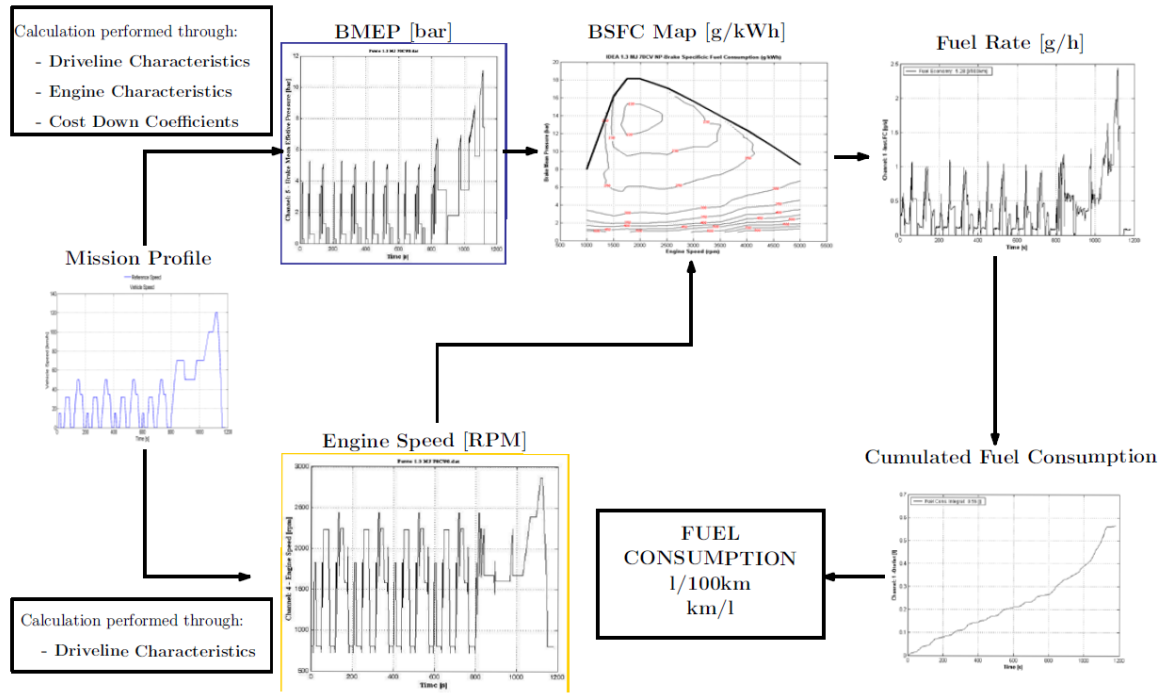


Figure 3.5: Fuel consumption evaluation in a backward kinematic model [24]

The simple formulations used in the backward kinematic model are reported in the following paragraphs.

Wheel rotational speed (ω_{wh}) in a pure rolling condition and inlet of gearbox angular speed (ω_{gb}) are equal to:

$$\omega_{wh} = \frac{v}{r_{wh}} \quad \text{Eq. 3.1}$$

$$\omega_{gb} = \omega_{wh} \cdot i_{fd} \cdot i_{gb} \quad \text{Eq. 3.2}$$

Where:

- v is the longitudinal vehicle speed.
- r_{wh} is the effective wheel rolling radius (equal to 97/98% free wheel radius in normal driving).
- i_{fd} and i_{gb} are respectively the final drive and gearbox gear ratio.

The main forces are calculated as follow:

$$F_{acc} = M_{eq} \cdot a \quad \text{Eq. 3.3}$$

$$F_{res} = f_0 + M_{veh} \cdot g \cdot \sin(\delta) + f_1 \cdot v + f_2 \cdot v^2 \quad \text{Eq. 3.4}$$

$$F_{tot} = F_{acc} + F_{res} \quad \text{Eq. 3.5}$$

Where:

- F_{acc} is the force needed to contrast vehicle inertia.
- M_{eq} is the equivalent mass of the vehicle.
- F_{res} is the force needed to contrast resistance force of motion (i.e. aerodynamic, rolling and road slope forces).
- f_0 , f_1 and f_2 are the coast down coefficients, they summarize aerodynamic and rolling resistance force.
- g is the gravitational force ($g = 9.81 \text{ m/s}^2$).
- M_{veh} is the mass of the vehicle.
- δ is the road inclination.
- F_{tot} is the total force to the wheels.

The equivalent mass is equal to:

$$M_{eq} = M_{veh} + \frac{2 \cdot I_{wh,f} + 2 \cdot I_{wh,r}}{r_{wh}^2} + \frac{I_{ICE}}{r_{wh}^2} \cdot i_{fd}^2 \cdot i_{gb}^2 + \frac{I_{EM}}{r_{wh}^2} \cdot i_{fd}^2 \cdot i_{gb}^2 \quad \text{Eq. 3.6}$$

Where:

- $I_{wh,f}$ and $I_{wh,r}$ is the front and rear wheel inertia respectively.
- I_{ICE} is the ICE inertia.
- I_{EM} is the EM inertia.

The main powers are calculated as follows:

$$P_{gb} = F_{tot} \cdot v \cdot \eta_{gb}^{sign(-F_{tot})} \quad \text{Eq. 3.7}$$

$$P_{dmd} = P_{gb} \quad \text{Eq. 3.8}$$

$$P_{dmd} = P_{gb} - P_{lim,ICE,min} \quad \text{if } P_{gb} < 0 \text{ \& ICE is ON} \quad \text{Eq. 3.9}$$

$$u = \frac{P_{EM}}{P_{EM} + P_{ICE}} \quad \text{Eq. 3.10}$$

$$P_{EM,e} = P_{EM} \cdot \eta_{EM}^{sign(-P_{EM})} \quad \text{Eq. 3.11}$$

$$P_{batt} = P_{EM,e} + P_{el,acc} \quad \text{Eq. 3.12}$$

Where:

- P_{gb} is the gearbox power.
- η_{gb} is the gearbox efficiency.
- P_{dmd} is the power demand from ICE and EM.
- $P_{lim,ICE,min} (< 0)$ is the minimum power of ICE (dragging resistance power).
- u is the power split among ICE and EM ($u = 1$ is the electrical drive).
- P_{EM} is the EM power.
- P_{ICE} is the ICE power.
- $P_{EM,e}$ is the electrical power request or delivered by the EM.
- η_{EM} is the EM efficiency.
- P_{batt} is the request or delivered battery power.
- $P_{el,acc}$ is the power request by electrical accessories.

The SoC:

$$\Delta SoC = \frac{i \cdot t}{cap} \quad \text{Eq. 3.13}$$

$$SoC(t) = \frac{Q(t)}{Q_{max}} = \frac{\int_0^t i(t) dt}{Q_{max}} \quad \text{Eq. 3.14}$$

Where:

- i is the current flowing into or from the battery, $i = \frac{P_{batt}}{V_{batt}}$ where V_{batt} is the battery voltage.
- t is the time.
- cap is the battery capacity.
- $Q(t)$ is the actual battery charge.
- Q_{max} is the maximum battery charge level.

3.2.2 Modelling Tools

The DPM function is an algorithm which finds discrete-time optimal strategy using Bellman's principle of optimality [31]. It is worth saying that the term "time" is to be considered in a general way, in fact the problem discretization can be done time-based or based on another quantity (e.g. distance). In order to utilize DPM function the user has to provide the system model where the model equations (which can be time-variant) and the objective function are reported. Also, the input and state variables can be time-variant. The computational time of the DP algorithm is exponential in the number of input and state variables.

In order to understand how deterministic DP algorithm is implemented in DPM function it gives a brief overview.

We have to solve continuous-time problem; therefore, it must discretize in time first (Eq. 3.15)

$$x_{k+1} = f_k(x_k, u_k) \quad \text{Eq. 3.15}$$

Where:

- $k = 0, 1, \dots, N - 1$ where N is the total number of time step in the time discretized problem.
- x_k is the continuous state variable at discretized time k , $x_k \in X_k$ where X_k is its domain in k .
- u_k is the continuous control variable at discretized time k , $u_k \in U_k$ where U_k is its domain in k .

The time-discretized cost of the policy (also known as cost function or objective function) is reported in Eq. 3.16. The optimal policy has to be selected among the feasible ones, and will give a solution by minimizing (or maximizing) over an entire driving cycle the cost J reported in Eq. 3.17.

The DP algorithm is founded on the Bellman's principle of optimality therefore DP proceeds backward, from the last time step to the first (Eq.3.18).

$$J_{\pi_0}(x_0) = g_N(x_N) + \Phi_N(x_N) + \sum_{k=0}^{N-1} h_k(x_k, \mu_k(x_k)) + \Phi_k(x_k) \quad \text{Eq. 3.16}$$

$$J^*(x_0) = \min_{\pi_0 \in \Pi_0} J_{\pi_0}(x_0) \quad \text{Eq. 3.17}$$

$$J_{\pi_i}(x_i) = g_N(x_N) + \Phi_N(x_N) + \sum_{k=i}^{N-1} h_k(x_k, \mu_k(x_k)) + \Phi_k(x_k) \quad \text{Eq. 3.18}$$

Where:

- $\pi_0 = \{\mu_0, \mu_1, \dots, \mu_{N-1}\}$ is the control policy over the N time step.

- $J_{\pi_0}(x_0)$ is the time discretized cost using the control policy π_0 starting at initial conditions x_0 .
- $g_N(x_N) + \Phi_N(x_N)$ is the total final cost, where $g_N(x_N)$ is the final cost and $\Phi_N(x_N)$ is a penalty function to apply a constrain on the final state to the state variable.
- $h_k(x_k, \mu_k(x_k)) + \Phi_k(x_k)$ is the total instantaneous cost function (also called *arc cost*) of applying the policy μ_k at x_k where $h_k(x_k, \mu_k(x_k))$ is the instantaneous cost function and $\Phi_k(x_k)$ is a penalty function to apply a constrain to the state variable at x_k .
- $J^*(x_0)$ is the optimal policy at initial conditions x_0 .
- $\pi_0^* = \{\mu_0^*, \mu_1^*, \dots, \mu_{N-1}^*\}$ is the corresponding optimal control policy over the N time step.
- Π_0 is the set of feasible policies from initial time step.
- $\pi_i = \{\mu_i, \mu_{i+1}, \dots, \mu_{N-1}\}$ is the control policy over the “tail sub-problem”.
- $J_{\pi_i}(x_i)$ is the time discretized cost using the control policy π_i starting at initial conditions x_i .

The optimal policy is firstly found for the final part of the “tail sub-problem” (Eq. 3.19) and then it is gradually extended to the previous time steps. Applying Bellman’s principle of optimality, the optimal policy for the “tail sub-problem” is the “tail policy” $\pi_i^* = \{\mu_i^*, \mu_{i+1}^*, \dots, \mu_{N-1}^*\}$ of the entire problem optimal policy π_0^* :

$$J^*(x_i) = \min_{\pi_i \in \Pi_i} J_{\pi_i}(x_i) \quad \text{Eq. 3.19}$$

Where:

- $J^*(x_i)$ is the optimal policy at initial conditions x_i .
- $\pi_i^* = \{\mu_i^*, \mu_{i+1}^*, \dots, \mu_{N-1}^*\}$ is the corresponding optimal control policy for the “tail sub-problem”.
- Π_i is the set of feasible policies for the “tail sub-problem”.
- $J_{\pi_i}(x_i)$ is the time discretized cost using the control policy π_i starting at initial conditions x_i .

Now state and input variable discretizations are introduced. It proceeds backward to generate the optimal cost-to-go function ($Y_k(x_k^i)$) at every node in the discretized state-time space [31]. Therefore, the output of the algorithm (Eq. 3.20/Eq. 3.21) is the optimal control signal map that is given by the argument that minimizes Eq. 3.19 for each state x_k^i of the discretized state-time space [29][31]:

For end step ($k = N$):

$$Y_N(x_N^i) = g_N(x_N^i) + \Phi_N(x_N^i) \quad \text{Eq. 3.20}$$

Where:

- $Y_N(x_N^i)$ is the last time step cost-to-go function, x_N^i is the discretized state variable with state-index i at discretized time N .
- $g_N(x_N^i) + \Phi_N(x_N^i)$ is the total final cost, where $g_N(x_N^i)$ is the final cost and $\Phi_N(x_N^i)$ is a penalty function to apply a constrain on the final state to the state variable.

For intermediate step ($k = N - 1$ to 0):

$$Y_k(x_k^i) = \min_{u_k \in U_k} \{h_k(x_k^i, u_k) + \Phi_k(x_k^i) + Y_{k+1}(f_k(x_k^i, u_k))\} \quad \text{Eq. 3.21}$$

Where:

- $Y_k(x_k^i)$ is the cost-to-go function, x_k^i is the discretized state variable with state-index i at discretized time k .
- $h_k(x_k^i, u_k) + \Phi_k(x_k^i)$ is the total instantaneous cost function where $h_k(x_k^i, u_k)$ is the instantaneous cost function and $\Phi_k(x_k^i)$ is a penalty function to apply a constrain to the state variable at x_k^i .
- $Y_{k+1}(f_k(x_k^i, u_k))$ is the cost-to-go function from time $k + 1$, is evaluated on discretized points in the state grid. $f_k(x_k^i, u_k)$ is the output of the model function, it is continuous in the state space, therefore the cost-to-go function must be evaluated correctly because can be among the nodes: in the DPM function is used linear

interpolation; the computational cost of this linear interpolation is neglectable due to the equally spaced state and input grids.

The optimal control signal map is used to find the optimal u_k during the forward simulation, to create the optimal state trajectory. As mentioned above, the control signal is discretized, therefore in the optimal control signal map, the control signal must be interpolated if the actual state does not be equal to the discretized point of the state grid.

3.3 Distance-based Model

For implementing the optimization model, based on DP to ensure global optimality, the model equations are expressed and discretized in distance-based coordinates. The independent variable used in this approach is distance, instead of time, which is usually used. This change ensures an appropriate handling of route features e.g. traffic lights, stop signs, speed limits, elevation data: which position remain fixed in distance-based coordinates. If a HEV is considered, in order to minimize the fuel consumption over a given route using route information, the optimizer have to jointly decide the optimal vehicle speed profile and the EMS (the power split), satisfying for each step state-dependent and route dependent constraints, described from Eq. 3.22 to Eq. 3.27.

$$v_{min}(k_i) \leq v(k_i) \leq v_{max}(k_i) \quad \text{Eq. 3.22}$$

$$SoC_{min}(k_i) \leq SoC(k_i) \leq SoC_{max}(k_i) \quad \text{Eq. 3.23}$$

$$P_{ICE,min}(k_i) \leq P_{ICE}(k_i) \leq P_{ICE,max}(k_i) \quad \text{Eq. 3.24}$$

$$P_{EM,min}(k_i) \leq P_{EM}(k_i) \leq P_{EM,max}(k_i) \quad \text{Eq. 3.25}$$

$$a_{min}(k_i) \leq a(k_i) \leq a_{max}(k_i) \quad \text{Eq. 3.26}$$

$$SoC(k_0) = SoC(k_N) \quad \text{if PHEV in CS mode} \quad \text{Eq. 3.27}$$

Where:

- v_{min} and v_{max} are lower and upper speed limit.
- SoC_{min} and SoC_{max} are lower and upper SoC limit.
- $P_{ICE,min}$ and $P_{ICE,max}$ are lower and upper ICE power, the first is negative and it is equal to the maximum power absorbed by the ICE in dragging mode, the last is obviously positive both are function of ICE rotational speed.
- $P_{EM,min}$ and $P_{EM,max}$ are the lower and upper EM power, the first is negative and it is equal to the maximum power absorbed by the EM when it works like a generator, the last is positive and it is equal to the maximum power provided by the EM when it works like a motor.
- a_{min} and a_{max} are the minimum and maximum acceleration permitted.

In the distance-based model the cost plays a key role: it is the quantity to be minimized globally. In the above-mentioned problem, the cost function is expressed as defined in Eq. 3.28

$$C = \alpha \cdot \frac{dx}{X} + (1 - \alpha) \cdot \frac{dt}{T} \quad \text{Eq. 3.28}$$

Where:

- X is the total quantity of interest in the reference cycle to be minimized for a given travel time; in our analysis the reference cycle is the NEDC or the RDE cycle, as it will be described in the following sections. X can be ΔSoC , fuel consumption or energy depending on the vehicle under analysis. dx the same quantity of X evaluated on a single distance step of the optimization problem.
- $\alpha \in (0,1)$ is a weighting factor which gives much or less importance to travel time with respect to the quantity to be minimized: the trade-off between the two quantities depend on the tuning of this factor.

- T is the total travel time of the reference cycle, while dt is the time taken on each step of the driving cycle.

The weighting factor α has the function to obtain a non-banal solution and the dt and dx are normalized with respect to the quantity in the non-optimal initial problem so that the two terms can be comparable.

Speed optimization V2X

In a first analysis the stops are imposed where the speed of the analysed cycle is zero and the duration of each stop is equal to the mean stop time of the initial cycle. In order to take into account V2X communication, it was also performed an analysis where it is considered the possibility to skip the stops in the cycle under analysis. More in detail, the generic cycle stop is supposed to be a traffic light intersection where in case of green sign there are not a stop constraint, an example is reported in Figure 4.7.

Furthermore, an infeasibility was introduced to make the vehicle stop only at a traffic light with a red signal. The phases are randomly assigned while red and green durations for all traffic lights are equal to 40 and 20 seconds respectively. The phases and the traffic light timing are identical for a given cycle for all the three cases in the sensitivity analysis described in the following sections.

3.3.1 PHEV Final Drive Energy Minimization

In this case study the optimization is performed until final drive. The simulation goal is to find the optimal speed profile within speed limits that permit to minimize the cost function (Eq. 3.29), therefore reduce the positive energy at final drive level for a given travel time:

$$C = \alpha \cdot \frac{dE_{fd}}{E_{fd}} + (1 - \alpha) \cdot \frac{dt}{T} \quad \text{Eq. 3.29}$$

Where:

- dE_{fd} is the positive energy at final drive level at each step of the driving cycle and E_{fd} is the total final drive positive energy along the entire reference cycle.

The state variable is the vehicle speed, the control variable is the acceleration.

3.3.1.1 PHEV Final Drive Energy Minimization V2X

The V2X communication impacts on the model complexity: the time and the vehicle speed are the state variables while the control variable remains the acceleration. In order to reduce computational time, state variables changeable grids assume a key role: it is imposed an upper and a lower limit that can be different for each distance step. In particular the time grid was chosen in order to not influence the output: the travel time function of distance must be sufficiently distant for each distance step from the time limits, an example is reported in Figure 4.9. The speed grid changes according to the less restrictive upper and lower speed limit, an example is reported in Figure 4.7. Both state variables grids and control variable grid are equally spaced. The computational time comparison between fixed grid and variable grid for the analysed cycles is reported in Table 3.4.

Table 3.4: Computational time comparison between fixed grid and variable grid in PHEV final drive energy minimization model

Parameter	Cycle	Unit	Fixed grid	Variable grid
Computational time	UDC	[min]	43.0	6.6
Computational time	Urban RDE	[min]	194.3	20.5
Processor: Intel(R) Core(TM) i7-1065G7 CPU @ 1.30GHz 1.50 GHz RAM: 16 GB				

3.3.2 CV Fuel Minimization

In this model the entire vehicle is taken into account and its fuel consumption is minimized. Starting from the previous case study, a CV was created, featuring the ICE of the PHEV. The simulation goal is to find the optimal speed profile within speed limits that permit to minimize the cost function (Eq. 3.30), therefore enhance fuel economy for a given travel time:

$$C = \alpha \cdot \frac{dm_f}{m_f} + (1 - \alpha) \cdot \frac{dt}{T} \quad \text{Eq. 3.30}$$

Where:

- dm_f is the fuel consumption on each step of the driving cycle and m_f is the total fuel burned along the entire reference cycle.

In order to obtain a fuel consumption, the ICE rotational speed is needed. Since the gear optimization would have excessively increased the computational burden of the model, a simple rule-based logic was modelled for gear selection. The rule-based gear selection is based on a severe ICE under speeding: the shifting to a higher gear is allowed when, for the new gear, the rotational speed at the gearbox inlet is slightly greater than 1000 rpm. Similarly, the shifting to a lower gear is allowed when, for the new gear, the rotational speed at the gearbox inlet is slightly greater than 1000 rpm. Rule-based gear selection avoid a more model complexity which leads to a higher computational cost, unsustainable in case of CV fuel minimization V2X.

The state variable is the vehicle speed, the control variable is the acceleration.

3.3.2.1 CV Fuel Minimization V2X

Similarly PHEV Final Drive Energy Minimization V2X model, the computational cost is reduced thanks to variable grid of state variables. The same considerations already done in section 3.3.1.1, can be repeated. The computational time comparison between fixed grid and variable grid for the analysed cycles is reported in Table 3.5.

Table 3.5: Computational time comparison between fixed grid and variable grid in CV fuel minimization model

Parameter	Cycle	Unit	Fixed grid	Variable grid
Computational time	UDC	[min]	30.5	4.7
Computational time	Urban RDE	[min]	284.1	30
Processor: Intel(R) Core(TM) i7-1065G7 CPU @ 1.30GHz 1.50 GHz RAM: 16 GB				

3.3.3 BEV Δ SoC Minimization

In this model is taken into account the entire vehicle. Starting from the initial case study, a BEV was created, featuring the electrical side of the PHEV powertrain. The simulation goal is to find the optimal speed profile within speed limits that permit to minimize the cost function (Eq. 3.31), therefore minimize the difference between initial and final SoC for a given travel time:

$$C = \alpha \cdot \frac{dSoC}{\Delta SoC} + (1 - \alpha) \cdot \frac{dt}{T} \quad \text{Eq. 3.31}$$

Where:

- $dSoC$ is the SoC consumption on each step of the driving cycle and $\Delta SoC = SoC_i - SoC_f$, where SoC_i is the initial and SoC_f is the final SoC of the non-optimal initial cycle.

The two main difference between PHEV and BEV specifications are:

- **BEV gearbox:** the BEV is modelled with only 1-speed transmission, where gear ratio is defined in Eq. 3.32. Overall transmission efficiency is imposed equal to 0.9.

$$i_{gb} = \frac{\omega_{EM,max}}{\omega_{wh,max} \cdot i_{fd}} \quad \text{Eq. 3.32}$$

Where:

- $\omega_{EM,max}$ is the maximum EM rotational speed, $\omega_{EM,max} = 5000 \text{ rpm}$.
 - $\omega_{wh,max}$ is the maximum wheel rotational speed, $\omega_{wh,max} = v_{veh,max}/r_{wh}$ where $v_{veh,max}$ is the maximum vehicle speed imposed equal to 160 km/h and r_{wh} is the wheel radius.
 - i_{fd} is the final drive gear ratio.
- **BEV battery:** the battery is scaled in order to increase the range. The BEV battery specifications are reported in Table 3.6.

Table 3.6: BEV battery specifications

HV Battery	
Type	Li-NMC
Rated Voltage	365 V
Capacity	54 kWh / 37 Ah
Number of Cell in Parallel	4
Number of String	63
Cooling System	Water Cooled

It is worth mentioning that in this model it is also considered the regenerative braking, therefore during deceleration the battery is charged. In order to take into account the regeneration, it is introduced the regenerative braking mechanical efficiency created from PHEV experimental data. The efficiency is a 2D map, function of vehicle speed and deceleration.

The state variable is the vehicle speed and SoC, the control variable is the acceleration. Therefore, the SoC become the second state variable, it is due to the SoC dependency of battery variables, i.e. the battery discharge and charge resistances, the open circuit voltage and maximum and minimum battery current.

In this work the V2X analysis for the BEV has not been performed due to the high computation time effort.

4. Results

4.1 Speed optimization for PHEV Final Drive Energy Minimization

4.1.1 NEDC

The NEDC, reported in the following paragraphs, was mainly used for debugging thanks to its simplicity. In the UDC the upper and the lower speed limit are set according from Eq. 4.1 to Eq. 4.5.

$$v_{min} = 0.8 \cdot v_{NEDC} \quad \text{if } a = 0 \quad \text{Eq. 4.1}$$

$$v_{min} = 0 \text{ km/h} \quad \text{if } a \neq 0 \text{ or } v_{NEDC} = 0 \quad \text{Eq. 4.2}$$

$$v_{max} = 1.2 \cdot v_{NEDC} \quad \text{if } a = 0 \quad \text{Eq. 4.3}$$

$$v_{max} = 60 \text{ km/h} \quad \text{if } a \neq 0 \quad \text{Eq. 4.4}$$

$$v_{max} = 0 \text{ km/h} \quad \text{if } v_{NEDC} = 0 \quad \text{Eq. 4.5}$$

For the EUDC the only difference is reported in Eq. 4.6.

$$v_{max} = 135 \text{ km/h} \quad \text{if } a \neq 0 \quad \text{Eq. 4.6}$$

Where:

- v_{min} and v_{max} are lower and upper speed limit.
- v_{NEDC} is the NEDC speed.

- a is the vehicle acceleration in the NEDC.

Therefore:

- In constant speed parts the speed must be within $\pm 20\%$ of reference cycle.
- During accelerations or decelerations no restrictive speed constraints are imposed.
- The stops are imposed.

The stop time of each stop is equal to 21 seconds, id est the mean time stop on the NEDC.

This leads to the limits reported in Figure 4.1.

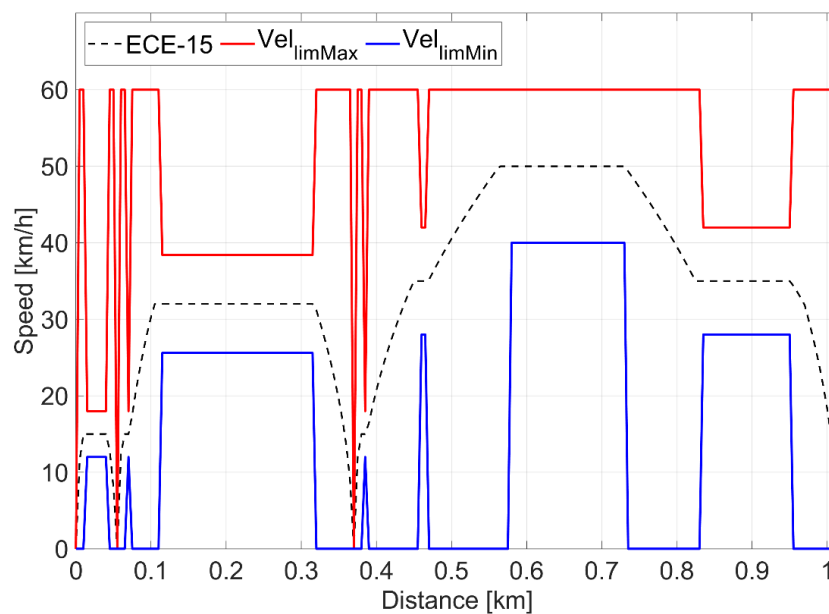


Figure 4.1: Speed limits for the first ECE-15

A sensitivity analysis on the NEDC was performed by means of a different cost function parameter α in Eq. 3.29: the value of α for the different cases is shown in Table 4.1.

Table 4.1: Cost function parameter for the sensitivity analysis

Parameter	Case 1	Case 2	Case 3
α	0.2	0.5	0.8

Therefore, as shown in Figure 4.2, a value of α closer to 0 leads to a greater importance to travel time, at the expense of energy consumption (Case 1), a value closer to 1 gives more importance to energy minimization (Case 3) and an intermediate value of α gives a similar weight to both (Case 2).

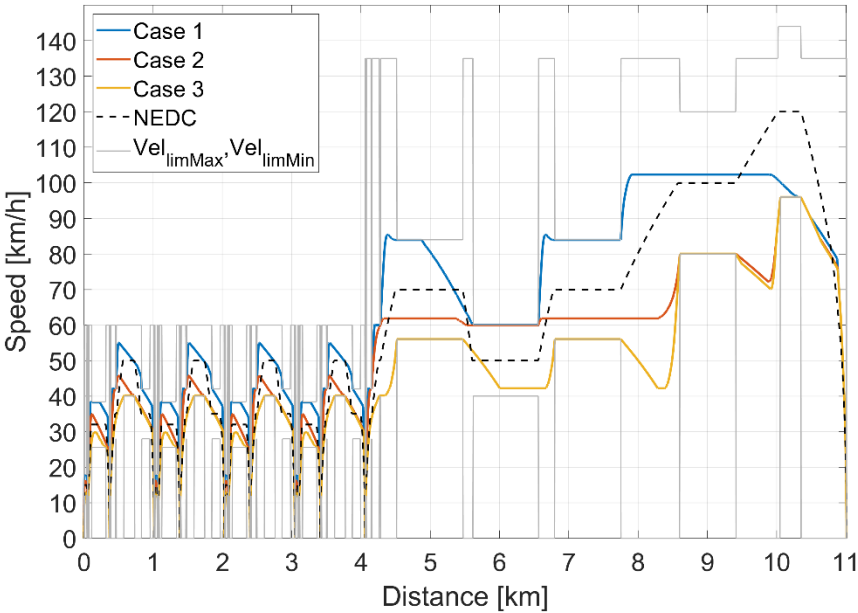


Figure 4.2: Vehicle speed profile with different values of cost function parameter, for the NEDC performed with a PHEV

The Case 1 which is characterized by a minor cost function parameter has a higher speed globally, respecting all the speed constrains. A zoom on the first ECE-15, to understand speed profiles differences between the three cases, is shown in Figure 4.3. Generally, on the UDC, it can be seen that the optimization chooses a coasting trend of the vehicle speed.

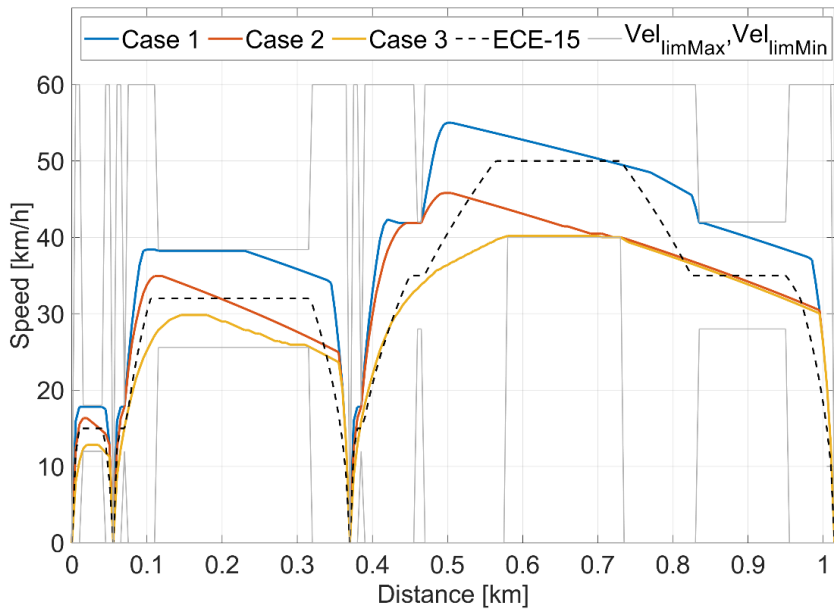


Figure 4.3: Vehicle speed profile with different values of cost function parameter, for the first ECE-15 performed with a PHEV

In Figure 4.4 the travel time for the three cases, along with the one for the reference cycle, is plotted against the travelled distance.

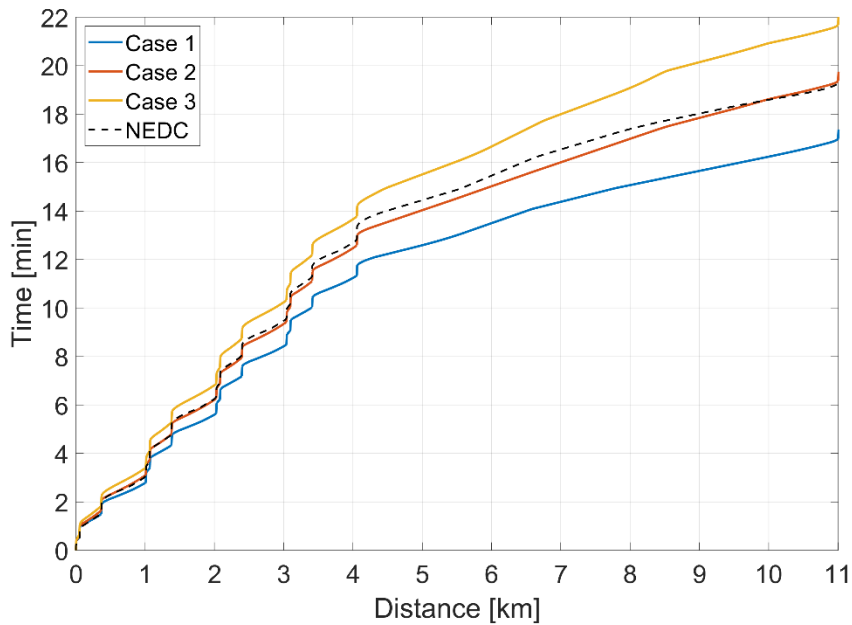


Figure 4.4: Travel time with different values of cost function parameter, for the NEDC performed with a PHEV

Then, the final drive positive energy request is shown in Figure 4.5. In all the three cases, the positive energy request is lower than the reference cycle: the major energy economy is

obtained for the Case 3. Regarding the travel time, for the Case 1 is lower than the NEDC, for the Case 2 is comparable and for the Case 3 is higher. The final values of this analysis are reported in Table 4.2.

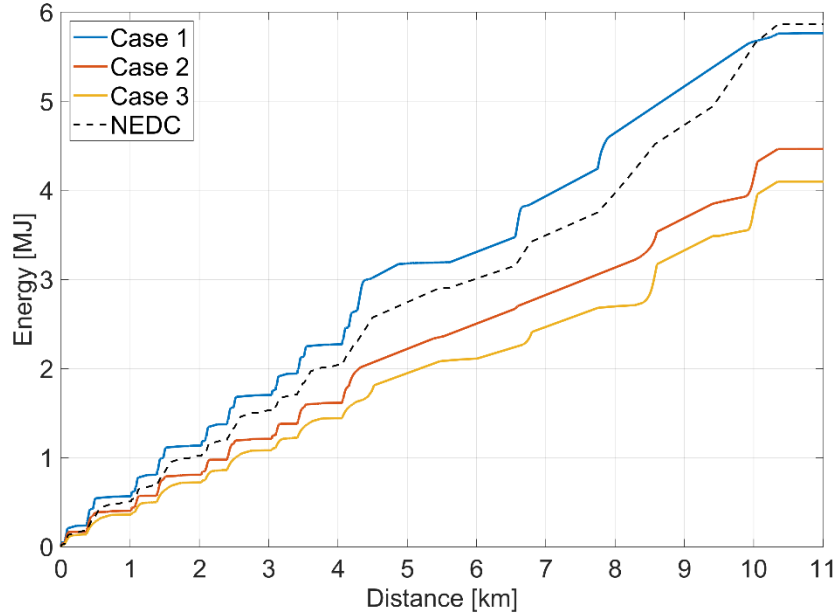


Figure 4.5: Final drive positive energy request with different values of cost function parameter, for the NEDC performed with a PHEV

Table 4.2: Total travel time, final drive positive energy request and final drive positive energy request per kilometre with different values of cost function parameter, for the NEDC performed with a PHEV

Parameter	Unit	NEDC	Case 1	Case 2	Case 3
Total travel time	[s]	19.7	17.4	17.8	22.1
Final drive positive energy request	[MJ]	5.86	5.76	4.46	4.10
Final drive positive energy request per kilometre	[MJ/km]	0.53	0.52	0.41	0.37

It is important to report the trade-off between the total positive energy request at final level and the total travel time for the eco-driving sensitivity analysis and compare the results to the reference fixed-speed cycle. As show in Figure 4.6, the three cases form an equilateral hyperbola, typical geometric place of trade-off plots and they move towards

the origin of the axes. Therefore, the solutions have a best trade-off with respect to the NEDC.

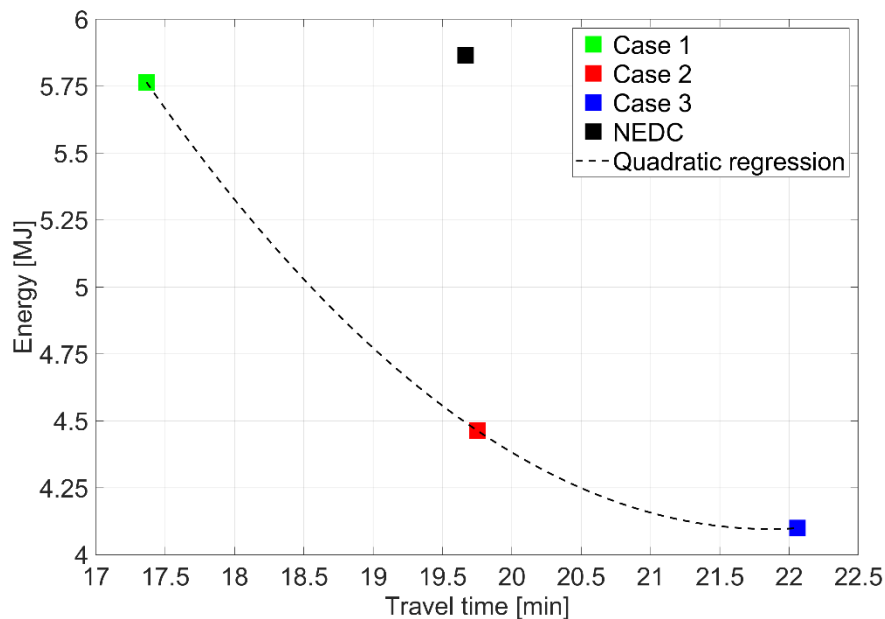


Figure 4.6: Trade-off between positive energy request at final level and travel time with different values of cost function parameter, for the NEDC performed with a PHEV

4.1.1.1 NEDC V2X

As mentioned in section 3.3, in order to take into account V2X communication, it was also performed an analysis where it is considered the possibility to skip the stops in the NEDC. The generic cycle stop is supposed to be a traffic light intersection where in case of green sign there are not a stop constraint.

In the NEDC with V2X communication the maximum speed limits are:

- **With red sign:** equal to the maximum speed limit previously defined.
- **With green sign:** equal to the maximum speed limit previously defined except for the traffic light where it is imposed to 60 km/h.

The minimum speed limit is equal to the lower limit previously defined. In this section only the results obtained for the UDC will be shown since it is the most interesting part for this type of analysis: in fact, the EUDC does not contain any additional stop.

The speed limits for the first ECE-15 are reported in Figure 4.7.

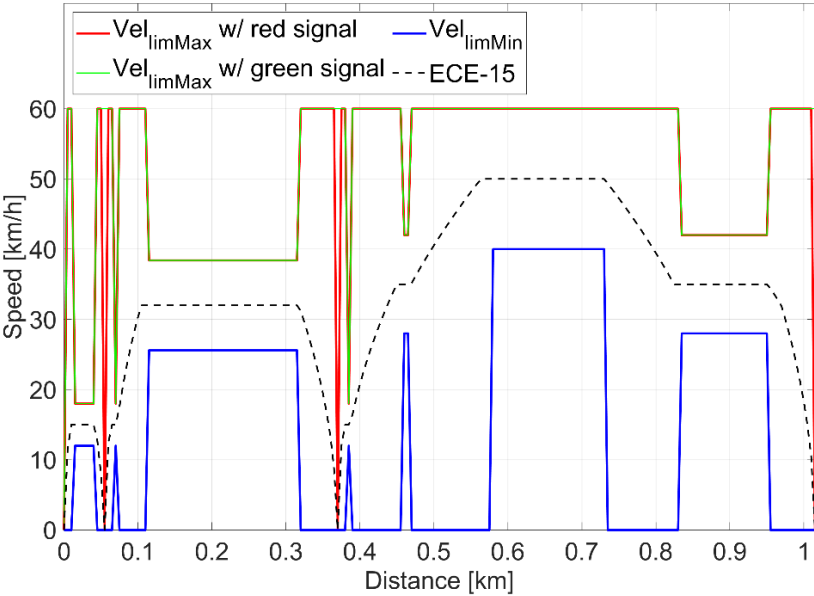


Figure 4.7: Speed limits with red or green signal for the first ECE-15

The speed profiles for the sensitivity analysis are reported in Figure 4.8. As shown, there are not substantial differences until the last traffic light: it is due to the presence of identical traffic light signal among the three cases, the problem constrains (e.g. speed, acceleration) and the relative long signal timing compared to the limited distance between traffic lights.

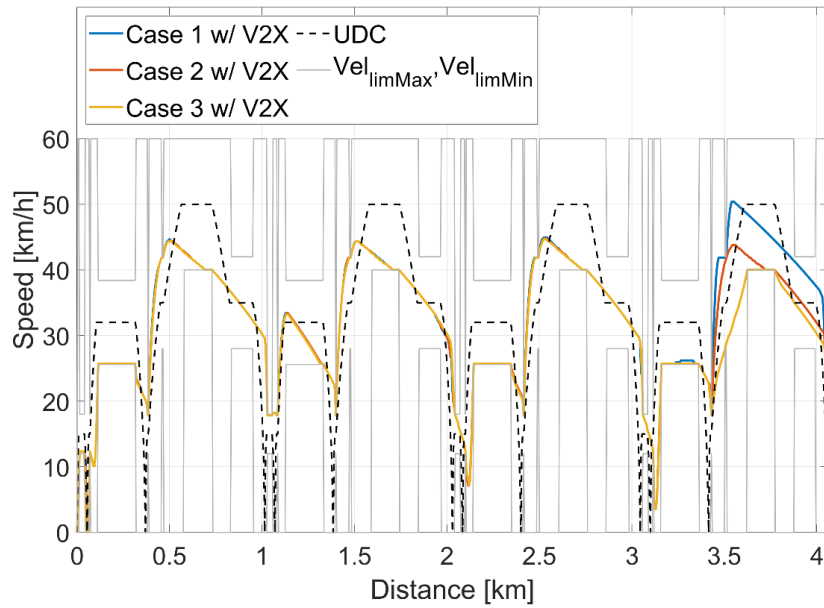


Figure 4.8: Vehicle speed profile with different values of cost function parameter, for the UDC with V2X communication performed with a PHEV

The travel time function of distance is shown in Figure 4.9. It is also reported the time limits: as mentioned above, they were necessary to reduce the computational cost of the problem; in order to not influence the output, they must be sufficiently distant for each distance step of each case from the time limits.

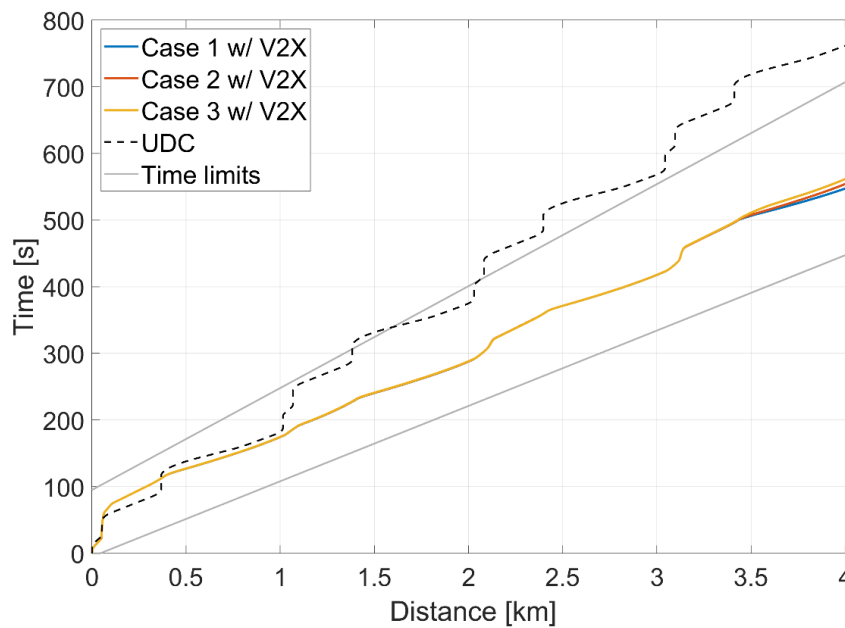


Figure 4.9: Travel time with different values of cost function parameter, for the UDC with V2X communication performed with a PHEV

Then, the final drive positive energy request is shown in Figure 4.10. The final values of this analysis are reported in Table 4.3.

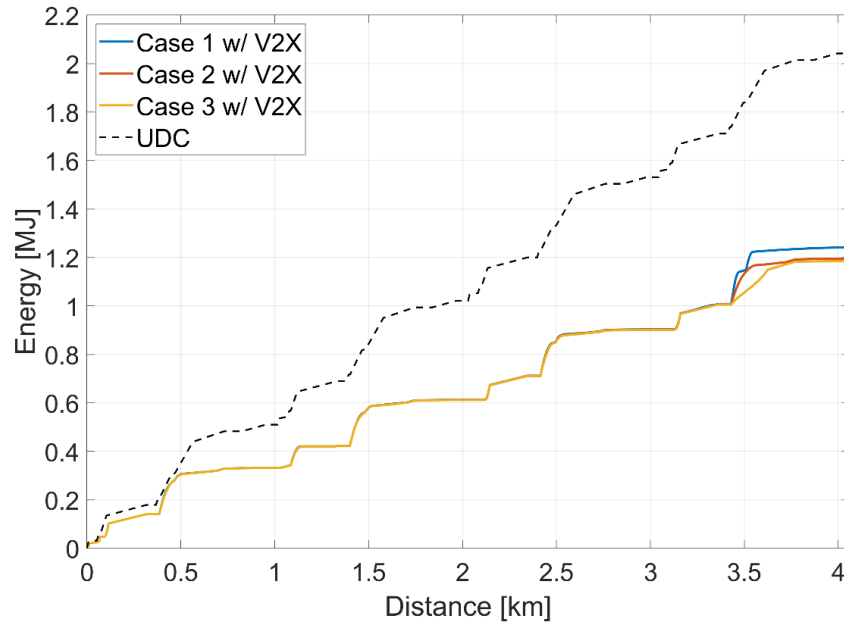


Figure 4.10: Final drive positive energy request with different values of cost function parameter, for the UDC with V2X communication performed with a PHEV

Table 4.3: Total travel time, final drive positive energy request and final drive positive energy request per kilometre with different values of cost function parameter, for the UDC with V2X communication performed with a PHEV

Parameter	Unit	UDC	Case 1 w/ V2X	Case 2 w/ V2X	Case 3 w/ V2X
Total travel time	[s]	773	555	563	571
Final drive positive energy request	[MJ]	2.04	1.24	1.20	1.18
Final drive positive energy request per kilometre	[MJ/km]	0.50	0.31	0.30	0.29

A comparison among different optimizations with a fixed value of cost function, equal to Case 2 (i.e. $\alpha = 0.5$), is shown in Figure 4.11, Figure 4.12 and Figure 4.13. The speed profile under the name “DP w/ V2X” is identical to the Case 2 in Figure 4.8, the ones called “UDC optimized” is the Case 2 reported in Figure 4.2. Since these profiles are not comparable (only the DP w/V2X has the possibility to skip the stop if finding the green sign), an

additional model was created, the “DP w/o V2X”, allowing to properly compare the model with and without V2X communication. The “DP w/o V2X” is identical to “UDC optimized” except from the stops: the vehicle will eventually stop or not depending on the initial random phase of the traffic lights in the V2X communication (Figure 4.14). In this case the stop time is equal to the remaining time of the first red signal.

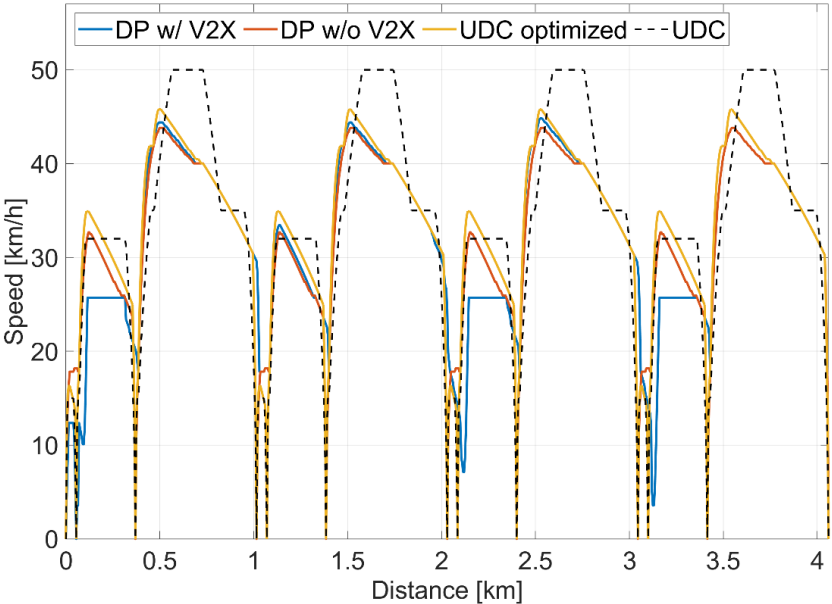


Figure 4.11: Vehicle speed profile comparison among different optimizations with a fixed value of cost function parameter, for the UDC performed with a PHEV

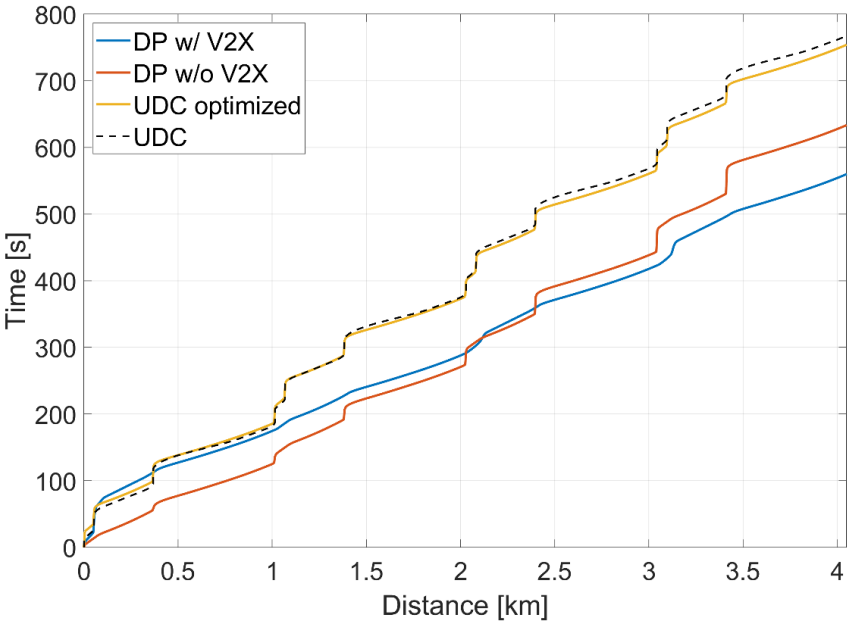


Figure 4.12: Travel time comparison among different optimizations with a fixed value of cost function parameter, for the UDC performed with a PHEV

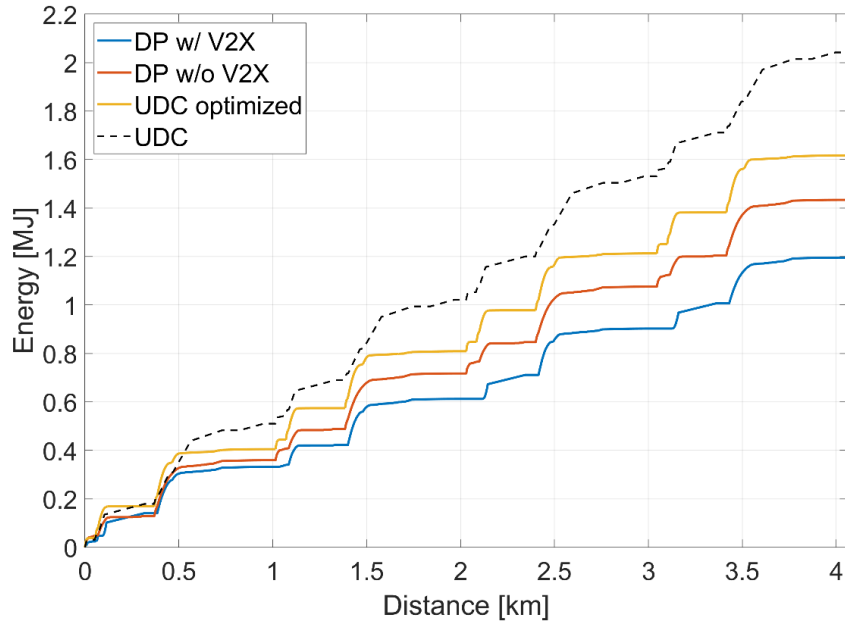


Figure 4.13: Final drive positive energy request comparison among different optimizations with a fixed value of cost function parameter, for the UDC performed with a PHEV

Therefore, the model with V2X communication needs less energy and at the same time takes less time to cover the route.

In Figure 4.14 the vehicle speed profile is shown for the model with and without V2X communication and the traffic light signal at the traffic light intersections. For the sake of clarity, in Figure 4.15 and Figure 4.16 only the model with V2X is reported: as it can see, in order to minimize the energy request and the travel time, when V2X communication are available, the optimizer is able to optimize the vehicle speed in order to catch green at traffic lights. The final values of the model with and without V2X communication are reported in Table 4.4. Figure 4.16 shows traffic light signals and travel time in a time-distance graph for the Case 2 with V2X: the vehicle can overcome the traffic light only when it catches the green signal; it can also be seen clearly the random phases.

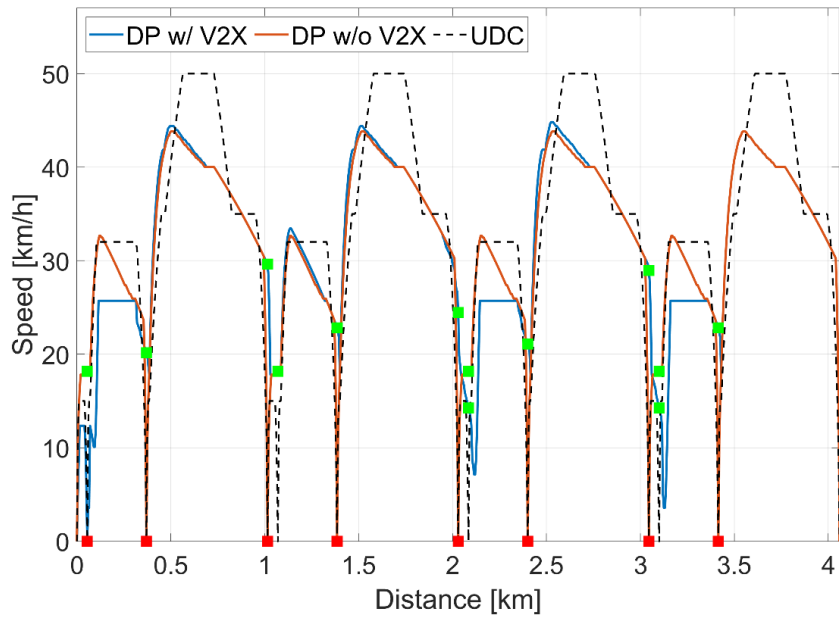


Figure 4.14: Vehicle speed profile comparison among the UDC with and without V2X communication and traffic light signal with a fixed value of cost function parameter, performed with a PHEV

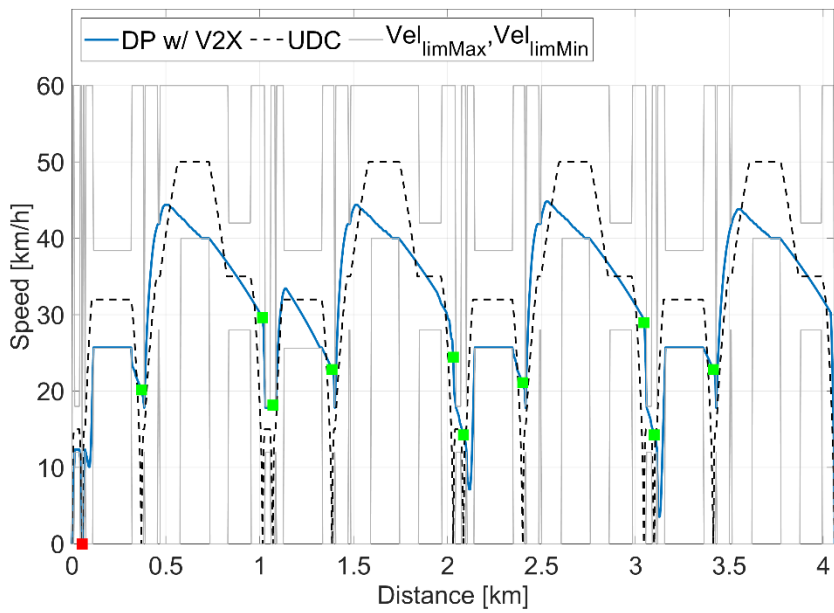


Figure 4.15: Vehicle speed profile and traffic light signal with a fixed value of cost function parameter, for UDC with V2X communication performed with a PHEV

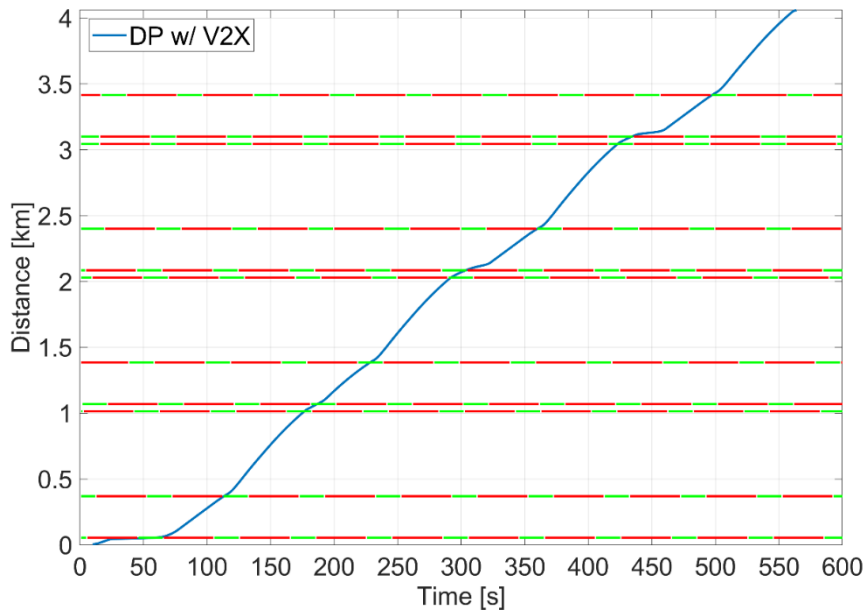


Figure 4.16: Traffic light signals and travel time in a time-distance graph with a fixed value of cost function parameter, for the UDC with V2X communication performed with a PHEV

Table 4.4: Total travel time, final drive positive energy request and final drive positive energy request per kilometre, comparison among the UDC with and without V2X communication with a fixed value of cost function parameter, performed with a PHEV

Parameter	Unit	Case 2 w/o V2X	Case 2 w/ V2X
Total travel time	[s]	636	563
Final drive positive energy request	[MJ]	1.43	1.20
Final drive positive energy request per kilometre	[MJ/km]	0.35	0.30

The trade-off between the total positive energy request at final level and the total travel time for the eco-driving sensitivity analysis for the UDC with and without V2X communication are reported in Figure 4.17. The UDC with V2X communication has a best trade-off with respect to UDC without V2X.

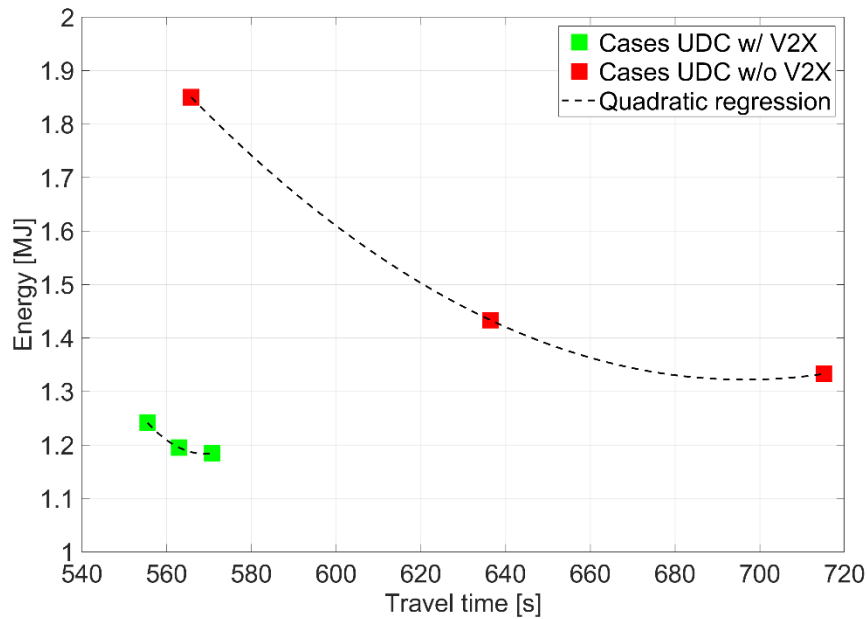


Figure 4.17: Trade-off between positive energy request at final level and travel time for the UDC with and without V2X communication with different values of cost function parameter, performed with a PHEV

4.1.2 RDE

As already stated, the NEDC was mainly used for model debugging. In order to obtain more interesting results, the same methodology was applied to a real-world cycle. In particular the RDE cycle respecting all the RDE test requirement described in section 3.1.2.2 was taken into account. For the RDE cycle the speed limits are:

- **The maximum speed limit** is equal to a moving average of the experimental speed (over an interval of 500 meters) incremented of 20 km/h; the upper limit is saturated to 135 km/h; at the stop the maximum limit is equal to 0 km/h. The limit was chosen in order to have realistic results: the experimental data were considered as a sort of mean speed value of that route taking into account mean traffic and road features (e.g. road signal, curves, slope) and the moving average is necessary in order to smooth the speed limits.

- **The minimum speed limit** is equal to a moving average of the experimental speed (over an interval of 500 meters) decremented of 20 km/h; a 0 km/h limit is imposed 100 meters before and after each stop in order to allow the vehicle stop.

The speed limits for the first part of RDE cycle is reported in Figure 4.18.

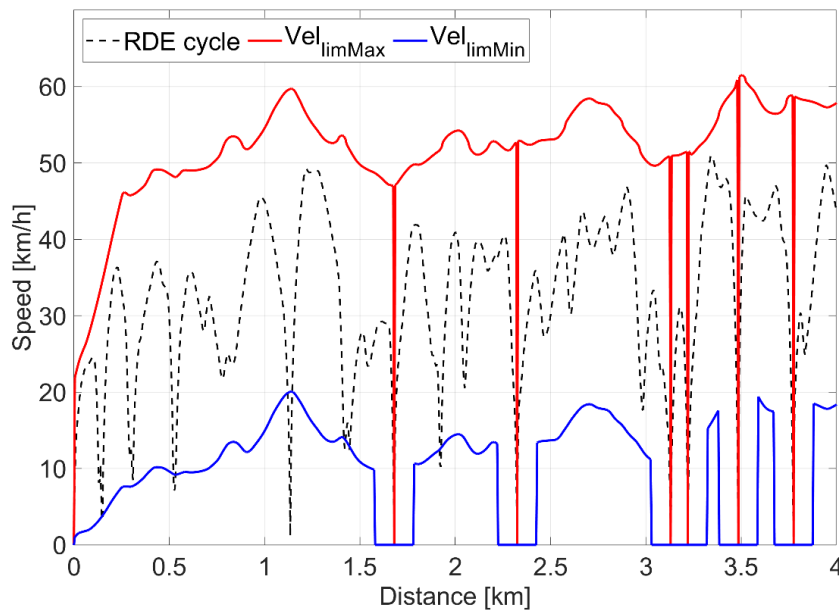


Figure 4.18: Speed limits for the initial part of the RDE cycle

As reported for the NEDC, also for the RDE cycle a sensitivity analysis was performed by means of a different cost function parameter α in Eq. 3.29: the value of α for the different cases is shown in Table 4.1.

Speed profiles for the entire RDE cycle are reported in Figure 4.19 and a zoom of the initial part of urban and rural parts are shown in Figure 4.20 and Figure 4.21, respectively.

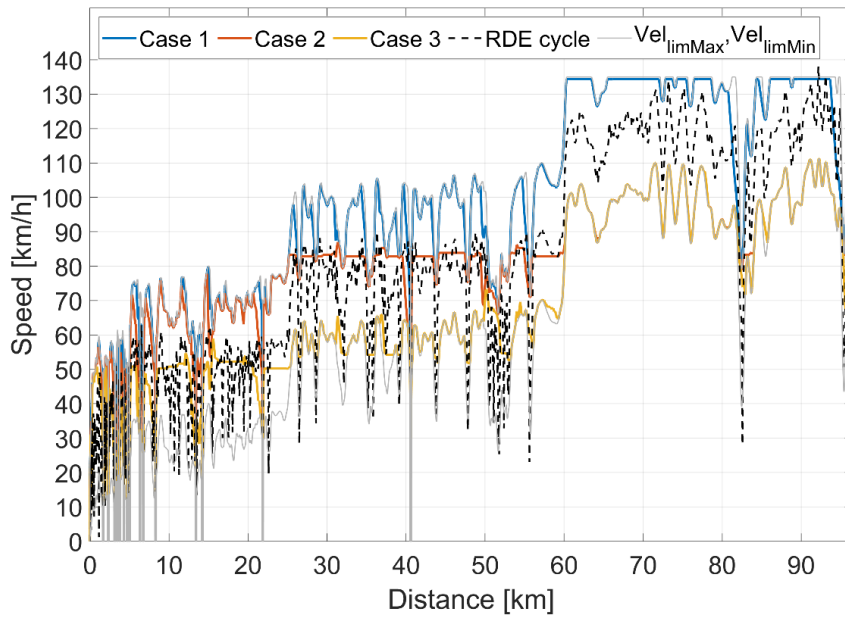


Figure 4.19: Vehicle speed profile with different values of cost function parameter, for the RDE cycle performed with a PHEV

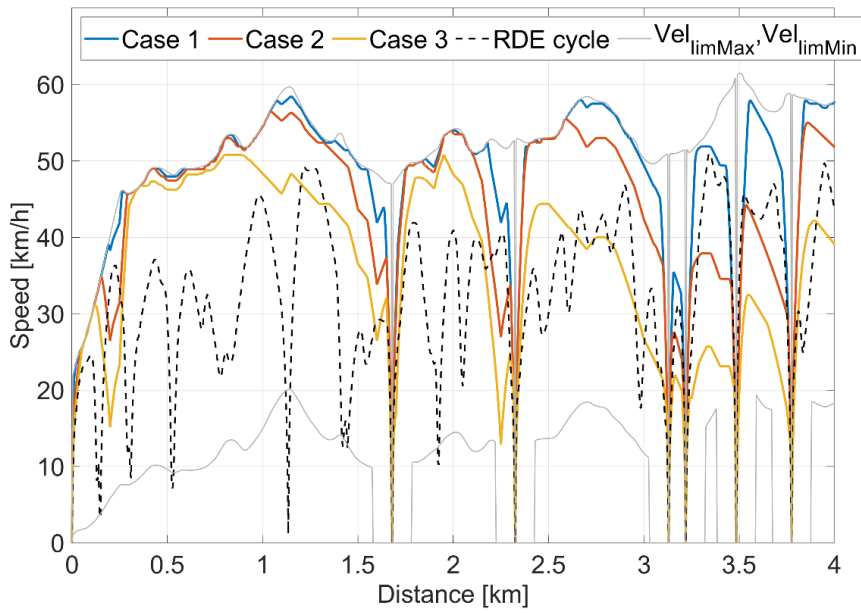


Figure 4.20: Vehicle speed profile with different values of cost function parameter, for the initial part of urban RDE cycle performed with a PHEV

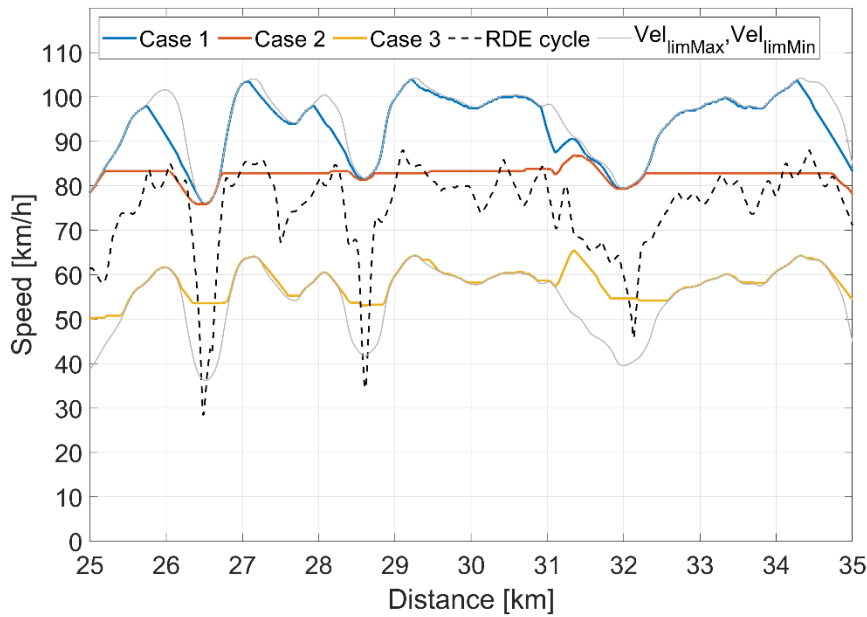


Figure 4.21: Vehicle speed profile with different values of cost function parameter, for the initial part of rural RDE cycle performed with a PHEV

As already seen for the NEDC, it is evident that the higher the value assigned to the parameter α , the lower the energy consumption: it means that the optimizer chooses lower vehicle speeds entailing lower energy consumption. Generally, an about constant speed is preferred a part from some points in which the speed limits and the elevation change play a major role. Therefore, the solution strictly depends on the speed limits. The travel times and the energy requests are reported in Figure 4.22 and Figure 4.23. The main final values of this analysis are reported in Table 4.5.

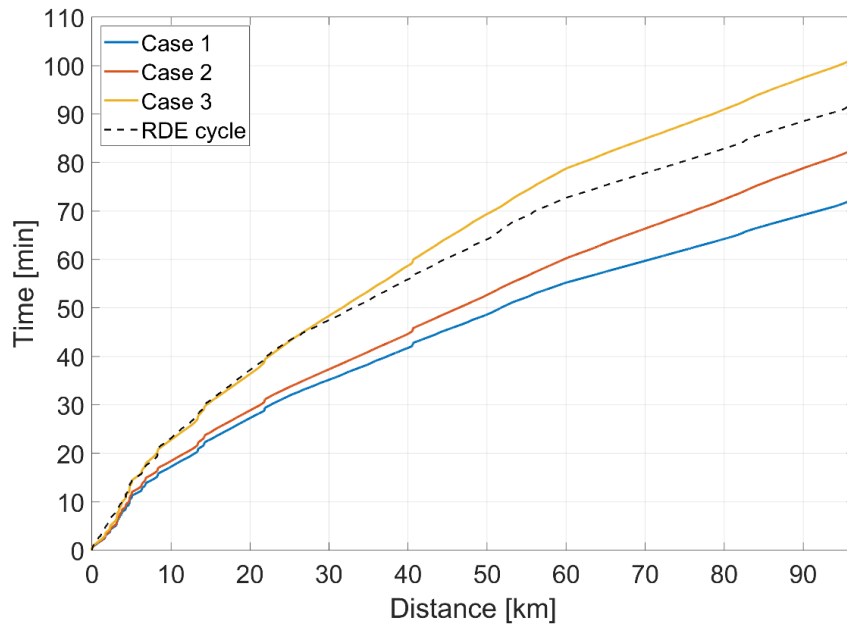


Figure 4.22: Travel time with different values of cost function parameter, for the RDE cycle performed with a PHEV

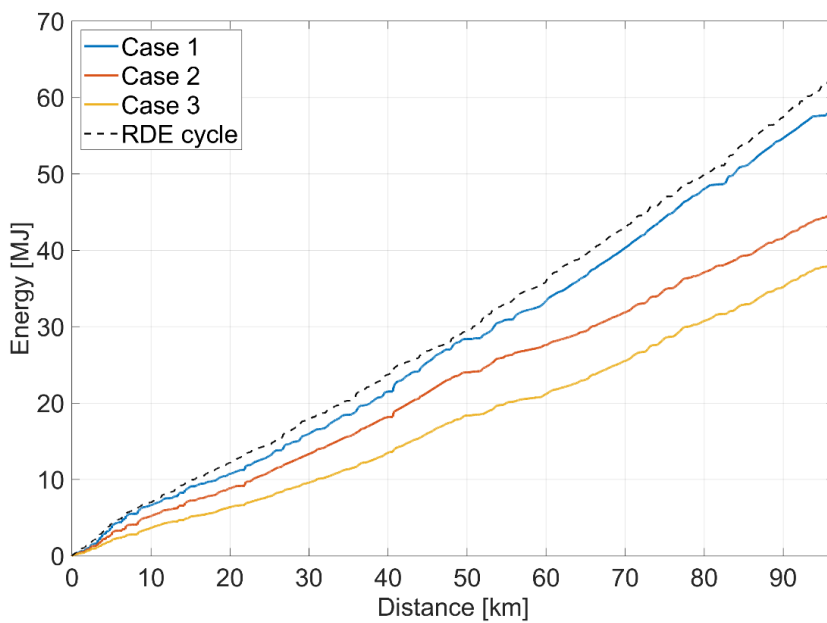


Figure 4.23: Final drive positive energy request with different values of cost function parameter, for the RDE cycle performed with a PHEV

As it can be seen from Figure 4.22 and Figure 4.23, in all the three cases less energy is consumed if compared to the RDE cycle thanks to the smoother accelerations, but only in the Case 2 and the Case 3 the travel time is lower.

Table 4.5: Total travel time, final drive positive energy request and final drive positive energy request per kilometre with different values of cost function parameter, for the RDE cycle performed with a PHEV

Parameter	Unit	RDE cycle	Case 1	Case 2	Case 3
Total travel time	[min]	92.2	73.3	83.6	102.3
Final drive positive energy request	[MJ]	62.86	57.97	44.62	38.19
Final drive positive energy request per kilometre	[MJ/km]	0.65	0.60	0.46	0.40

The trade-off between the total positive energy request at final level level and the total travel time for the eco-driving sensitivity analysis are reported in Figure 4.24. The same considerations already done for the NEDC, can be repeated.

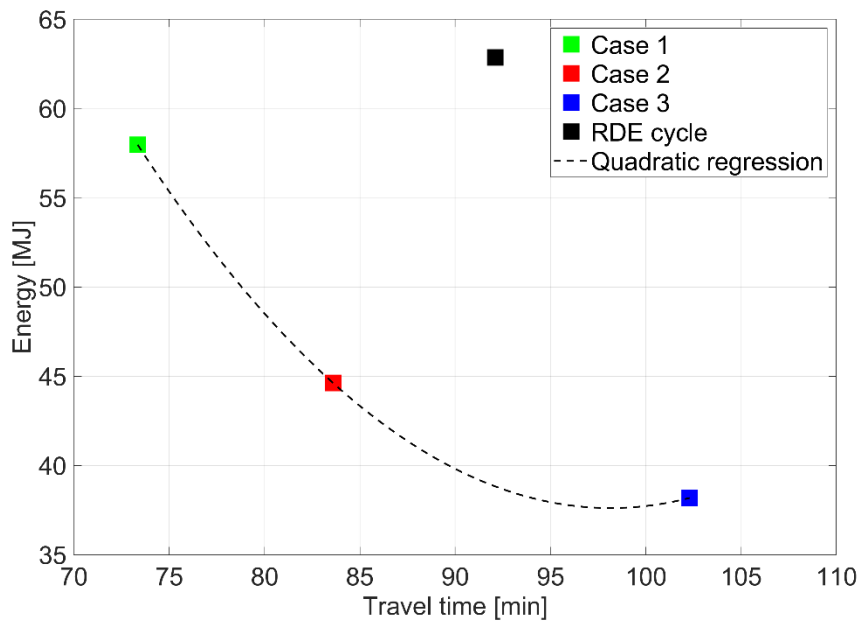


Figure 4.24: Trade-off between positive energy request at final level and travel time with different values of cost function parameter, for the RDE cycle performed with a PHEV

4.1.2.1 RDE V2X

As mentioned, in order to take into account V2X communication, it was also performed an analysis where it is considered the possibility to skip the stops in the RDE cycle. The generic cycle stop is supposed to be a traffic light intersection where in case of green sign there are not a stop constraint.

For the RDE cycle with V2X communication the maximum speed limits are:

- **With red sign:** equal to the maximum speed limit previously defined.
- **With green sign:** equal to the maximum speed limit previously defined except for the traffic light where it remains the moving average of the experimental speed (over an interval of 500 metres) incremented of 20 km/h.

The minimum speed limit is equal to the lower limit previously defined. In this section only the results obtained for the first 14.22 kilometres of the RDE cycle will be shown since it is the most interesting part for this type of analysis: in fact, the remaining part contains few stops.

The speed limits for the firsts 4 kilometres of the urban RDE cycle are reported in Figure 4.25.

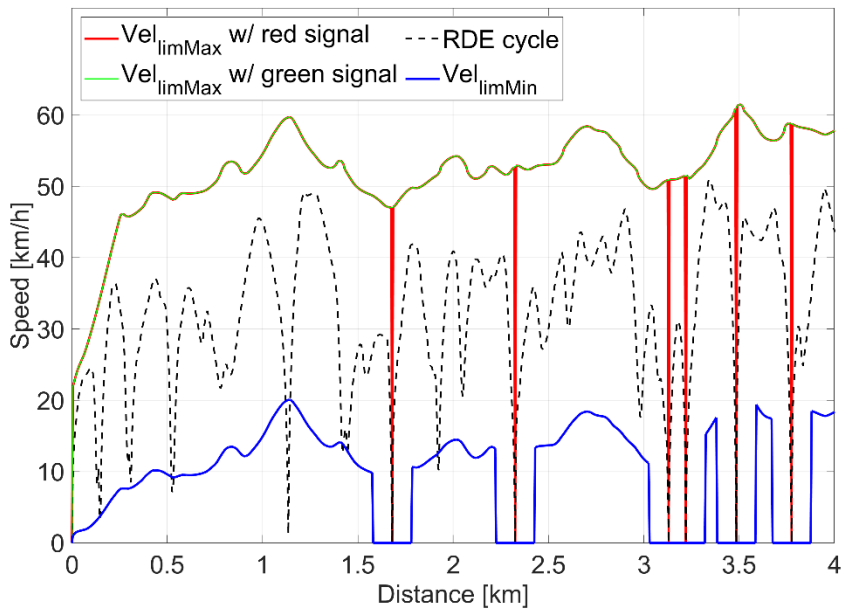


Figure 4.25: Speed limits with red or green signal for the initial part of the RDE cycle

The vehicle speeds, travel time and energy consumption are reported in Figure 4.26, Figure 4.27 and Figure 4.28. As for the UDC, in the first part of the RDE cycle there are no substantial differences among the different cases due to the limited distance between the traffic lights. From around the 7th kilometre on, the speed profile tends to diverge. It should be noted that, differently from the analysis in section 4.1.2, the speed profiles are not about constant. In fact, it can be mainly linked the presence of traffic light, so the speed profiles changes to obtain the “green wave”. The final values of this analysis are reported in Table 4.6.

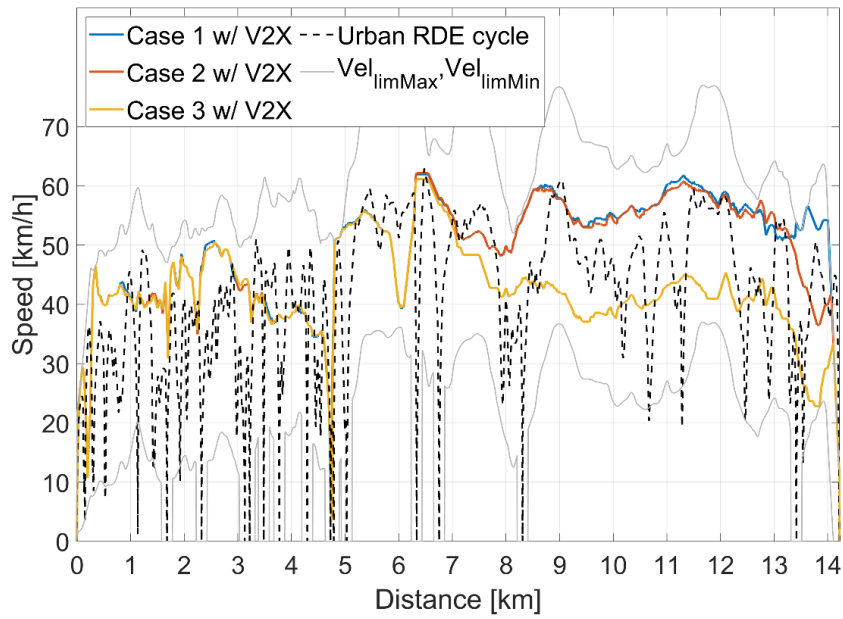


Figure 4.26: Vehicle speed profile with different values of cost function parameter, for the urban RDE cycle with V2X communication performed with a PHEV

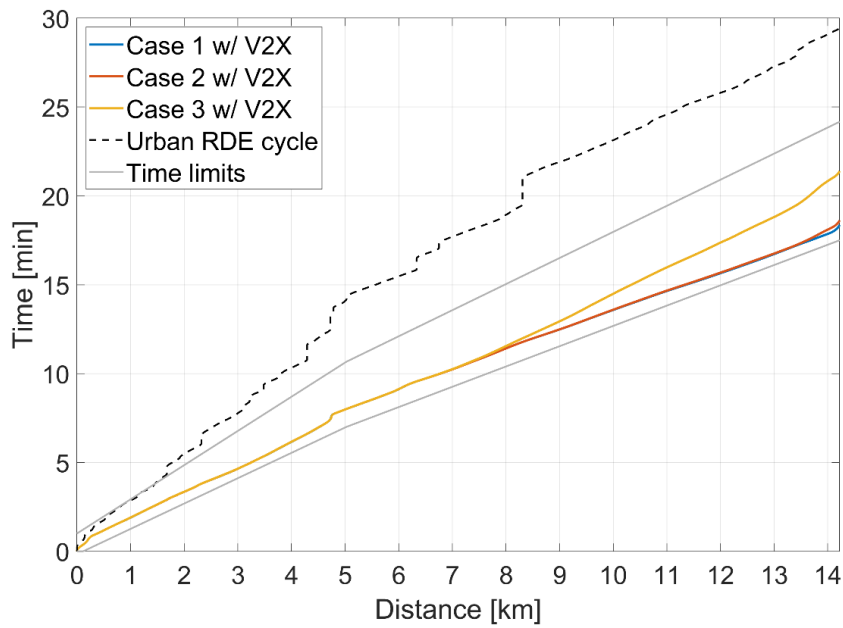


Figure 4.27: Travel time with different values of cost function parameter, for the urban RDE cycle with V2X communication performed with a PHEV

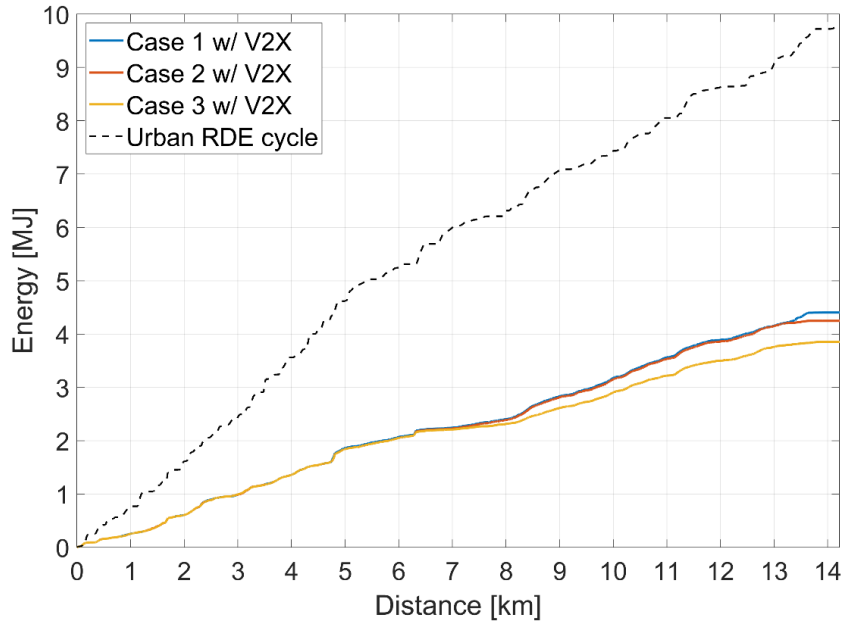


Figure 4.28: Final drive positive energy request with different values of cost function parameter, for the urban RDE cycle with V2X communication performed with a PHEV

Table 4.6: Total travel time, final drive positive energy request and final drive positive energy request per kilometre with different values of cost function parameter, for the urban RDE cycle with V2X communication performed with a PHEV

Parameter	Unit	Urban RDE cycle	Case 1 w/ V2X	Case 2 w/ V2X	Case 3 w/ V2X
Total travel time	[min]	29.5	18.4	18.6	21.4
Final drive positive energy request	[MJ]	9.75	4.40	4.25	3.85
Final drive positive energy request per kilometre	[MJ/km]	0.69	0.31	0.30	0.27

A comparison among different optimizations with a fixed value of cost function, equal to the Case 2 (i.e. $\alpha = 0.5$), is shown in Figure 4.29, Figure 4.30 and Figure 4.31. The same considerations already done for the NEDC with V2X, can be repeated. The final values of the model with and without V2X communication are reported in Table 4.7. So, the model with V2X communication, takes less time and less energy to cover the route if compared to the model without V2X.

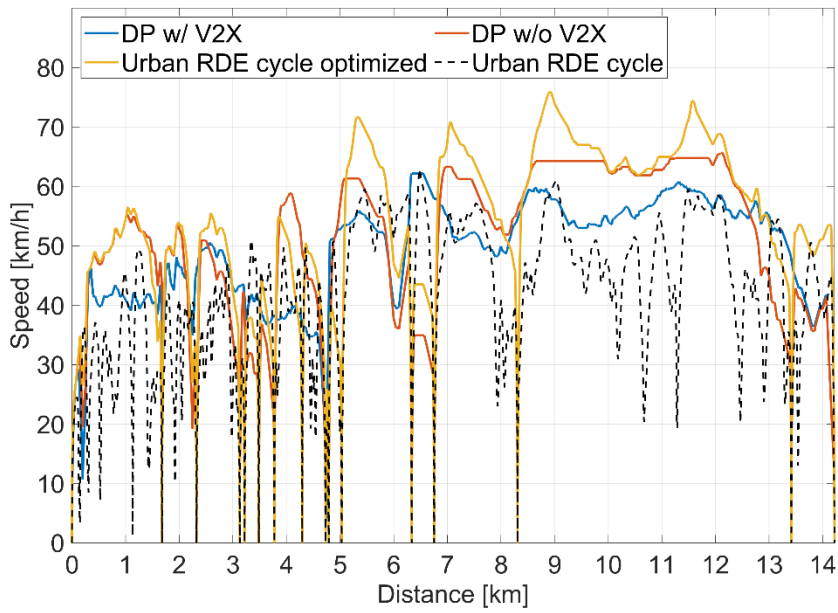


Figure 4.29: Vehicle speed profile comparison among different optimizations with a fixed value of cost function parameter, for the urban RDE cycle performed with a PHEV

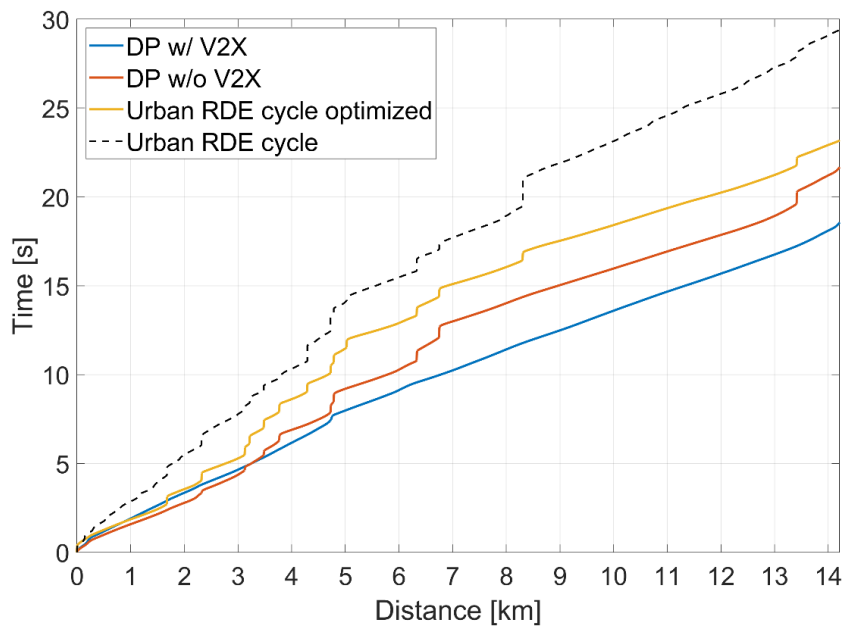


Figure 4.30: Travel time comparison among different optimizations with a fixed value of cost function parameter, for the urban RDE cycle performed with a PHEV

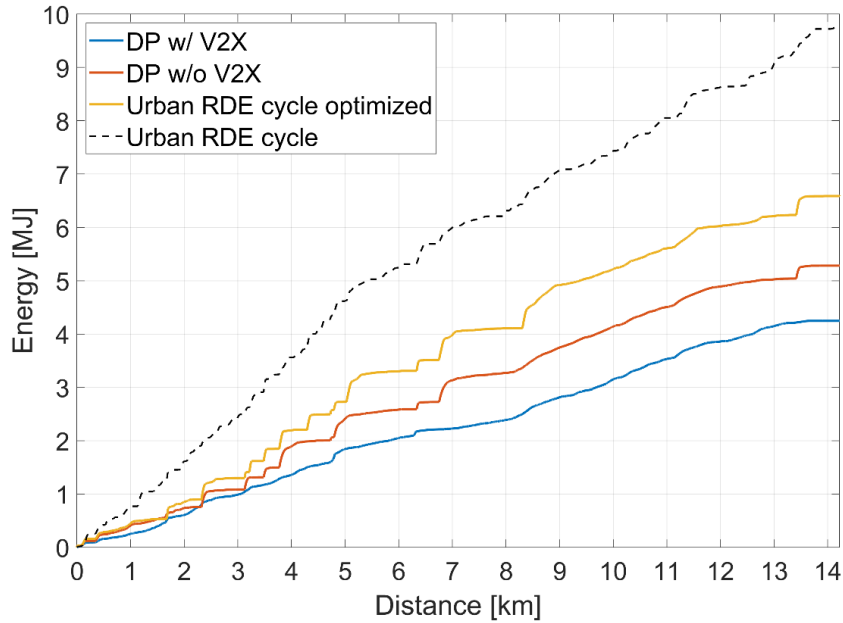


Figure 4.31: Final drive positive energy request comparison among different optimizations with a fixed value of cost function parameter, for the urban RDE cycle performed with a PHEV

In Figure 4.32 the vehicle speed profiles are shown for the model with and without V2X communication. It is eye-catching that, when V2X communication are available, the optimizer is able to optimize the vehicle speed in order to catch only green at traffic lights. For the sake of clarity, in Figure 4.33 and Figure 4.34 is only reported the model with V2X. Figure 4.34 shows traffic light signals and travel time in a time-distance graph for the Case 2 with V2X: the vehicle can overcome the traffic light only when it catches the green signal; it can also be seen clearly the random phases.

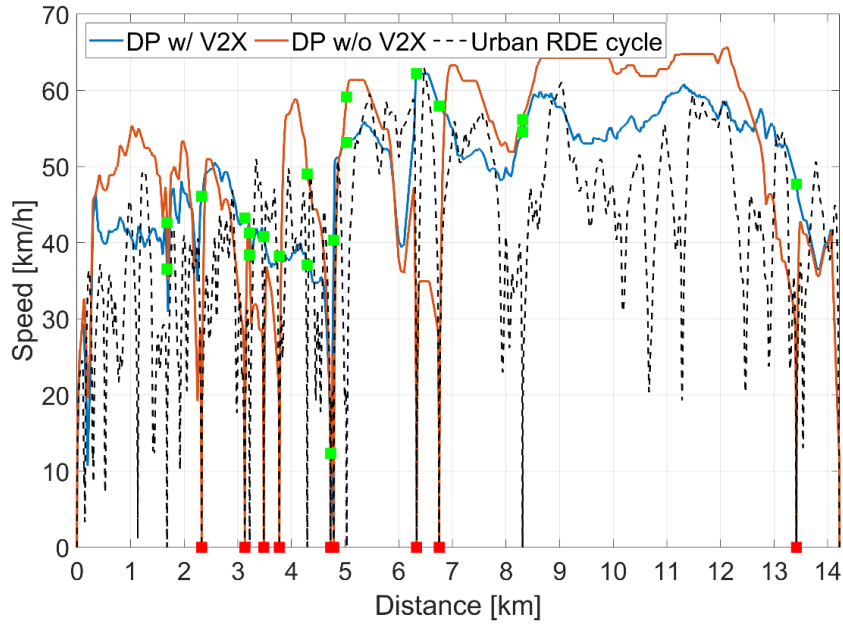


Figure 4.32: Vehicle speed profile comparison among the urban RDE cycle with and without V2X communication and traffic light signal with a fixed value of cost function parameter, performed with a PHEV

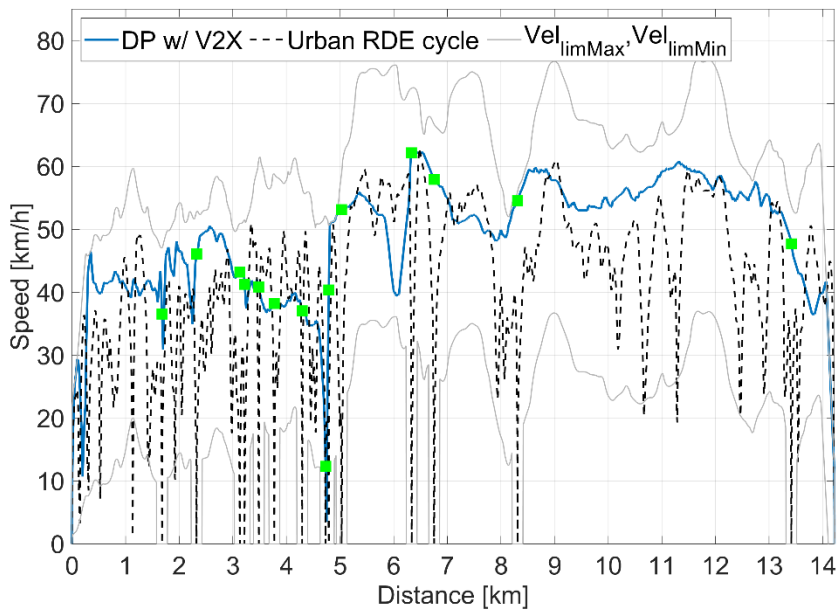


Figure 4.33: Vehicle speed profile and traffic light signal with a fixed value of cost function parameter, for the urban RDE cycle with V2X communication performed with a PHEV

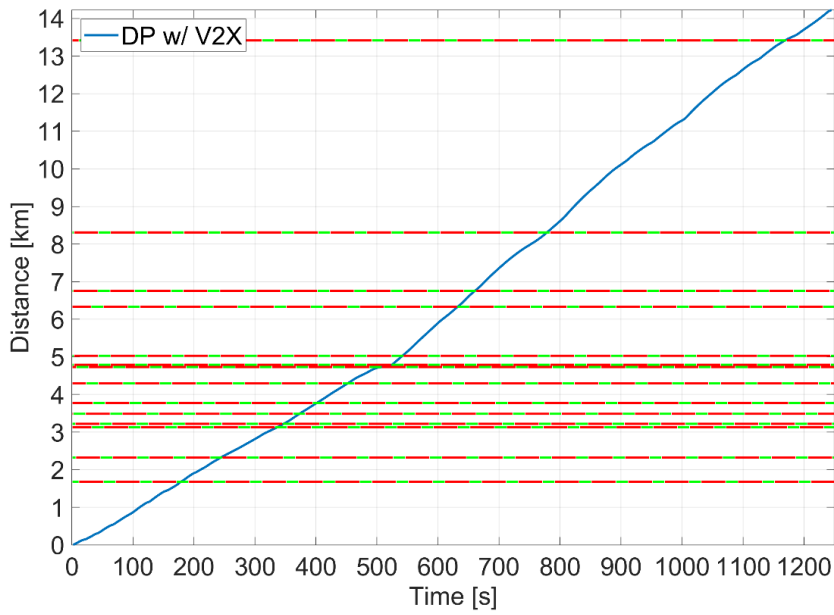


Figure 4.34: Traffic light signals and travel time in a time-distance graph with a fixed value of cost function parameter, for the urban RDE cycle with V2X communication performed with a PHEV

Table 4.7: Total travel time, final drive positive energy request and final drive positive energy request per kilometre, comparison among the urban RDE cycle with and without V2X communication with a fixed value of cost function parameter, performed with a PHEV

Parameter	Unit	Case 2 w/o V2X	Case 2 w/ V2X
Final travel time	[min]	21.7	18.6
Final drive positive energy request	[MJ]	5.28	4.25
Final drive positive energy request per kilometre	[MJ/km]	0.37	0.30

The trade-off between the total positive energy request at final level and the total travel time for the eco-driving sensitivity analysis for the urban RDE cycle with and without V2X communication are reported in Figure 4.35. The urban RDE cycle with V2X communication has a best trade-off with respect to the urban RDE cycle without V2X.

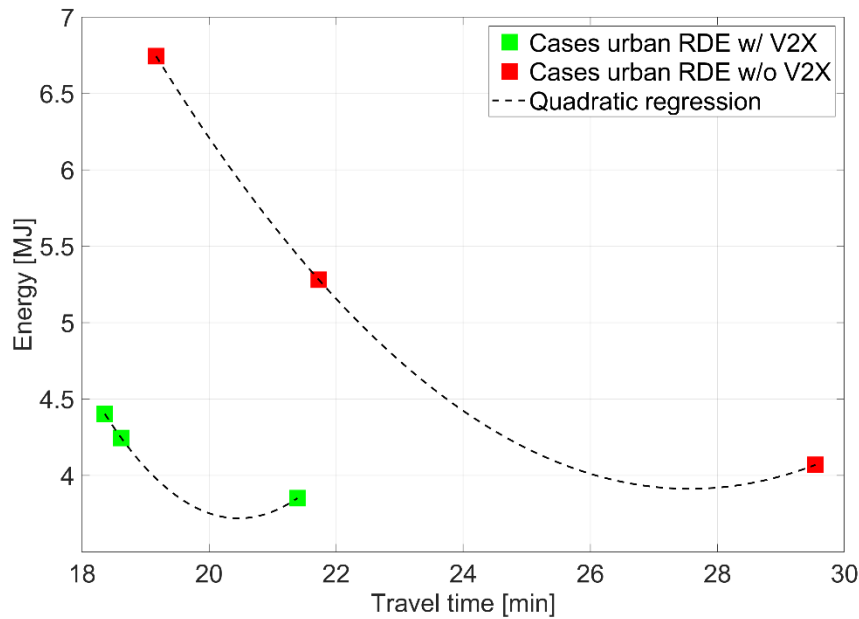


Figure 4.35: Trade-off between positive energy request at final level and travel time for the urban RDE cycle with and without V2X communication with different values of cost function parameter, performed with a PHEV

4.2 Speed Optimization for CV Fuel Consumption Minimization

4.2.1 NEDC

Analogously to the PHEV analysis described in the previous sections, a sensitivity analysis was performed in order to show the optimal speed profile for different values of cost function, i.e. the parameter α , as shown in Figure 4.36 and Figure 4.37. Since the minimization is performed on the fuel consumption, differently from the PHEV where the energy at the final drive was minimized, no coasting trend of the vehicle speed can be seen.

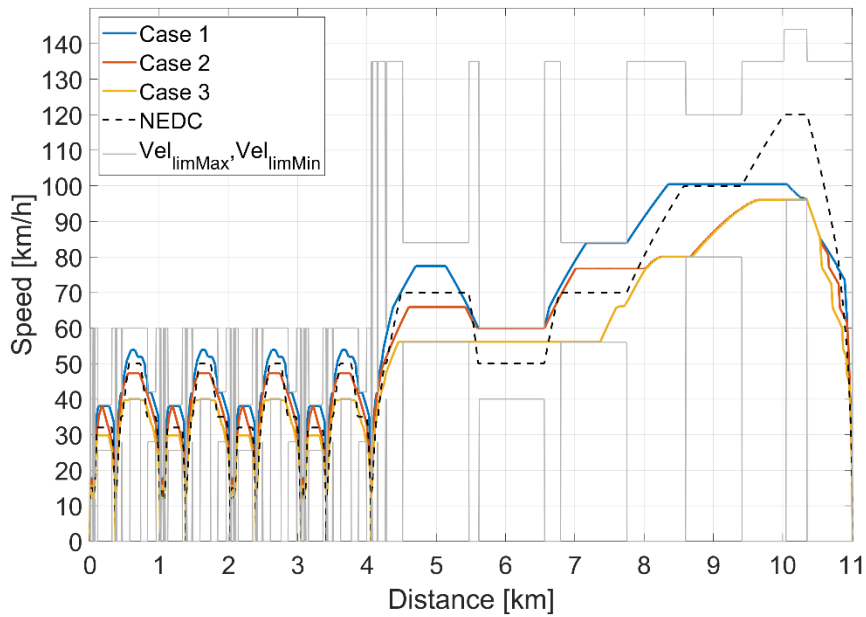


Figure 4.36: Vehicle speed profile with different values of cost function parameter, for the NEDC performed with a conventional vehicle

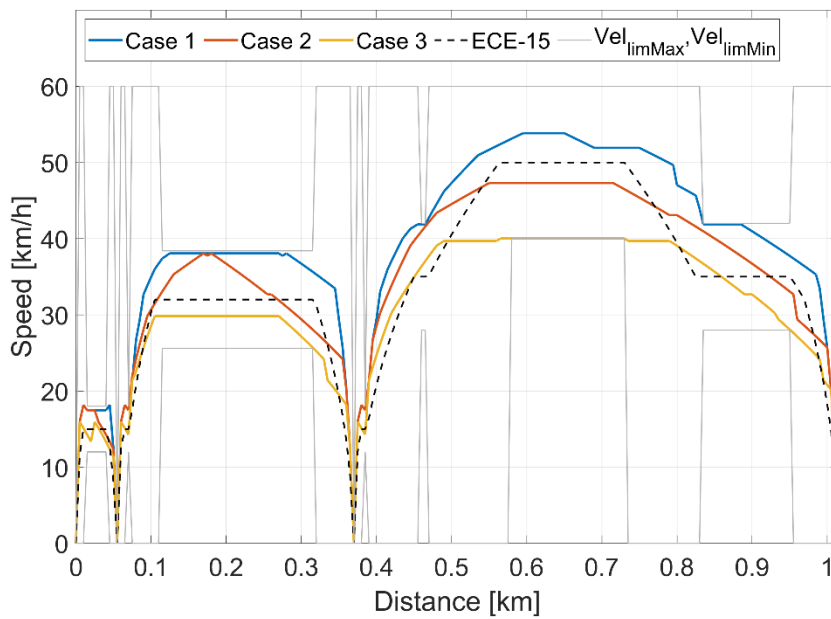


Figure 4.37: Vehicle speed profile Travel time with different values of cost function parameter, for the first ECE-15 performed with a conventional vehicle

The sensitivity analysis on travel time, fuel consumption and average fuel consumptions over the NEDC for different values of cost function parameter are reported in Figure 4.38 and Figure 4.39. The travel time for the Case 1 and the Case 2 are lower than the NEDC and the Case 3 is higher, but the fuel consumption for all the cases are lower than the NEDC. The final values of this analysis are reported in Table 4.8.

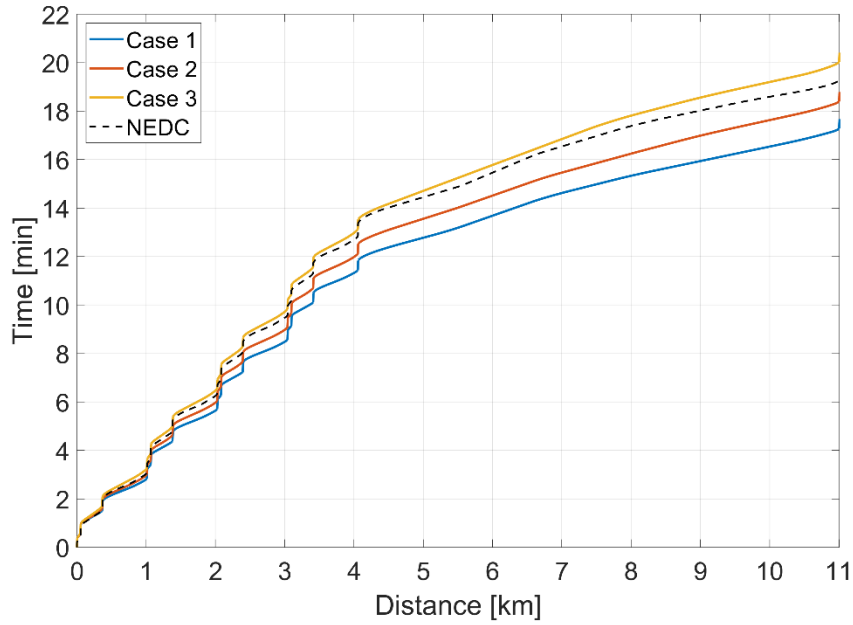


Figure 4.38: Travel time with different values of cost function parameter, for the NEDC performed with a conventional vehicle

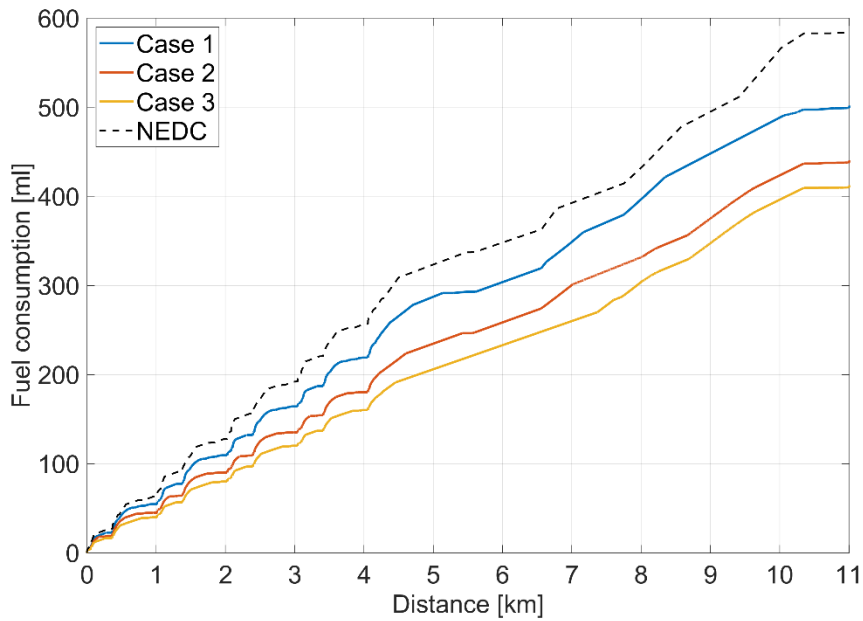


Figure 4.39: Fuel consumption with different values of cost function parameter, for the NEDC performed with a conventional vehicle

Table 4.8: Final travel time, fuel consumption and average fuel consumption with different values of cost function parameter, for the NEDC performed with a conventional vehicle

Parameter	Unit	NEDC	Case 1	Case 2	Case 3
Final travel time	[min]	19.7	17.7	18.8	20.4
Fuel consumption	[ml]	584	502	441	413
Average fuel consumption	[km/l]	18.9	21.9	25.0	26.7

The trade-off between the fuel consumption and the total travel time for the eco-driving sensitivity analysis are reported in Figure 4.40. The same considerations already done for the equivalent PHEV analysis, can be repeated.

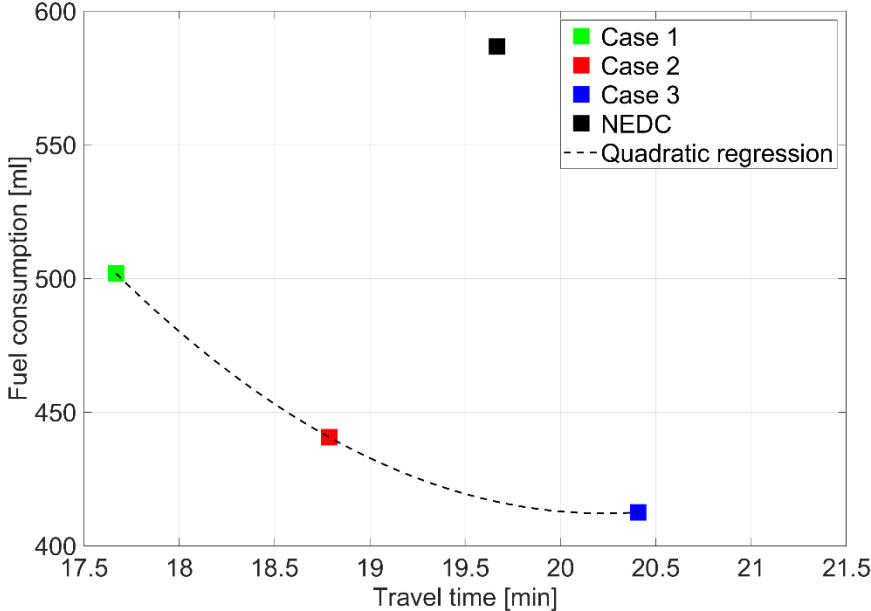


Figure 4.40: Trade-off between fuel consumption and travel time with different values of cost function parameter, for NEDC performed with a conventional vehicle

4.2.1.1 NEDC V2X

As already shown for the PHEV analysis, in order to take into account V2X communication, it was also performed an analysis where it is considered the possibility to skip the stops in the NEDC. The generic cycle stop is supposed to be a traffic light intersection where in case of green sign there are not a stop constraint. Only the results obtained for the UDC will be shown since it is the most interesting part for this type of analysis: in fact, the EUDC does not contain any additional stop. The vehicle speeds, travel time and energy consumption are reported in Figure 4.41, Figure 4.42 and Figure 4.43. The final values of this analysis are reported in Table 4.9. As it is shown there are only little differences among the cases.

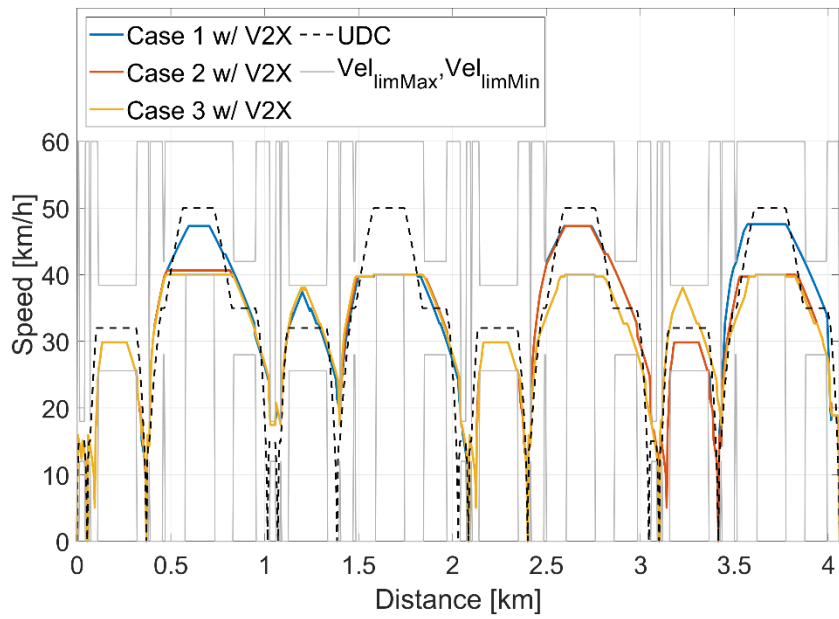


Figure 4.41: Vehicle speed profile with different values of cost function parameter, for the UDC with V2X communication performed with a conventional vehicle

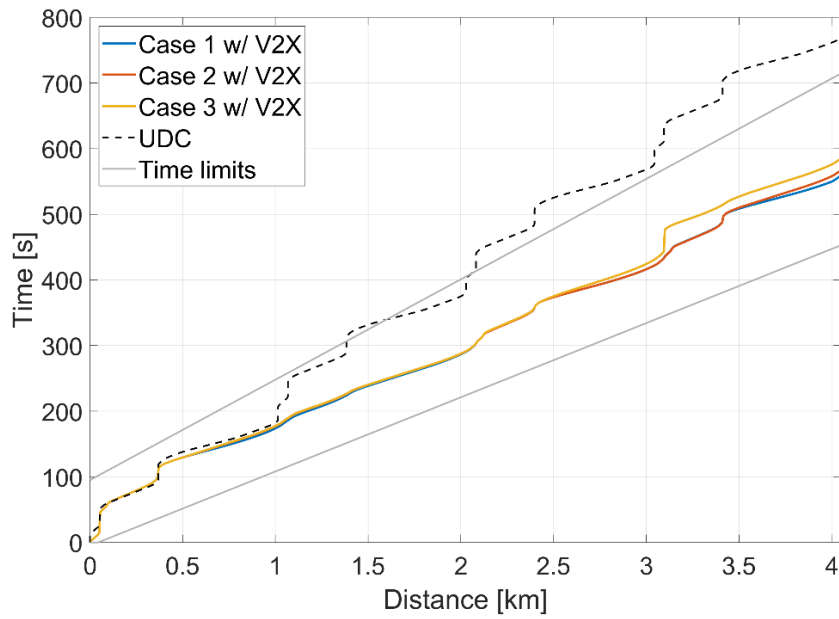


Figure 4.42: Travel time with different values of cost function parameter, for the UDC with V2X communication performed with a conventional vehicle

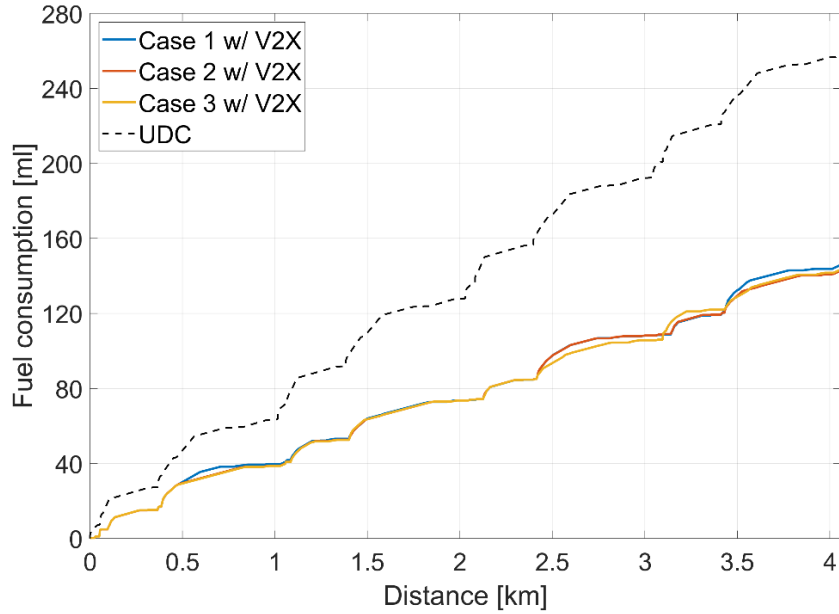


Figure 4.43: Fuel consumption with different values of cost function parameter, for the UDC with V2X communication performed with a conventional vehicle

Table 4.9: Final travel time, fuel consumption and average fuel consumption with different values of cost function parameter, for the UDC with V2X communication performed with a conventional vehicle

Parameter	Unit	UDC	Case 1 w/ V2X	Case 2 w/ V2X	Case 3 w/ V2X
Final travel time	[s]	773	568	570	584
Fuel consumption	[ml]	257	145	142	143
Average fuel consumption	[km/l]	15.8	28.0	28.6	28.4

A comparison among different optimizations with a fixed value of cost function, equal to Case 2 (i.e. $\alpha = 0.5$), is shown in Figure 4.44, Figure 4.45 and Figure 4.46. The same considerations already done for the equivalent PHEV analysis, can be repeated. The final values of the model with and without V2X communication are reported in Table 4.10. So, the model with V2X communication, takes less time and consumes less fuel to cover the route if compared to the model without V2X.

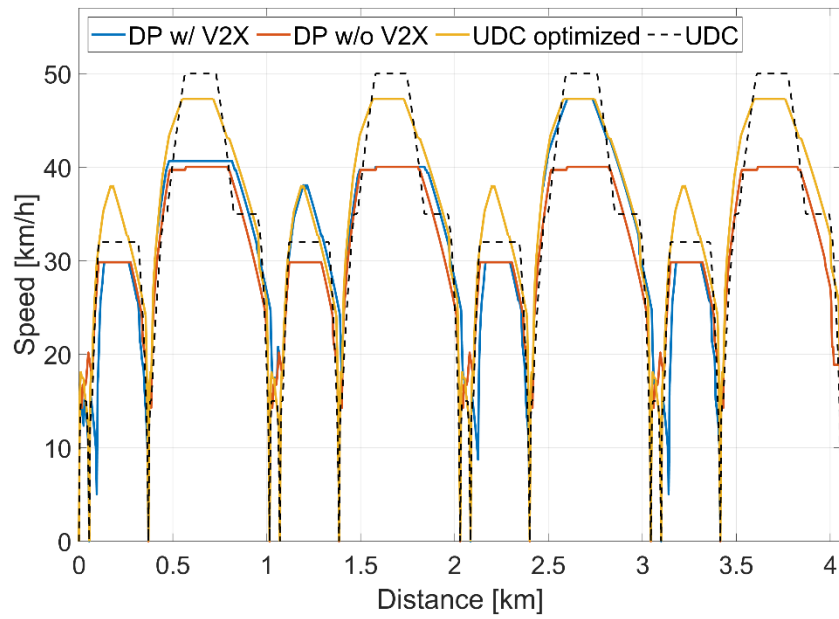


Figure 4.44: Vehicle speed profile comparison among different optimizations with a fixed value of cost function parameter, for the UDC performed with a conventional vehicle

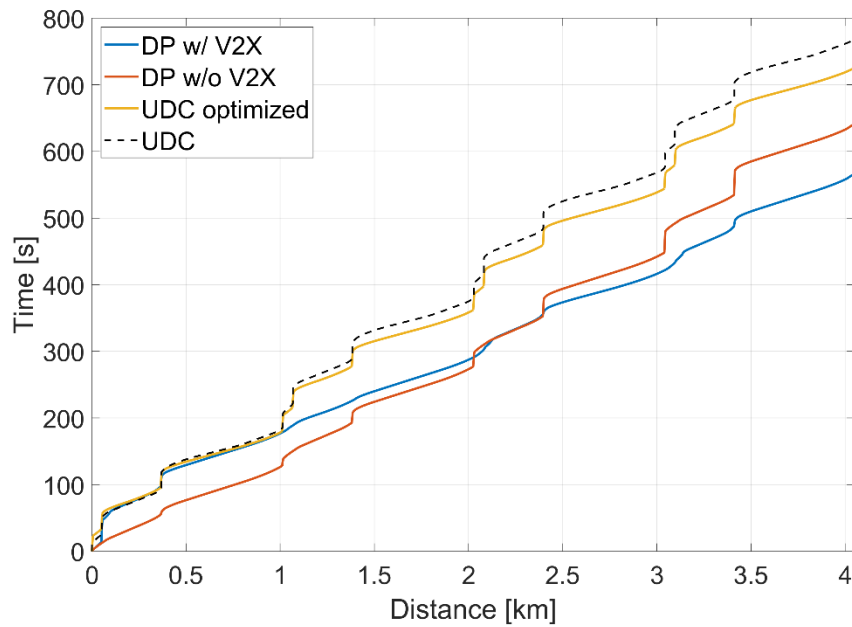


Figure 4.45: Travel time comparison among different optimizations with a fixed value of cost function parameter, for the UDC performed with a conventional vehicle

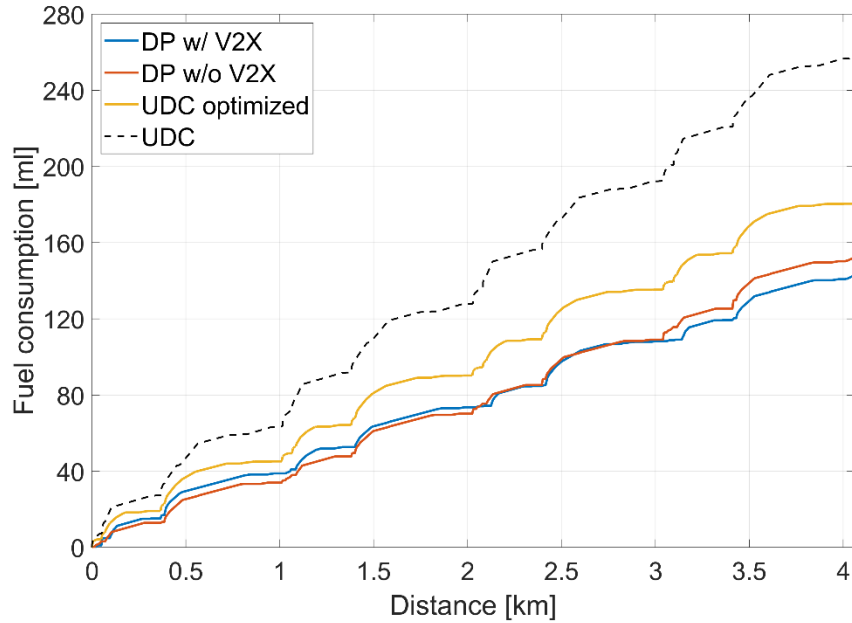


Figure 4.46: Fuel consumption comparison among different optimizations with a fixed value of cost function parameter, for the UDC performed with a conventional vehicle

In Figure 4.47 the vehicle speed profiles are shown. DP w/ and w/o V2X feature the cases with and without V2X communication and traffic light signals at traffic light intersections, respectively. For clarity, in Figure 4.48 and Figure 4.49 only the model with V2X is reported. Figure 4.49 shows traffic light signals and travel time in a time-distance graph for the Case 2 with V2X: the vehicle can overcome the traffic light only when it catches the green signal; it can also be seen clearly the random phases.

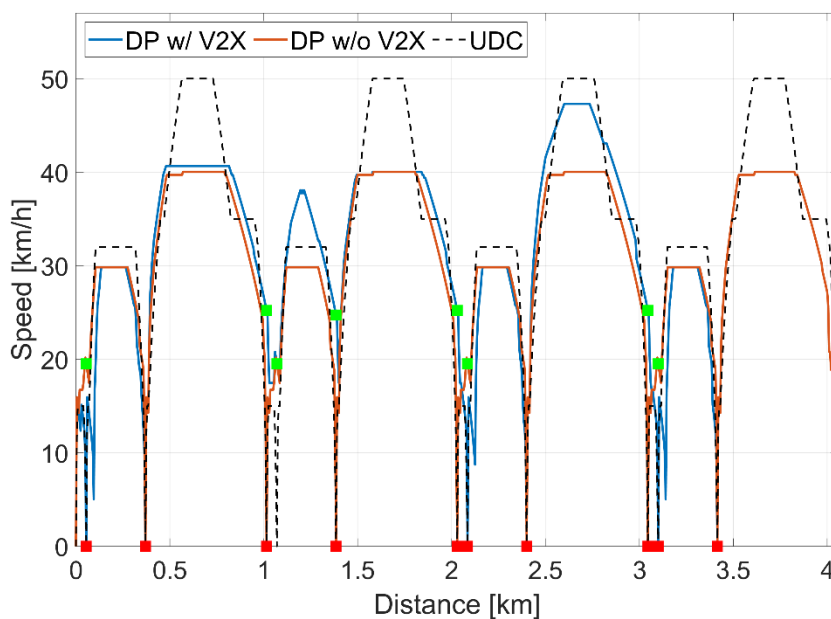


Figure 4.47: Vehicle speed profile comparison among the UDC with and without V2X communication and traffic light signal with a fixed value of cost function parameter, performed with a conventional vehicle

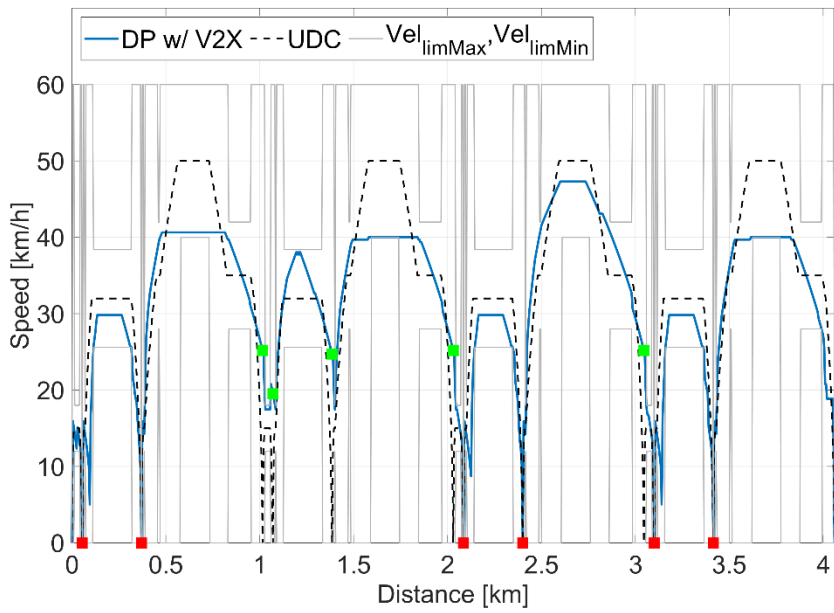


Figure 4.48: Vehicle speed profile and traffic light signal with a fixed value of cost function parameter, for UDC with V2X communication performed with a conventional vehicle

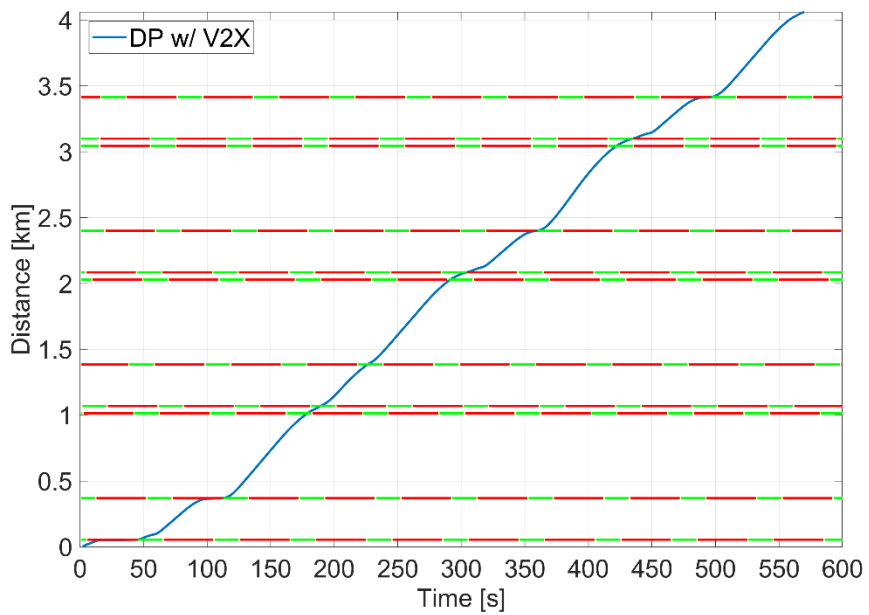


Figure 4.49: Traffic light signals and travel time in a time-distance graph with a fixed value of cost function parameter, for the UDC with V2X communication performed with a conventional vehicle

Table 4.10: Final travel time, fuel consumption and average fuel consumption, comparison among the UDC with and without V2X communication with a fixed value of cost function parameter, performed with a conventional vehicle

Parameter	Unit	Case 2 w/o V2X	Case 2 w/ V2X
Final travel time	[s]	642	570
Fuel consumption	[ml]	152	142
Average fuel consumption	[km/l]	26.7	28.6

The trade-off between the fuel consumption and the total travel time for the UDC with and without V2X communication are reported in Figure 4.50. The UDC with V2X communication has a best trade-off with respect to the UDC without V2X.

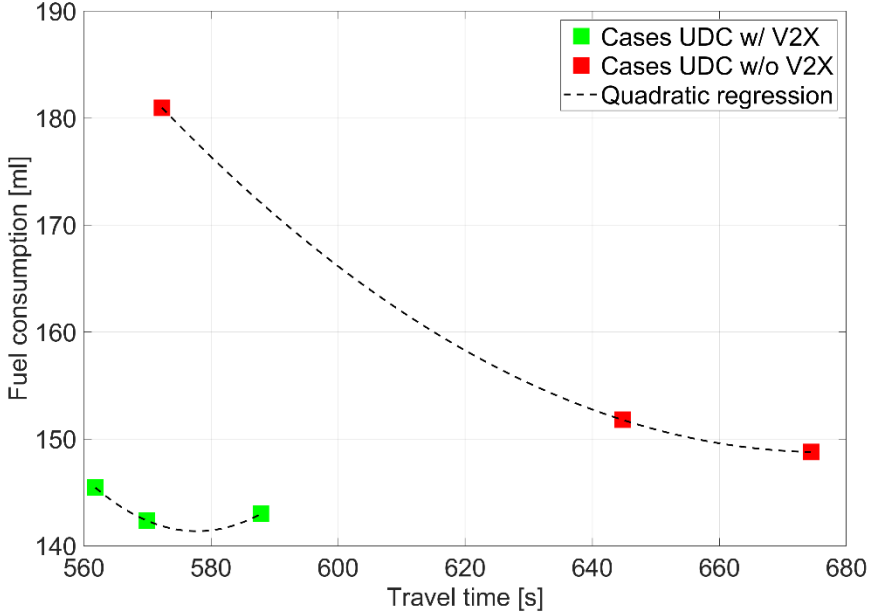


Figure 4.50: Trade-off between fuel consumption and travel time for the UDC with and without V2X communication with different values of cost function parameter, performed with a conventional vehicle

4.2.2 RDE

As previously shown for the PHEV analysis, the vehicle speed profile of a conventional vehicle was optimized on a RDE cycle in order to obtain more interesting results. Speed profiles for the entire RDE cycle are reported in Figure 4.51 and a zoom of the initial part of urban and rural part are shown in Figure 4.52 and Figure 4.53, respectively.

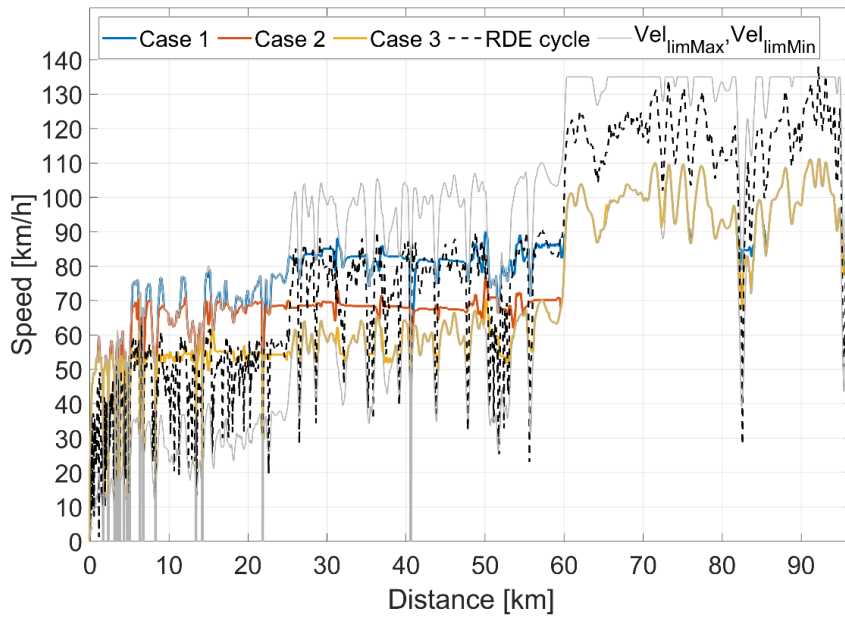


Figure 4.51: Vehicle speed profile with different values of cost function parameter, for the RDE cycle performed with a conventional vehicle

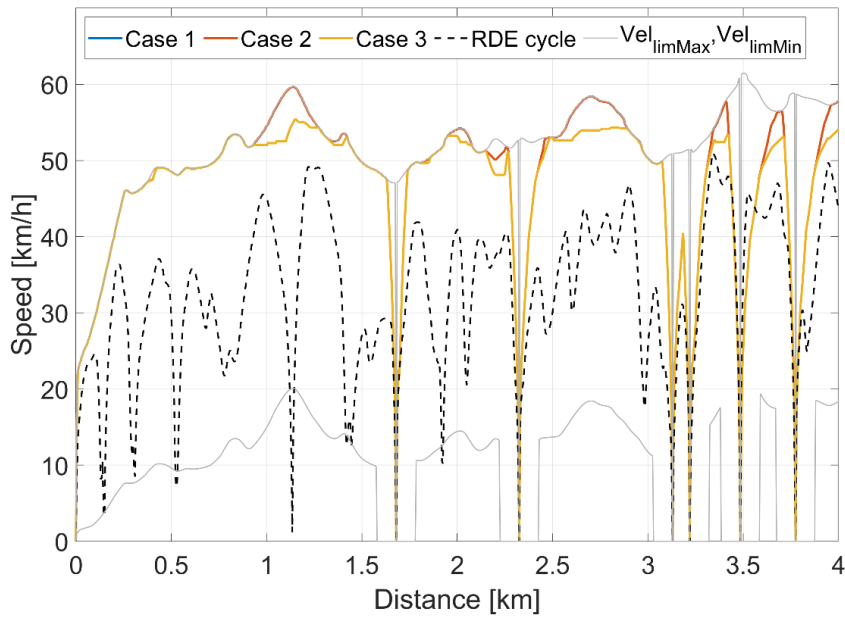


Figure 4.52: Vehicle speed profile with different values of cost function parameter, for the initial part of urban RDE cycle performed with a conventional vehicle

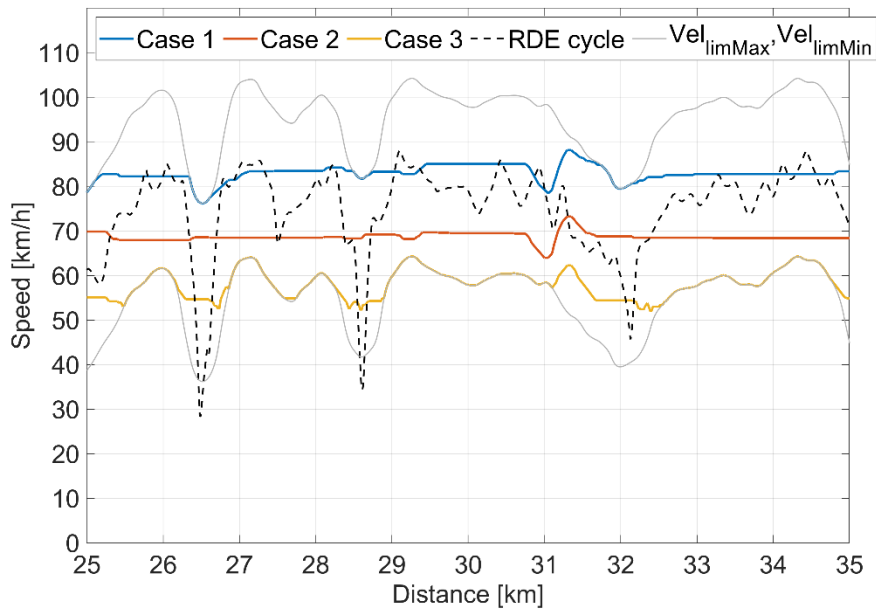


Figure 4.53: Vehicle speed profile with different values of cost function parameter, for the initial part of rural RDE cycle performed with a conventional vehicle

As previously seen for the PHEV analysis, the vehicle speed tends to be constant unless the speed limits and the route elevation change this trend. The travel times and the energy requests are reported in Figure 4.54 and Figure 4.55. The final values of this analysis are reported in Table 4.11.

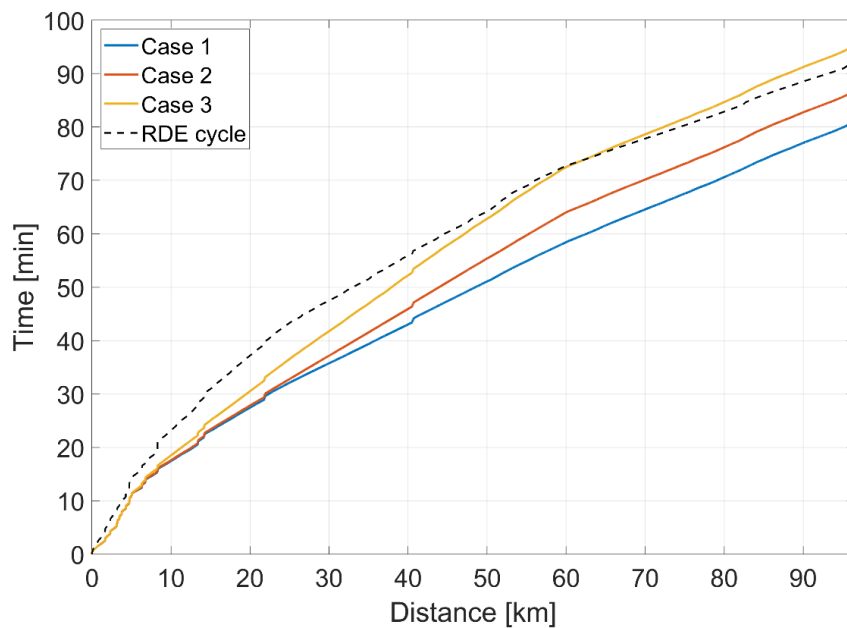


Figure 4.54: Travel time with different values of cost function parameter, for the RDE cycle with a conventional vehicle

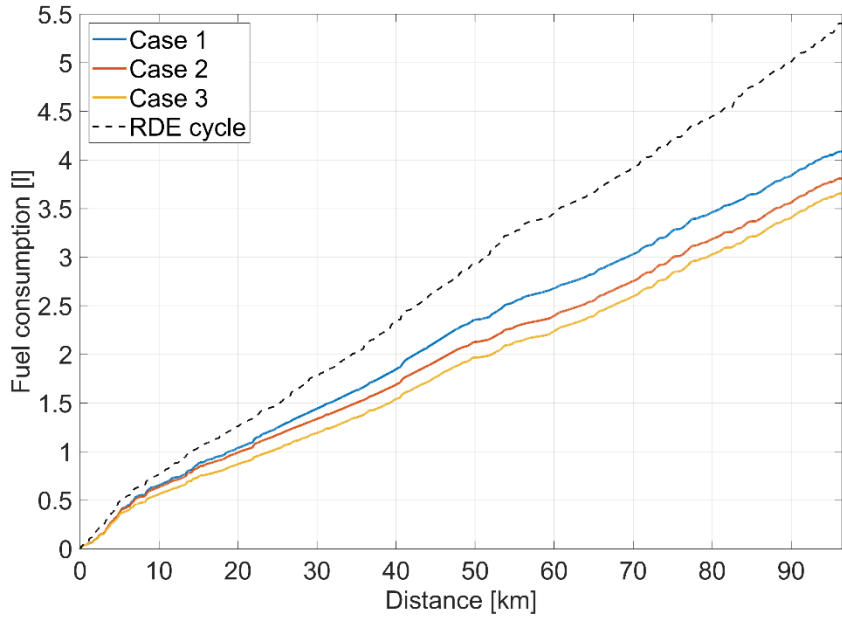


Figure 4.55: Fuel consumption with different values of cost function parameter, for the RDE cycle performed with a conventional vehicle

Table 4.11: Final travel time, fuel consumption and average fuel consumption with different values of cost function parameter, for the RDE cycle performed with a conventional vehicle

Parameter	Unit	RDE cycle	Case 1	Case 2	Case 3
Final travel time	[min]	92.2	81.4	87.2	95.7
Fuel consumption	[l]	5.41	4.09	3.81	3.66
Average fuel consumption	[km/l]	17.8	23.6	25.3	26.4

The trade-off between the fuel consumption and the total travel time for the eco-driving sensitivity analysis are reported in Figure 4.56. The same considerations already done for the equivalent PHEV analysis, can be repeated.

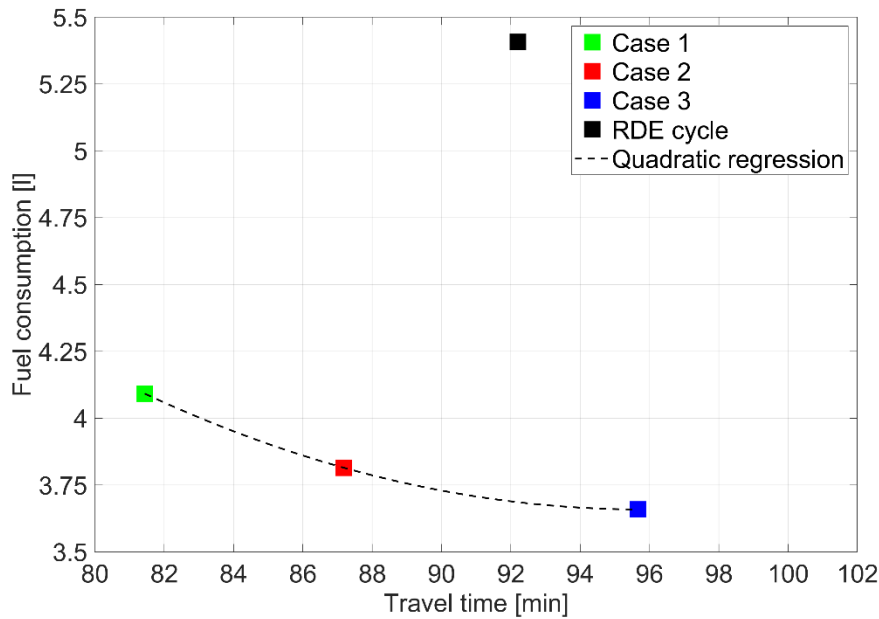


Figure 4.56: Trade-off between fuel consumption and travel time with different values of cost function parameter, for the NEDC performed with a conventional vehicle

4.2.2.1 RDE V2X

As previously seen for the PHEV analysis, in order to take into account V2X communication, it was also performed an analysis where it is considered the possibility to skip the stops in the RDE cycle. The generic cycle stop is supposed to be a traffic light intersection where in case of green sign there are not a stop constraint. Only the results obtained for the first 14.22 kilometres of the RDE cycle will be shown since it is the most interesting part for this type of analysis: in fact, the remaining part contains few stops. The vehicle speeds, travel time and energy consumption are reported in Figure 4.57, Figure 4.58 and Figure 4.59. There are little differences between the Case 1 and the Case 2 along all the route. The final values of this analysis are reported in Table 4.12.

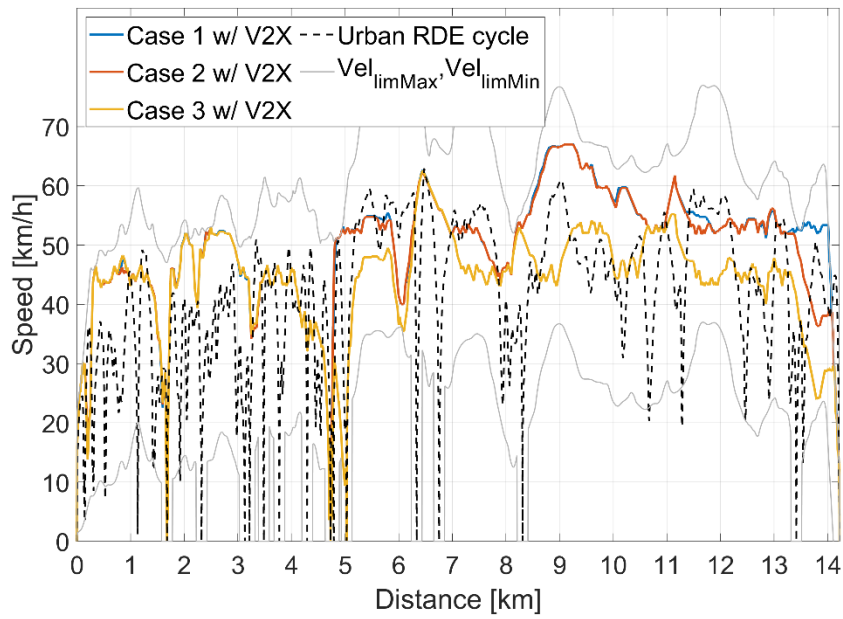


Figure 4.57: Vehicle speed profile with different values of cost function parameter, for the urban RDE cycle with V2X communication performed with a conventional vehicle

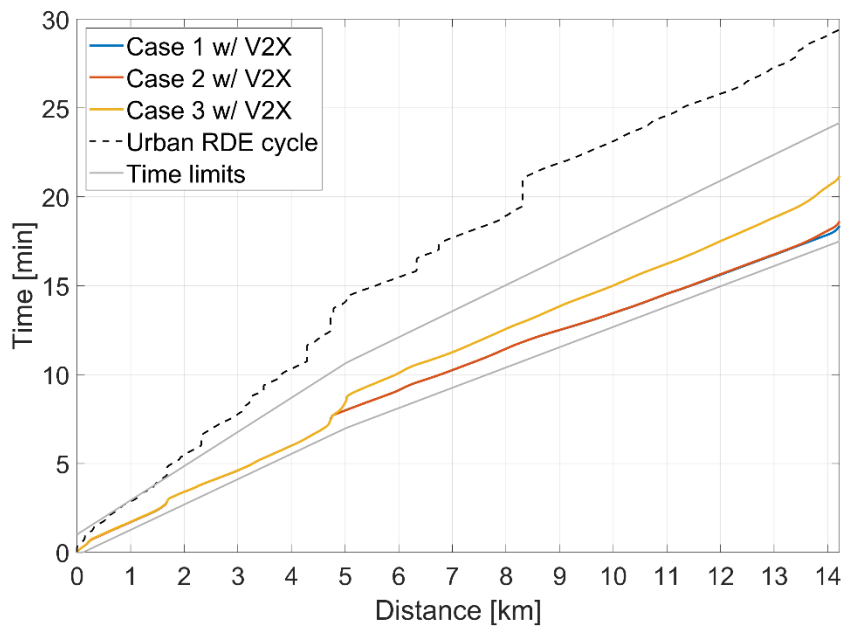


Figure 4.58: Travel time with different values of cost function parameter, for the urban RDE cycle with V2X communication performed with a conventional vehicle

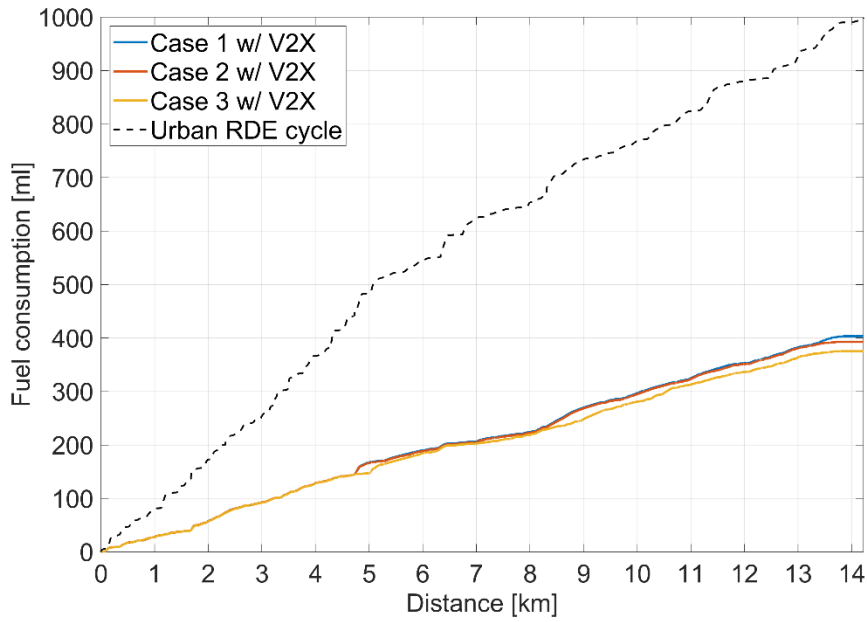


Figure 4.59: Fuel consumption with different values of cost function parameter, for the urban RDE cycle with V2X communication performed with a conventional vehicle

Table 4.12: Final travel time, fuel consumption and average fuel consumption with different values of cost function parameter, for the urban RDE cycle with V2X communication performed with a conventional vehicle

Parameter	Unit	Urban RDE cycle	Case 1 w/ V2X	Case 2 w/ V2X	Case 3 w/ V2X
Final travel time	[min]	29.5	18.4	18.6	21.2
Fuel consumption	[ml]	994	404	392	375
Average fuel consumption	[km/l]	14.3	35.2	36.3	37.9

A comparison among different optimizations with a fixed value of cost function, equal to Case 2, is shown in Figure 4.60, Figure 4.61 and Figure 4.62. The same considerations already done for the equivalent PHEV analysis, can be repeated. The final values of the model with and without V2X communication are reported in Table 4.13. So, the model with V2X communication, takes less time and less energy to cover the route with respect to the comparable model without V2X.

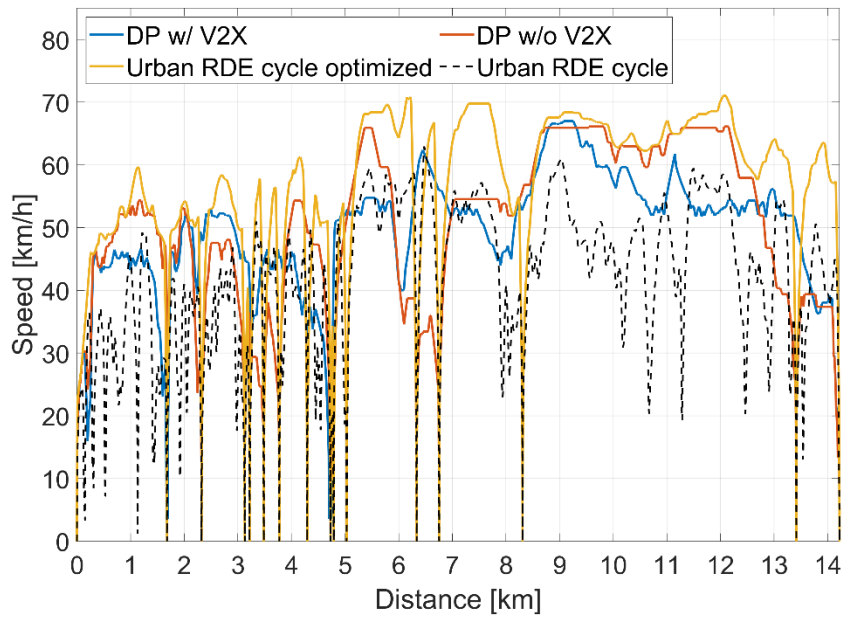


Figure 4.60: Vehicle speed profile comparison among different optimizations with a fixed value of cost function parameter, for the urban RDE cycle performed with a conventional vehicle

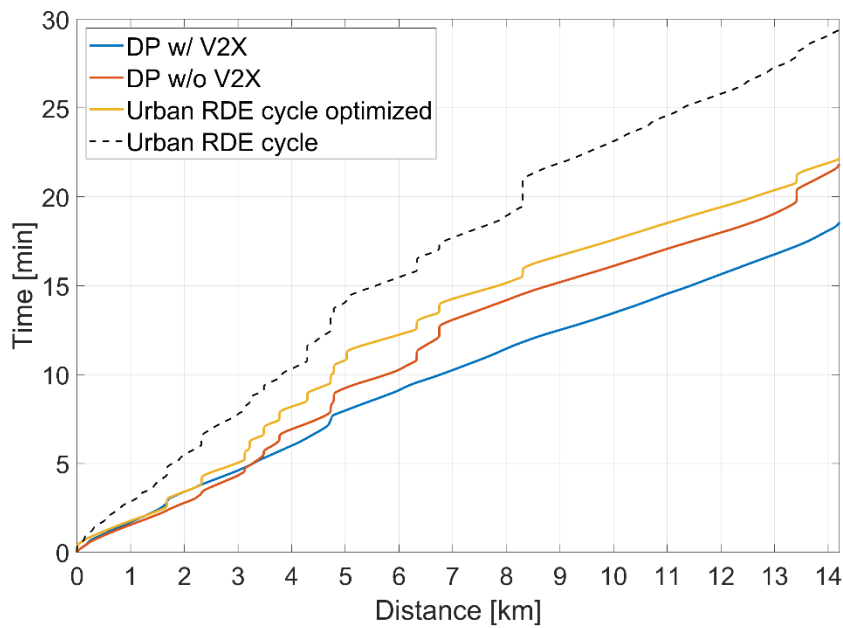


Figure 4.61: Travel time comparison among different optimizations with a fixed value of cost function parameter, for the urban RDE cycle performed with a conventional vehicle

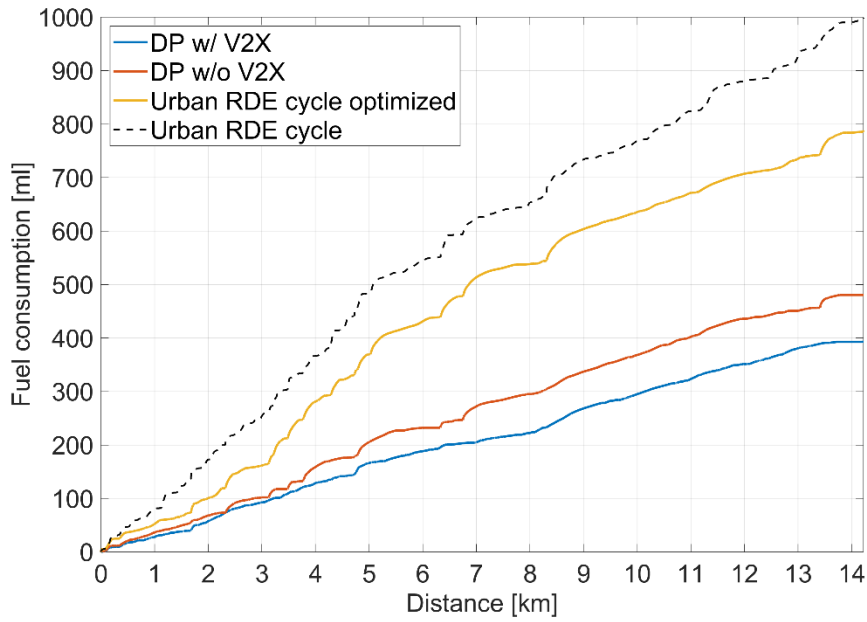


Figure 4.62: Fuel consumption comparison among different optimizations with a fixed value of cost function parameter, for the urban RDE cycle performed with a conventional vehicle

In Figure 4.63 the vehicle speed profile is shown for the model with and without V2X communication and the traffic light signal at the traffic light intersections. For the sake of clarity, in Figure 4.64 and Figure 4.65 is only reported the model with V2X. Figure 4.65 shows traffic light signals and travel time in a time-distance graph for the Case 2 with V2X: the vehicle can overcome the traffic light only when it catches the green signal; it can also be seen clearly the random phases.

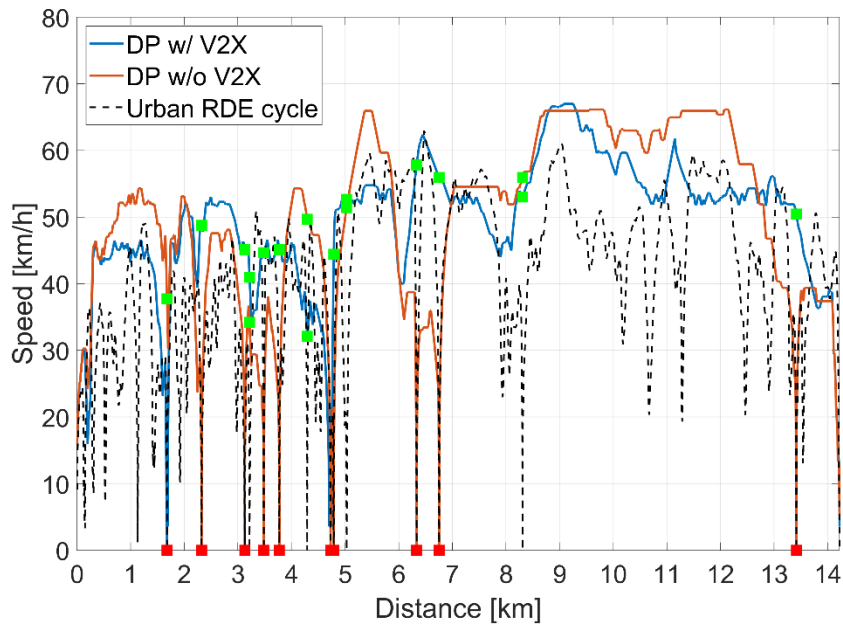


Figure 4.63: Vehicle speed profile comparison among the urban RDE cycle with and without V2X communication and traffic light signal with a fixed value of cost function parameter, performed with a conventional vehicle

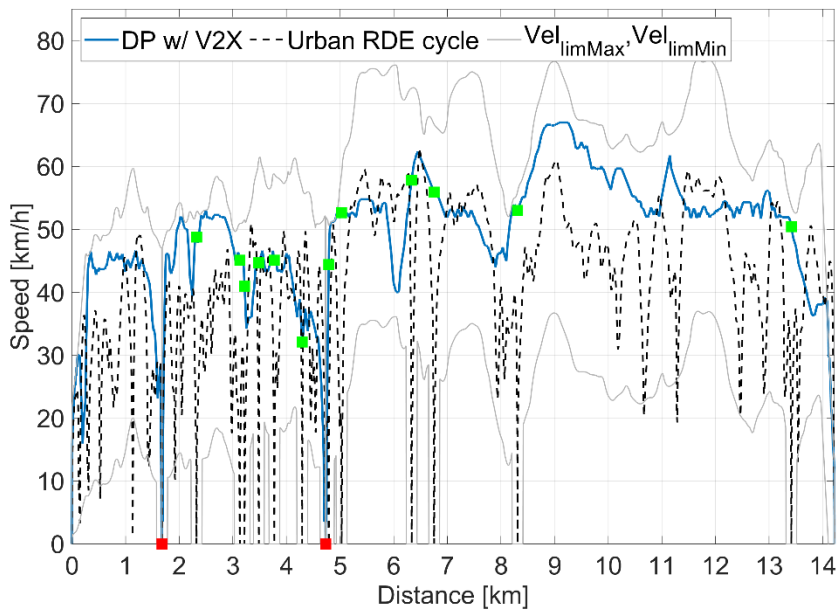


Figure 4.64: Vehicle speed profile and traffic light signal with a fixed value of cost function parameter, for the urban RDE cycle with V2X communication performed with a conventional vehicle

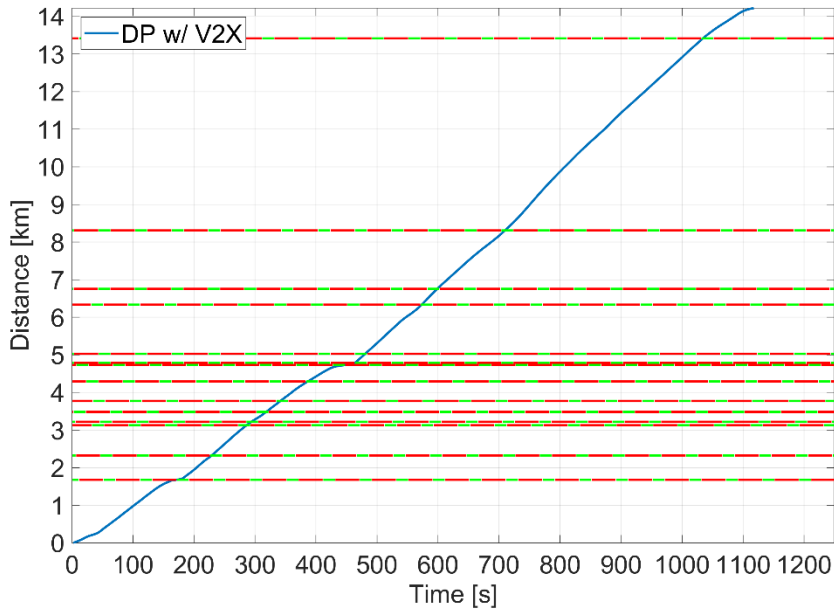


Figure 4.65: Traffic light signals and travel time in a time-distance graph with a fixed value of cost function parameter, for the urban RDE cycle with V2X communication performed with a PHEV

Table 4.13: Final travel time, fuel consumption and average fuel consumption, comparison among the urban RDE cycle with and without V2X communication with a fixed value of cost function parameter, performed with a conventional vehicle

Parameter	Unit	Case 2 w/o V2X	Case 2 w/ V2X
Final travel time	[min]	21.9	18.6
Fuel consumption	[ml]	481	392
Average fuel consumption	[km/l]	29.6	36.3

The trade-off between the fuel consumption and the total travel time for the eco-driving sensitivity analysis for the urban RDE cycle with and without V2X communication are reported in Figure 4.66. The urban RDE cycle with V2X communication has a best trade-off with respect to urban RDE cycle without V2X.

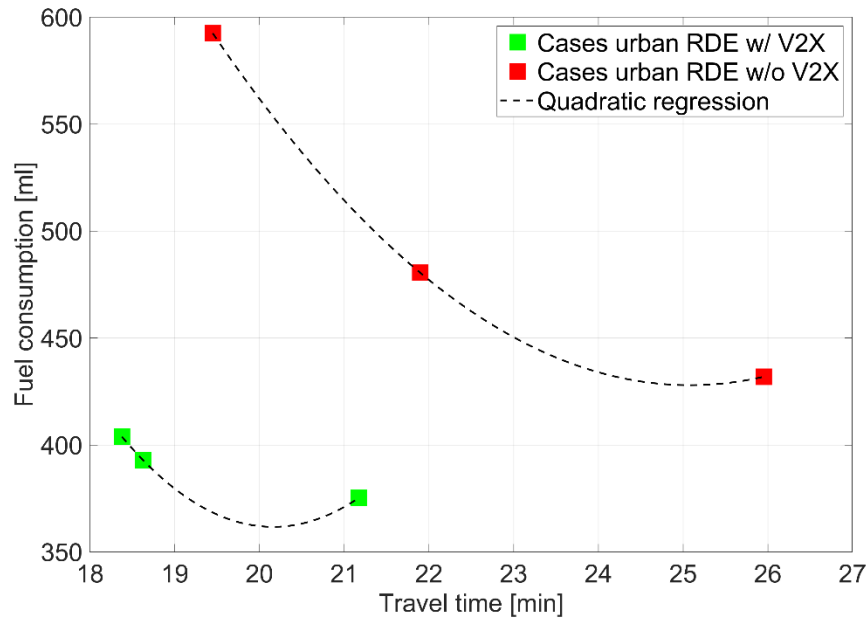


Figure 4.66: Trade-off between fuel consumption and travel time for the urban RDE cycle with and without V2X communication with different values of cost function parameter, performed with a conventional vehicle

4.3 Speed Optimization for BEV Δ SoC Minimization

4.3.1 NEDC

The sensitivity analysis was performed in order to show the optimal speed profile for different cost function parameter α (Figure 4.67 and Figure 4.68). Generally, on the UDC, it can be seen that the optimization chooses a coasting trend of the vehicle speed, as it happened for the PHEV final drive energy minimization model.

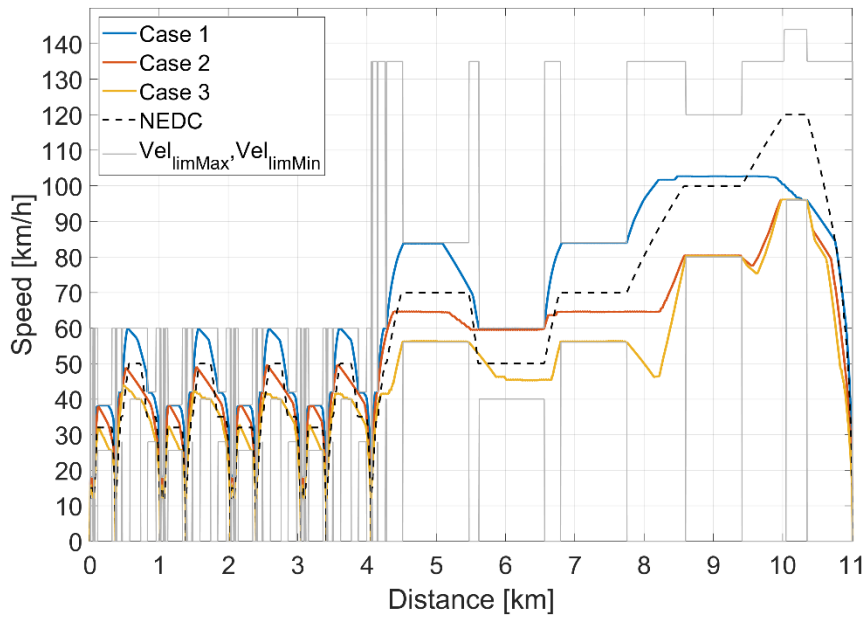


Figure 4.67: Vehicle speed profile with different values of cost function parameter, for the NEDC performed with a battery electric vehicle

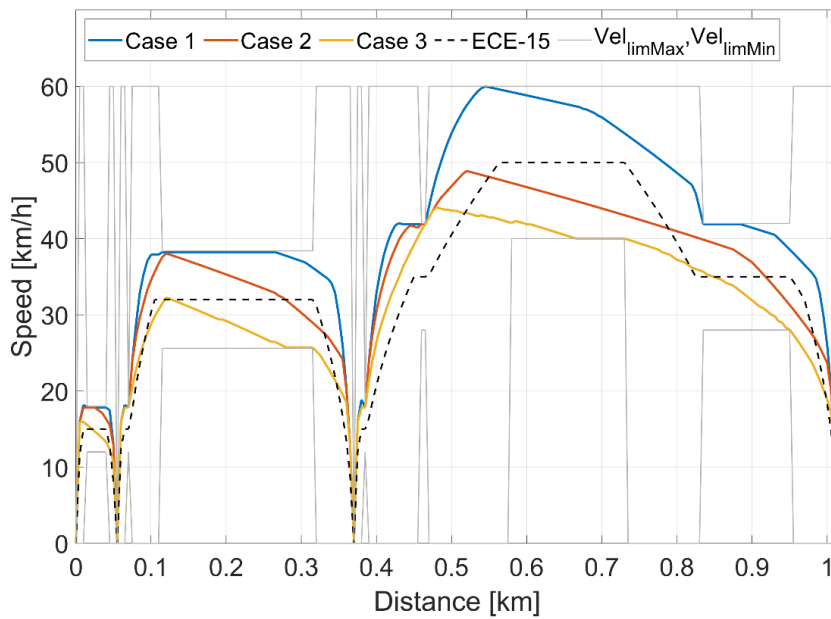


Figure 4.68: Vehicle speed profile with different values of cost function parameter, for the first ECE-15 performed with a battery electric vehicle

The travel times and the SoC profile for the NEDC and the cases of sensitivity analysis are reported in Figure 4.69 and Figure 4.70. The travel time for the Case 1 and the Case 2 are lower than the NEDC and the Case 3 is higher, but the SoC variation for all the cases are lower than the NEDC. In Figure 4.70 it is also reported the SoC limits, they are necessary

to reduce the computational cost of the problem; in order to not influence the output, they must be sufficiently distant for each distance step of each case from the SoC limits. The final values of this analysis are reported in Table 4.14.

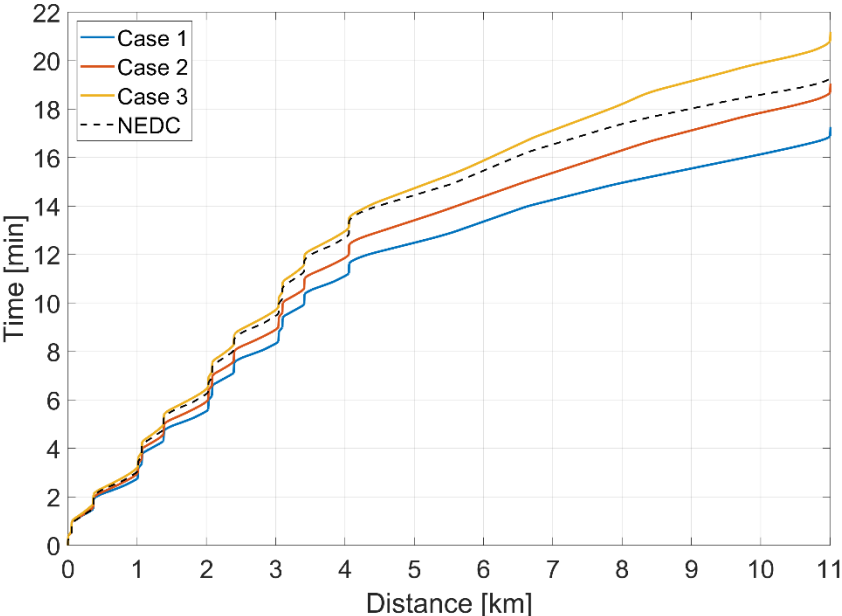


Figure 4.69: Travel time with different values of cost function parameter, for the NEDC performed with a battery electric vehicle

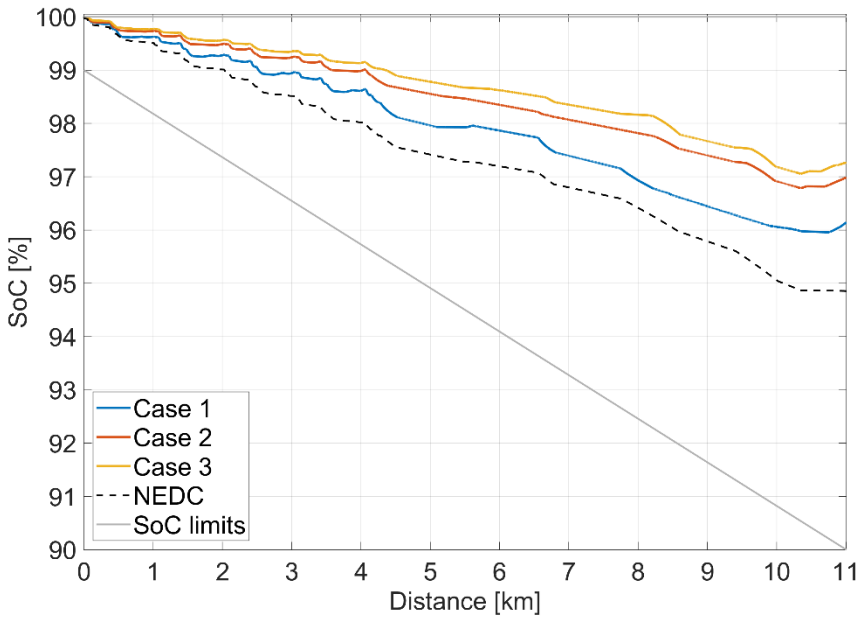


Figure 4.70: SoC profile with different values of cost function parameter, for the NEDC performed with a battery electric vehicle

Table 4.14: Final travel time, SoC variation and battery energy request per kilometre with different values of cost function parameter, for the NEDC performed with a battery electric vehicle

Parameter	Unit	NEDC	Case 1	Case 2	Case 3
Final travel time	[min]	19.7	17.3	19.1	21.2
Soc variation	[%]	5.2	3.9	3.0	2.7
Battery energy request per kilometre	[MJ/km]	0.92	0.69	0.53	0.48

The trade-off between the SoC variation and the total travel time for the eco-driving sensitivity analysis are reported in Figure 4.71. The same considerations already done for the equivalent PHEV analysis, can be repeated.

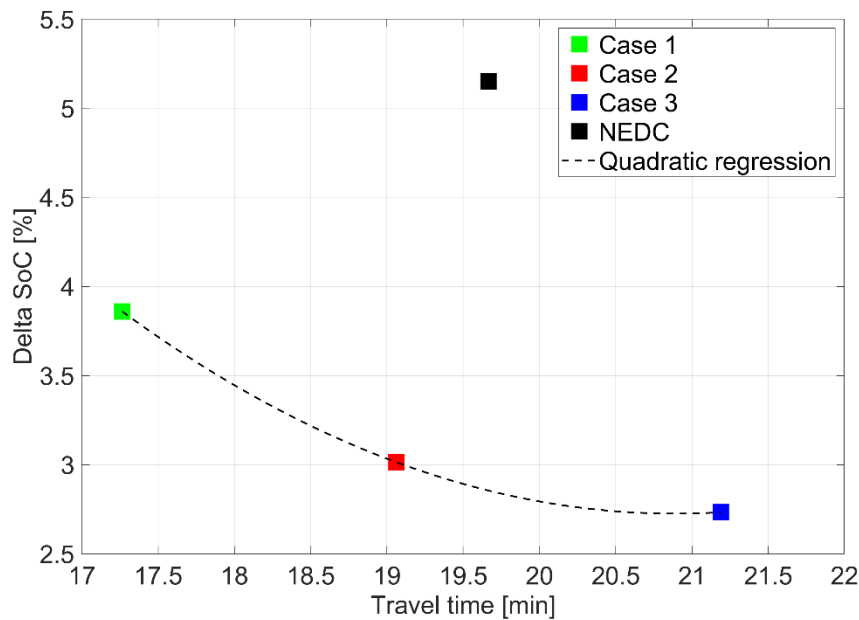


Figure 4.71: Trade-off between SoC variation and travel time with different values of cost function parameter, for the NEDC performed with a battery electric vehicle

4.3.2 RDE

As previously shown for the PHEV analysis, the vehicle speed profile of a conventional vehicle was optimized on a RDE cycle in order to obtain more interesting results. Speed

profiles for the entire RDE cycle are reported in Figure 4.72 and a zoom of a part of urban and rural route are shown in Figure 4.73 and Figure 4.74, respectively.

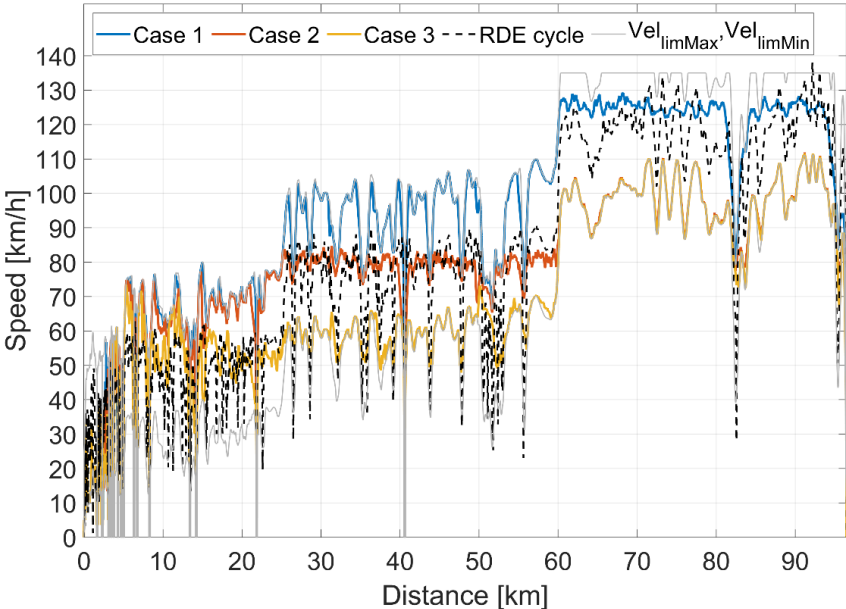


Figure 4.72: Vehicle speed profile with different values of cost function parameter, for the RDE cycle performed with a battery electric vehicle

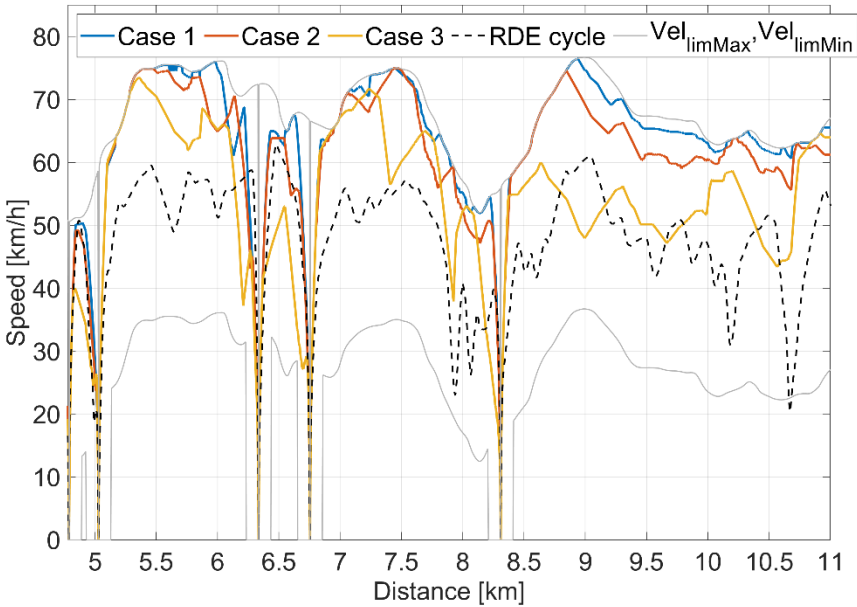


Figure 4.73: Vehicle speed profile with different values of cost function parameter, for the initial part of urban RDE cycle performed with a battery electric vehicle

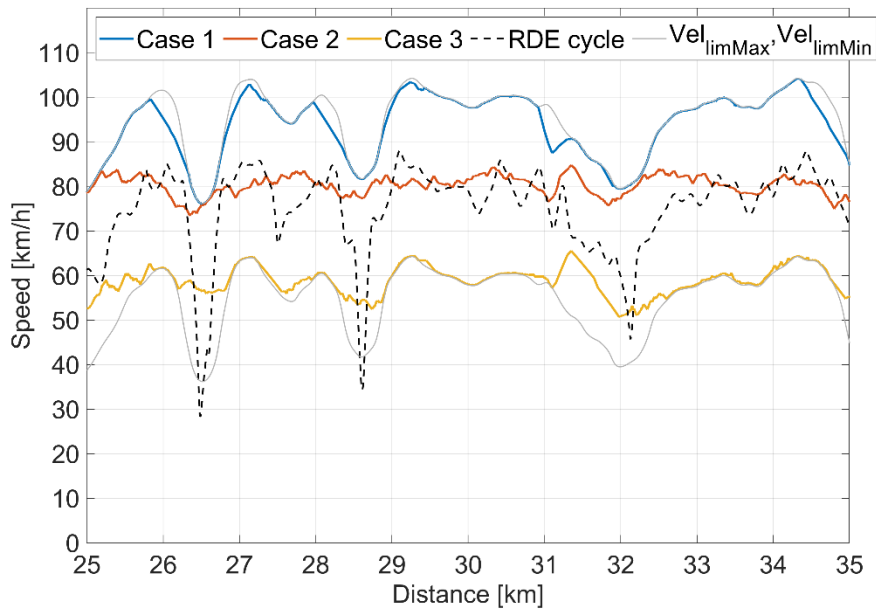


Figure 4.74: Vehicle speed profile with different values of cost function parameter, for the initial part of rural RDE cycle performed with a battery electric vehicle

Generally, an about constant speed is preferred unless the speed limits imposed and the route elevation change this trend. The travel times and the SoC variation are reported in Figure 4.75 and Figure 4.76. The final values of this analysis are reported in Table 4.15.

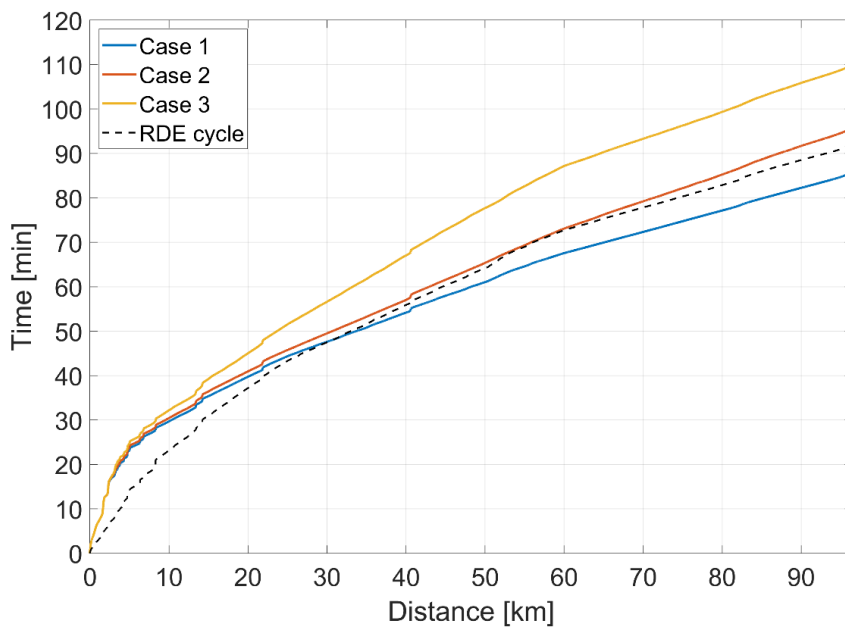


Figure 4.75: Travel time with different values of cost function parameter, for the RDE cycle performed with a battery electric vehicle

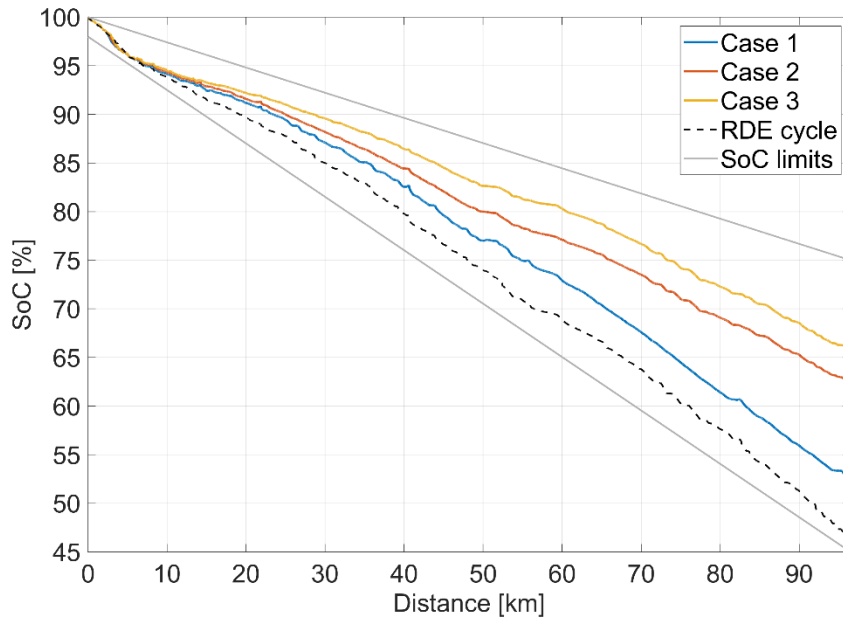


Figure 4.76: SoC profile with different values of cost function parameter, for the RDE cycle performed with a battery electric vehicle

Table 4.15: Final travel time, SoC variation and battery energy request per kilometre with different values of cost function parameter, for the RDE cycle performed with a battery electric vehicle

Parameter	Unit	RDE cycle	Case 1	Case 2	Case 3
Final travel time	[min]	92.2	81.4	87.2	95.7
SoC variation	[%]	53.9	46.8	37.1	33.8
Battery energy request per kilometre	[MJ/km]	1.09	0.94	0.75	0.68

The trade-off between the SoC variation and the total travel time for the eco-driving sensitivity analysis are reported in Figure 4.77. The same considerations already done for the equivalent PHEV analysis, can be repeated.

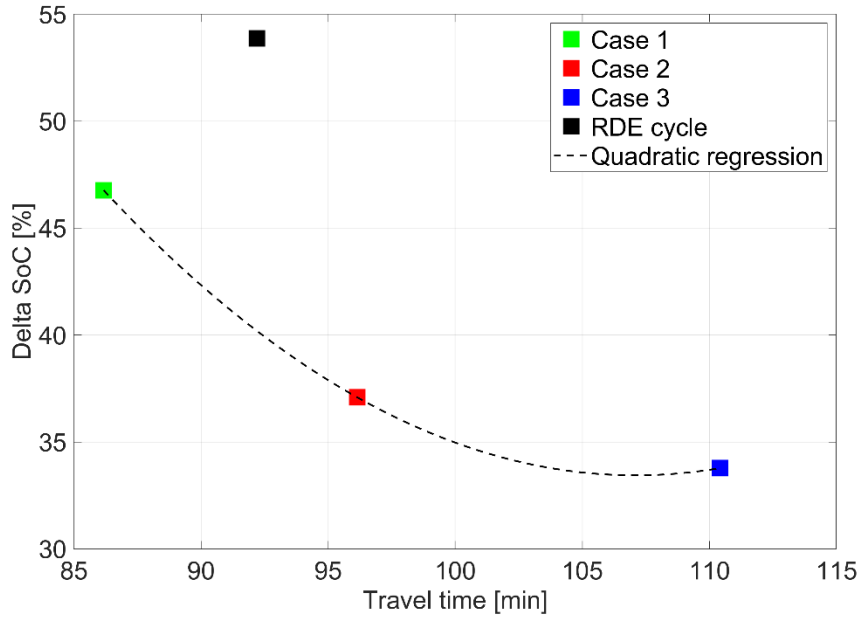


Figure 4.77: Trade-off between SoC variation and travel time with different values of cost function parameter, for RDE cycle performed with a battery electric vehicle

Conclusions

Over the last decades, the policy makers are concerned with the reduction of Greenhouse Gases (GHGs) emissions and the improvement of air quality. In this scenario, the use of a conventional Internal Combustion Engine (ICE) and one or more Electric Motors (EMs) is one of the most promising solution for car makers to meet the mid- and long-term legislation targets. In fact, regardless of the vehicle segment, all the car makers are increasing the degree of electrification of their vehicles.

However, the introduction of vehicle electrification introduces an increased complexity. To manage this complexity a Hybrid Electric Vehicle (HEV) requires an Energy Management System (EMS) deciding the power split among the actuators. The synergic use of the eco-driving technology and the optimal EMS can fully exploit the benefits provided by hybridization. It is found that the eco-driving is a simple and low-cost measure to significantly reduce fuel consumption. In fact, acceleration and deceleration, driving speed, idling and route characteristics are the major factors effecting the fuel consumption. Integrating eco-driving suggestions into vehicle hardware lead to actual improvements. In the literature, several optimization techniques have been suggested for this goal. Among them, the Dynamic Programming (DP) is one of the most promising technique.

This dissertation was focused on eco-driving optimization and three different case studies were considered. In the first one, the speed profile was optimized in order to minimize the energy request at the wheels level respecting a given travel time and all the problem constrains. The problem was solved by creating a distance-based model taking into account all the route constraints (i.e., stops, traffic lights, speed limits). Then, in order to take into account the fuel/energy consumption, two different vehicle models were obtained from the Plug-in Hybrid Electric Vehicle (PHEV): a Conventional Vehicle (CV) and a Battery Electric Vehicle (BEV) featuring, respectively, the thermal engine and the

EM of the real case study. In both cases, the energy minimization was performed (in terms of fuel or battery energy, respectively) respecting the constraints coming from the route and the travel time.

The eco-driving distance-based model developed adopted a backward kinematic approach and use Dynamic Programming Model (DPM) in the MATLAB environment. All the model outputs show a substantial improvement in the trade-off among fuel/energy consumption and travel time, comparing it with a fixed speed time-based model. The solution strictly depends on problem constrains choice, in particular speed limits; therefore, a correct evaluation of them assumes a key role. As demonstrated by the Vehicle-to-Everything (V2X) analysis, a further improvement in the trade-off can be achieved in the urban area thanks to the Vehicle-to-Grid (V2G) communication which allows to avoid the waste of energy and travel time linked to the stops at traffic lights intersections.

Bibliography

- [1] En.wikipedia.org. 2021. *Greenhouse gas* - Wikipedia. [online] Available at: <https://en.wikipedia.org/wiki/Greenhouse_gas> [Accessed 8 July 2021].
- [2] World Meteorological Organization. 2021. *The State of the Global Climate 2020*. [online] Available at: <<https://public.wmo.int/en/our-mandate/climate/wmo-statement-state-of-global-climate>> [Accessed 8 July 2021].
- [3] Hoegh-Guldberg, O., Jacob, D., Taylor, M., Bindi, M., Brown, S., Camilloni, I., Diedhiou, A., Djalante, R., Ebi, K., Engelbrecht, F., Guiot, J., Hijioka, Y., Mehrotra, S., Payne, A., Seneviratne, S., Thomas, A., Warren, R., Zhou, G. and Tschakert, P., 2018. *Impacts of 1.5°C global warming on natural and human systems*. [online] the UWA Profiles and Research Repository. Available at: <<https://research-repository.uwa.edu.au/en/publications/impacts-of-15%C2%BAc-global-warming-on-natural-and-human-systems>> [Accessed 8 July 2021].
- [4] Levin, K., 2021. *8 Things You Need to Know About the IPCC 1.5°C Report*. [online] World Resources Institute. Available at: <<https://www.wri.org/insights/8-things-you-need-know-about-ipcc-15c-report>> [Accessed 8 July 2021].
- [5] Hansen, J. and Sato, M., 2020. *Global Warming Acceleration*. [online] Columbia.edu. Available at: <http://www.columbia.edu/~jeh1/mailings/2020/20201214_GlobalWarmingAcceleration.pdf> [Accessed 8 July 2021].
- [6] CO2.Earth. 2021. *Earth's CO2 Home Page*. [online] Available at: <<https://www.co2.earth>> [Accessed 8 July 2021].
- [7] IEA. 2018. *World Energy Outlook 2018 – Analysis - IEA*. [online] Available at: <<https://www.iea.org/reports/world-energy-outlook-2018>> [Accessed 8 July 2021].
- [8] IEA. 2016. *World Energy Outlook 2016 – Analysis - IEA*. [online] Available at: <<https://www.iea.org/reports/world-energy-outlook-2016>> [Accessed 8 July 2021].
- [9] Climate Action - European Commission. 2021. *Paris Agreement - Climate Action - European Commission*. [online] Available at: <http://ec.europa.eu/clima/policies/international/negotiations/paris_en> [Accessed 8 July 2021].

- [10] Live-counter.com. 2021. *How Many Cars are There in the World?*. [online] Available at: <<https://www.live-counter.com/number-of-cars/>> [Accessed 8 July 2021].
- [11] Bolduc, D.A., Gibbs, N., Hetzner, C., Malan, A. and Sigal, P., 2018. *Automakers' road maps to full-electric and plug-in hybrid cars*. [online] Automotive News Europe. Available at: <<https://europe.autonews.com/article/20181006/ANE/180929838/automakers-road-maps-to-full-electric-and-plug-in-hybrid-cars>> [Accessed 8 July 2021].
- [12] Theicct.org. 2021. *International Council on Clean Transportation*. [online] Available at: <<https://theicct.org/>> [Accessed 8 July 2021].
- [13] 2021. [online] Available at: <<https://www.eea.europa.eu/data-and-maps/data/data-viewers/greenhouse-gases-viewer>> [Accessed 8 July 2021].
- [14] Ihsmarket.com. 2019. *Automotive Forecast, Light Vehicle Sales | IHS Markit*. [online] Available at: <<https://ihsmarkit.com/products/automotive-light-vehicle-sales-forecasts.html>> [Accessed 8 July 2021].
- [15] 2018. *Electric vehicles from life cycle and circular economy perspectives*. European Environment Agency. ISBN 978-92-9213-985-8.
- [16] US EPA. 2019. *Dynamometer Drive Schedules | US EPA*. [online] Available at: <<https://www.epa.gov/vehicle-and-fuel-emissions-testing/dynamometer-drive-schedules>> [Accessed 8 July 2021].
- [17] Tutuianu, M., Marotta, A., Steven, H., Ericsson, E., Haniu, T., Ichikawa, N. and Ishii, H., 2013. *Development of a World-wide Worldwide harmonized Light duty driving Test Cycle (WLTC)*. [online] Unece.org. Available at: <<https://www.unece.org/fileadmin/DAM/trans/doc/2014/wp29grpe/GRPE-68-03e.pdf>> [Accessed 8 July 2021].
- [18] Spessa, E., 2017. *Controllo delle emissioni di inquinanti*. University Course – Mechanical Engineering – Politecnico di Torino.
- [19] Theicct.org. 2021. *Real-Driving Emissions Test Procedure for Exhaust Gas Pollutant Emissions of Cars and Light Commercial Vehicles in Europe*. [online] Available at: <https://theicct.org/sites/default/files/publications/EU-RDE_policy-update_Jan2017_vF.pdf> [Accessed 8 July 2021].
- [20] Tinyurl.com. 2017. *EUR-Lex - 32017R1151 - EN - EUR-Lex*. [online] Available at: <<https://tinyurl.com/53ecjp7s>> [Accessed 8 July 2021].

- [21] DiPierro, G., Millo, F., Pulvirenti, L. and Rolando, L., 2021. *A Methodology for the Reverse Engineering of the Energy Management Strategy of a Plug-in Hybrid Electric Vehicle*. Under Review.
- [22] Pesaran, A.A., 2011. *Choices and requirements of batteries for EVs, HEVs, PHEVs*, in NREL/PR-5400-51474.
- [23] Tran, D., Vafaeipour, M., El Baghdadi, M., Barrero, R., Van Mierlo, J. and Hegazy, O., 2020. *Thorough state-of-the-art analysis of electric and hybrid vehicle powertrains: Topologies and integrated energy management strategies*. *Renewable and Sustainable Energy Reviews*, 119, p.109596. doi: 10.1016/j.rser.2019.109596.
- [24] Rolando, L., 2012. *An Innovative Methodology for the Development of HEVs Energy Management Systems*. Doctoral Thesis. Politecnico di Torino.
- [25] Zhang, Yang, Teng, Ouyang, Guo, Li and Du, 2019. *Comparative Analysis of Technical Route and Market Development for Light-Duty PHEV in China and the US*. *Energies*, 12(19), p.3753. doi:10.3390/en12193753.
- [26] Vda.de. 2021. VDA. [online] Available at: <<https://www.vda.de/en/topics/environment-and-climate/Global-WLTP-roll-out-for-more-realistic-results-in-fuel-consumption/WLTP-How-are-plug-in-hybrids-and-electric-cars-measured.html>> [Accessed 8 July 2021].
- [27] Theicct.org. 2017. [online] Available at: <https://theicct.org/sites/default/files/publications/EU-PHEV_ICCT-Briefing-Paper_280717_vF.pdf> [Accessed 8 July 2021].
- [28] Ali, A.M. and Söffker, D., 2018. *Towards Optimal Power Management of Hybrid Electric Vehicles in Real-Time: A Review on Methods, Challenges, and State-Of-The-Art Solutions*. *Energies*, 11(3), p.476. doi: 10.3390/en11030476.
- [29] Onori, S., Serrao, L. and Rizzoni, G., 2016. *Hybrid Electric Vehicles*. SpringerBriefs in Electrical and Computer Engineering,. doi: 10.1007/978-1-4471-6781-5.
- [30] Eolss.net. 2021. [online] Available at: <<http://www.eolss.net/sample-chapters/c18/E6-43-18-05.pdf>> [Accessed 8 July 2021].
- [31] Sundstrom, O. and Guzzella, L., 2009. *3rd IEEE Multi-conference on Systems and Control*. [S.l.]: IEEE Control Systems Society. ISBN 978-1-4244-4602-5.

- [32] Huang, Y., Ng, E., Zhou, J., Surawski, N., Chan, E. and Hong, G., 2018. *Eco-driving technology for sustainable road transport: A review*. *Renewable and Sustainable Energy Reviews*, 93, pp.596-609. doi: 10.1016/j.rser.2018.05.030.
- [33] De Nunzio, G., Sciarretta, A., Gharbia, I. and Ojeda, S., 2018. *A Constrained Eco-Routing Strategy for Hybrid Electric Vehicles Based on Semi-Analytical Energy Management*. 2018 IEEE Intelligent Transportation Systems Conference. ISBN 978-1-7281-0323-5.
- [34] Gupta, S., Rajakumar Deshpande, S., Tufano, D., Canova, M., Rizzoni, G., Aggoune, K., Olin, P. and Kirwan, J., 2020. *Estimation of Fuel Economy on Real-World Routes for Next-Generation Connected and Automated Hybrid Powertrains*. SAE Technical Paper Series,. doi: 10.4271/2020-01-0593.
- [35] Bodenheimer, R., Brauer, A. and Eckhoff, D., et al., 2014. *Enabling GLOSA for Adaptive Traffic Lights*. Vehicular Networking Conference (VNC), 2014 IEEE. ISBN 978-1-4799-7660-7.
- [36] Olin, P., Aggoune, K., Tang, L., Confer, K., Kirwan, J., Rajakumar Deshpande, S., Gupta, S., Tulpule, P., Canova, M. and Rizzoni, G., 2019. *Reducing Fuel Consumption by Using Information from Connected and Automated Vehicle Modules to Optimize Propulsion System Control*. SAE Technical Paper Series,. doi: 10.4271/2019-01-1213.
- [37] Plianos, A., Jokela, T. and Hancock, M., 2018. *Predictive Energy Optimization for Connected and Automated HEVs*. SAE Technical Paper Series,. doi: 10.4271/2018-01-1179.
- [38] Wan, N., Vahidi, A. and Luckow, A., 2016. *Optimal speed advisory for connected vehicles in arterial roads and the impact on mixed traffic*. *Transportation Research Part C: Emerging Technologies*, 69, pp.548-563. doi: 10.1016/j.trc.2016.01.011.
- [39] Rama, N., Wang, H., Orlando, J., Robinette, D. and Chen, B., 2019. *Route-Optimized Energy Management of Connected and Automated Multi-Mode Plug-In Hybrid Electric Vehicle Using Dynamic Programming*. SAE Technical Paper Series,.doi: 10.4271/2019-01-1209.
- [40] De Nunzio, G., Thibault, L. and Sciarretta, A., 2017. *Bi-Objective Eco-Routing in Large Urban Road Networks*. 2017 IEEE 20th International Conference on Intelligent Transportation Systems (ITSC). ISBN 978-1-5386-1526-3.
- [41] DiPierro, G., Galvagno, E., Mari, G., Millo, F., Velardocchia, M. and Perazzo, A., 2020. *A Reverse-Engineering Method for Powertrain Parameters Characterization Applied to a P2 Plug-In Hybrid Electric Vehicle with Automatic Transmission*. *SAE International Journal of Advances and Current Practices in Mobility*, 3(1), pp.715-730. doi:10.4271/2020-37-0021.

[42] Serrao, L., 2009. *A comparative analysis of energy management strategies for hybrid electric vehicle*. Ph.D. dissertation. The Ohio State University.

[43] Millo, F., Rolando, L., and Andreatta, M., 2011. *Numerical Simulation for Vehicle Powertrain Development* In: Tech. ch. 6.